End-to-end models of marine ecosystems: exploring the consequences of climate change and fishing using a minimal framework

Celina See Wing Wong

Doctor of Philosophy
University of York
Biology
March 2014

Abstract

Marine ecosystems are vital to human society: as a source of food, for economic growth and for their potential to mitigate climate change. With marine ecosystems threatened by climate change and overfishing, there is a need for sustainable fisheries management, which has been the basis for an ecosystem-based approach to management. This has led to considerable interest in end-to-end ecosystem models, where the physical effects of the environment and the population dynamics of all marine organisms are coupled together into one framework. In this thesis, I studied an end-to-end model which coupled together a box-component model representing phytoplankton and zooplankton, with a size-structured fish community model.

I investigated the potential artefacts in model results, caused by numerical methods or by model architecture. I found that care needs to be taken with the choice of numerical method used to simulate size-structured models, as the choice of numerical resolution can yield numerically stable results but can also affect large-scale behaviours of the system, such as the slope and mathematical stability of the size-spectra solutions. With regards to model architecture, coupling together two submodels which differ in structure and resolution can lead to large-scale behaviours of the system which appear plausible and consistent with empirical data, but which impose serious discrepancies in the underlying life-histories of the fish.

By distinguishing model artefacts from ecosystem-effects, the interactions and feedbacks between the higher and lower trophic level organisms can be investigated. I studied the potential impact of climate change upon the marine ecosystem, and in particular, upon the seasonal dynamics of phytoplankton. I found that under a warming climate, the spring phytoplankton bloom occurs earlier and for a longer duration, and the model predicts the loss of the autumn phytoplankton bloom. These changes were not solely due to the direct effect of temperature, but also due to the indirect effect of the interactions of the fish population with zooplankton. The effect of fishing upon the marine ecosystem was also explored with this end-to-end model, with two potential fishing strategies applied to the system. Regardless of the choice of fishing strategy, intensive exploitation of fish stocks can lead to a significant shift in the dynamics of phytoplankton. The phytoplankton's dynamics change from stable annual patterns to unpredictable periodic behaviours.

This thesis has developed an end-to-end model which uses a minimal framework to study the interactions of organisms at different trophic levels, and highlights the importance of these interactions and the associated feedbacks under different scenarios. It combines important theoretical insights into the consequences of model architecture and model-derived artefacts upon ecosystem-scale behaviours, at the same time as highlighting the potential for end-to-end models as a practical and flexible management tool.

Contents

List of Figures

List of Tables

Acknowledgements

I would like to begin with thanking my supervisors, Dr. Jon Pitchford, Professor Richard Law, Dr. Jonathan Beecham and Dr. Steve Mackinson for all their help and guidance over the last three and a half years. They have each been a role model for me and I have learnt a lot from my interactions with them.

I want to thank the staff and students at the University of York who have supported me throughout the years, particularly those in the York Centre for Complex Systems Analysis. My thanks goes to the members of my thesis advisory panel, Dr. Jamie Wood and Dr. Gustav Delius. I would also like to thank members of the Theoretical Ecology Group of the Biology Department, past and present, Dr. Jenny Burrow, Dr. Zoe Cook, Simon Croft, Sarah Collings and Sam Ellis, for their insights and discussions throughout the course of my PhD. In particular, thanks goes to Dr. Samik Datta and Dr. Mariella Canales, who helped me with my understanding of size-structured modelling and the McKendrick-von Foerster equation.

I would also like to thank those at Cefas who helped me during my PhD, Dr. Sonja Van Leeuwen, Dr. Rodney Forster, Dr. Liam Fernand and Dr. Andy Payne, as well as the scientists and crew of the Cefas Endeavour who taught me how to identify a fish. My gratitude goes to Professor Ken Andersen at the Technical University of Denmark, who helped to shape my ideas for size-structured modelling at the start of my PhD. My thanks also goes to Dr. Mike Plank at the University of Canterbury, New Zealand, for introducing me to size-spectra during my Masters, as well as for generously sharing his expertise with me to aid my grasp of numerically modelling size-structured populations.

Special thanks goes to my friends and family, who have been supporting me throughout my PhD. My mum and dad, my sisters and brother-in-law, and my wonderful niece have been there for me, every step of the way on this long journey. Finally, my deepest gratitude goes to John Adamthwaite. He has been my rock during the last year and a half, and most especially in the last two months, so thank you for standing beside me while I finished this journey.

Author's Declaration

I hereby declare that this submission is entirely my own work except where due acknowledgement is given. This work has not previously been presented for an award at this, or any other, University.

"No good fish goes anywhere without a porpoise."
- Lewis Carroll (1865)

Chapter 1

General Introduction

1.1 The modelling of marine ecosystems

Natural ecosystems are necessary for human life, providing us with essential services, from clean air to food. With over 70% of the Earth's surface covered by oceans and seas, the fisheries industry providing employment to over 600 million people and global fish consumption at 130.8 million tonnes in 2011 (FAO, 2012), marine ecosystems are essential for human survival. As well as being of economic value through the importance of commercial fisheries, marine ecosystems have huge potential for mitigating climate change by acting as a source or sink for atmospheric carbon dioxide (Boyd and Doney, 2002; Hoegh-Guldberg and Bruno, 2010). The complexity of marine ecosystems has led to a huge diversity of mathematical models: to understand the major processes and drivers of these systems (such as climate and human factors), as well as to forecast ecological responses to future scenarios (Fulton et al., 2011). Due to the vast magnitude of marine ecosystems, the ecological dynamics of the system has traditionally been represented using two independent components: biogeochemical and fish production models (Travers et al., 2009).

Biogeochemical models typically focus on the flux of a main nutrient, such as nitrogen, between three compartments: nutrients (N), phytoplankton (P) and zooplankton (Z) (Travers et al., 2009; Libralato and Solidoro, 2009; Carlotti and Poggiale, 2010). As a result of their biological simplicity, such models can be coupled to hydrodynamic models, which capture elements of the physical environment of the ocean (such as wind, temperature and irradiance) (Blackford, 2004). These hydrodynamic models can be one-dimensional models representing a water column (such as the General Ocean Turbulence model, GOTM (Blackford, 2004)) or completely three-dimensional models (such as the Regional Ocean Modelling System, ROMS (Shchepetkin and McWilliams, 2005)).

The connection between nutrients and the population dynamics of these lower trophic level (LTL) organisms included in biogeochemical models (i.e. phytoplankton and zooplankton) has traditionally been modelled using simple box compartments to represent each component, commonly referred to as nutrient-phytoplankton-zooplankton (NPZ) type models (Steele and Hendersen, 1981; Franks, 2002). These models have been extended by adding a detritus compartment (D), in order to represent bacterial nutrient cycling activities, leading to the NPZD models (Travers et al., 2007; Anderson, 2005).

Fasham et al. (1990) uses the basic NPZD framework, but expands it with explicit compartments for bacteria (B), nitrate nitrogen (N_n), ammonium nitrogen (N_r) and labile dissolved organic nitrogen (N_d). The European Regional Seas Ecosystem model (ERSEM), refines the NPZD components into several functional types (Baretta, 1995): for example, the phytoplankton module is divided into five groups: diatoms, flagellates, picoplankton, dinoflagellates and coccolithophores. Another approach for refining the NPZD components is through size-structure: the NEMURO model divides the zooplankton group into small, large and predatory (Kishi et al., 2007).

As can be seen, the approach in common with each of these biogeochemical models is retaining the plankton functional type within the framework, although the complexity of that implied disaggregation varies between models (from the most basic NPZD compartment model (Fasham et al., 1990) to the coarsely size-structured approach (Kishi et al., 2007), to a stage-structured representation (Moll and Stegert, 2007; Stegert et al., 2007)).

Fish production models, on the other hand, have been developed from the perspective of fisheries management (Travers et al., 2007). They tend to focus on exploited fish species, either in a single-species (Lassen and Medley, 2001) or multi-species context (Magnusson, 1995). These models are used to represent the survival and catch for a cohort of an exploited species and, as such, they are often species specific. Further approaches to modelling the dynamics of higher trophic level organisms (HTL) structure the fish population through some individual-based trait, such as age, size or stages (Mellin et al., 2009; Kamioka, 2005; Rudolf, 2007; de Roos et al., 2008; de Roos and Persson, 2002; de Roos et al., 2010).

To provide two instructive examples, OSMOSE (Object-oriented Simulator of Marine ecOSystem Exploitation) is an individual-based model of size-structured schools of organisms (Shin and Cury, 2001; Travers et al., 2007, 2009). Within each school, prey selection depends on being in the same place at the same time as the school of predators, but also upon size-ratios (predators prefer to feed upon prey which are a within a particular size-range, known as a predator-prey mass ratio (Andersen and Ursin, 1977; Law et al., 2009; Datta, 2011)). On the other hand, Ecopath with Ecosim (EwE) describes the system through functional groups (Christensen and Pauly, 1992). This model requires extensive empirical knowledge of the

food web being represented, in order to input diet preferences for the organisms.

The biogeochemical and fish production models have traditionally been modelled independently of each other, with 'closure' terms being used to represent the impact of one upon the other (Rose et al., 2010; Travers et al., 2007). The biogeochemical models (or LTL models) use a 'closure' term to represent the predation of fish on the phytoplankton and zooplankton. The functional form chosen for this term can influence the dynamics of the LTL model (Steele and Henderson, 1992; Edwards and Yool, 2000). Similarly, the fish production models (or HTL models) use a 'closure' term to represent the plankton pool that planktivorous fish species, and larval fish, require for survival. This can be done implicitly by assuming a 'carrying capacity' parameter (Travers et al., 2007).

Using a 'closure' term effectively assumes that there is no feedback between the dynamics of the HTLs and the LTLs. However, feedbacks do occur between these two marine subcompartments: plankton undergo seasonal influences which affect their dynamics, which would have a direct (or even indirect) impact upon the fish populations that feed upon them (Field et al., 2006; Rose et al., 2010), while human factors such as fishing would affect the predation pressures felt by the LTL organisms (Libralato and Solidoro, 2009; Megrey et al., 2007; Travers et al., 2007).

This has necessitated the development of 'end-to-end' (E2E) models, where the biogeochemical processes are coupled together with the lower and higher trophic level organisms into one framework (Rose et al., 2010; Fulton, 2010). It should be noted that 'end-to-end' models sometimes refers to models which not only couple together the lower and higher trophic level organisms into one framework, but also includes nutrient recycling (Heath, 2012; Heath et al., 2014). For the purposes of this thesis, I will be focussing on 'end-to-end' models which do not explicity include nutrient recycling.

1.2 Current developments in end-to-end modelling

Over the last ten years, there has been a considerable interest in the development of E2E models to understand the effects of climate change and fishing upon marine ecosystems (Travers et al., 2007; Rose et al., 2010; Libralato and Solidoro, 2009). There are two common approaches for constructing E2E models: coupling together existing submodels that represent LTL and HTL organisms, or creating an entirely new framework (Rose, 2012).

Fennel (2010) developed a NPZDF model, where the traditional NPZD model for the LTL dynamics are coupled to a fish community dominated by two prey species (sprat and herring)

and one predator (cod). The fish community is also coarsely size-structured, with 5 sprat size-classes, 6 herring size-classes and 7 cod size-classes. This model was applied to the Baltic Sea, with experimental runs over 40 years to study the effect of varying nutrient loads and fishing mortality of cod. Fennel uses this model to predict that management measures need to be enforced over several years to improve cod stocks.

Travers et al. (2009) coupled the ROMS-$N_2P_2Z_2D_2$ and OSMOSE submodels into one framework. As the LTL model assumes a constant mortality rate to the biological compartments, these rates needed to be decomposed so that part of it is determined by the HTL model. Travers et al. (2009) compared a one-way coupling (where the mortality rates of the plankton groups were kept constant) against a two-way coupling (the mortality rates of the plankton group were determined by the fish) for the southern Benguela ecosystem for the years 1990-1997. They showed that the coupling choice had a profound impact upon abundance (where the biomass of planktivorous species increased during the two-way coupling) and food web structure (where different food chains occurred during the two-way coupling due to changes in the dominant food chain which is supported by plankton).

These are two examples of E2E models which have been created by coupling together existing frameworks for the LTL and HTL communities. There are fewer examples of E2E models which have been developed from an entirely new framework, but one such example is the Atlantis model (Fulton et al., 2011; Smith et al., 2007; Link et al., 2010). Fulton et al. (2011) describes the Atlantis modelling framework as an E2E model which includes the biophysical system (environmental drivers as well as biological components), the human users of the modelled marine ecosystem (industrial fisheries), an adaptive management strategy (which includes monitoring, assessment and management decision processes) and socioeconomic drivers (human behaviours which influence the system, such as markets and social networks). Atlantis has been used to explore ecosystem dynamics (Link et al., 2010) and to predict future regime shifts (Fulton et al., 2011), due to either climate change or human practices.

There are advantages and disadvantages to either approach, and they both face similar challenges which arise in the development of E2E models. The advantage of coupling together existing submodels is that each system has been developed in great detail, and fully tested and understood over the years. The main issue lies with the fact that the submodels were created for different purposes. This leads to a difficulty in communication between the two submodels. For example, regarding the representation of the zooplankton: most LTL models represent the zooplankton by functional groups such as micro- and meso-zooplankton, whereas HTL models have represented the LTL organisms implicitly as a 'carrying capacity' parameter (Travers et al., 2007). Thus, when coupling together existing submodels, a 'library' needs to be created, in order for these two systems to communicate together: the re-

sources gained by the HTL organisms from feeding on phyto- and zooplankton is aggregated and distributed to the larval fish, and the predation pressures on the LTL organisms by the fish is allocated across the functional groups (Libralato and Solidoro, 2009; Travers et al., 2009).

This issue does not arise when creating a new framework for an E2E model, as the entire ecosystem is being considered during its development and specific diet niches can be introduced which span both the LTLs and HTLs. Building a new E2E model means that there is no focus on particular aspects of the marine ecosystem, such as phytoplankton dynamics or the life history of cod. Instead, wider ecosystem-scale questions can be addressed, where each component of the marine ecosystem can feedback and affect the others, either directly or indirectly. The disadvantage of this approach is the cost, both in time and money (Travers et al., 2007), as well as potential difficulties with mathematical stability, transparency and tractability due to increased model complexity.

1.3 The challenges involved in developing end-to-end models

When developing E2E models to represent marine ecosystems, either by coupling together existing submodels or through developing a new framework, there are two main challenges which need to be considered.

Firstly, there is the role of zooplankton within the marine ecosystem. As we have seen, zooplankton is the main link between the LTLs and the HTLs in mathematical models. However, in traditional marine ecosystem models, the zooplankton has been used as the 'model closure' and has not been represented in great detail. For example, in simple NPZ models, zooplankton mortality is often considered as density dependent and is modelled as being proportional to the square of the zooplankton concentration (Le Quéré et al., 2005), or else a linear function is assumed for model simplicity (Edwards and Brindley, 1999). Steele and Henderson (1992) showed that the choice of a linear function for the zooplankton mortality leads to limit cycle behaviour, which does not occur when a density dependent function for the zooplankton mortality is chosen. The zooplankton can be represented as one population, as in the NPZ models (Steele and Hendersen, 1981; Franks, 2002), size-structured into small, large and carnivorous (Kishi et al., 2007) or, most often, by functional type such as microzooplankton, heterotrophic flagellates, omnivorous or carnivorous (Baretta, 1995). On the other hand, zooplankton are often not explicitly considered in HTL models; they are represented by assuming no internal dynamics (so the total number of individuals remains

constant over time) (Law et al., 2009) or implicitly as a 'carrying capacity' parameter in a population growth equation (de Roos et al., 2008).

In an E2E framework, the zooplankton needs to realistically represent a range of prey for zooplanktivores such as herring and sprat, as well as larval fish, whose diet shifts and changes as it increases in body mass (Rose et al., 2010). One approach for this is to represent the zooplankton as a size-structured population, where the dynamics are governed by the body mass of the zooplankton (Fuchs and Franks, 2010; Zhou and Huntley, 1997; Carlotti and Poggiale, 2010).

The difference in scales between LTL and HTL dynamics, both temporal and spatial, also need to be addressed in E2E modelling (Rose et al., 2010). In traditional models for LTLs, it was assumed that the dynamics of fish varied so slowly in comparison to plankton that their actions upon the LTL organisms were assumed to be constant (Caswell and Neubert, 1998). A mixture of temporal scales need to be addressed in E2E modelling, in order to realistically represent the fast dynamics of phytoplankton (e.g. seasonal spring blooms) as well as the decadal effects that occur (e.g. impact upon the populations due to overharvesting) (Rose et al., 2010).

A range of spatial scales also need to be considered in an E2E model. Oceans are a spatially heterogeneous environment where plankton are distributed in 'patches' (Currie et al., 1998; Pitchford and Brindley, 2001; Martin et al., 2002; Brentnall et al., 2003), thus the survival of organisms whose diet consists of plankton is highly dependent on their movements. Fulton et al. (2004) show the effect that the spatial resolution has upon ecosystem models, and conclude that models with a coarse spatial resolution can lead to misleading results. The impact of fishing pressure can be misrepresented and over exaggerated using a coarse spatial scale, as predators and prey overlap for longer periods and over larger areas under these scenarios. Thus, a spatial dimension needs to be considered when developing end-to-end models. While there are tools which use an explicit spatial resolution within its framework, such as Ecospace which is a dynamic version of Ecopath, where the biomass within an ecosystem is dynamically allocated across a grid map (Pauly, 2000), spatial resolution could also be represented in an indirect way. The Atlantis model uses statistical distributions and coefficients of variation to capture patchiness in the marine environment, and thus avoids the need to explicitly represent them (Fulton, 2010). Thus, statistical indices which represent the probability of patchiness could be implemented into a predator's volume search rate, and the spatial heterogeneity of the ocean could be implemented into the modelling framework without an explicit spatial scale being considered. Ecopath with Ecosim assumes that prey are divided into vulnerable and invulnerable components (this is known as the foraging arena theory), or by defining consumption rates that reflect seasonal and spatial changes in consumption over the modelled period (Pauly, 2000; Travers et al., 2007).

1.4 The role of end-to-end models

End-to-end models are necessary tools for gaining insight of the impacts to the marine ecosystem under future management and environmental scenarios (Fulton et al., 2003b; Travers et al., 2007; Steele, 2012; Heath, 2012; Heath et al., 2014). For example, global warming is expected to lead to an increase in the sea surface temperature, with climate change models predicting a 1.1°C-6.4°C increase over the next 100 years (Huertas et al., 2011). This would have a direct effect on phytoplankton growth, which is highly influenced by temperature, nutrient availability and light intensity (McCauley and Murdoch, 1987; Moisan et al., 2002; Townsend et al., 1994). Any change within the phytoplankton population would have direct and indirect consequences for organisms at HTLs, in particular, upon the survival of fish larvae (Kristiansen et al., 2011).

An increase in sea surface temperature would also affect the physiological rates of organisms within the marine ecosystems, for example, metabolic rates or attack rates of predators (Clark et al., 2003; Pörtner and Knust, 2007). Clark et al. (2003) modelled North Sea cod populations and studied the effect of sea surface temperature on growth rates. They showed that an increase of temperature led to a decline in the cod spawning stock and recruitment, with growth rates optimal at 8.5°C.

End-to-end models are also tools that can be used for exploring various fisheries management strategies (Fulton, 2010). Traditional management strategies are established in order to protect the young and harvest the old, whilst still maintaining a strong spawning-stock population (Beverton and Holt, 1993; Law et al., 2013; Borrell, 2013). However, it has been argued that this selective fishing strategy has led to fish adapting by investing their energy into reaching sexual maturity as early as possible, as opposed to growing larger (Law, 2000; Reznick and Ghalambor, 2005; Enberg et al., 2011).

Recently, a balanced harvesting approach has been suggested as a more suitable fishing strategy, where fishing is distributed across a range of species and sizes, in proportion to their natural productivity (Law et al., 2012; Garcia et al., 2012). Law et al. (2012) used a dynamic size-spectrum single fish species model to compare selective fishing against balanced harvesting. They showed that balanced harvesting leads to good yields whilst reducing disruption to the ecosystem. However, the practical implementation needs more consideration as balanced harvesting requires knowledge of productivity (Maxwell et al., 2012; Jacobsen et al., 2014), although knowledge of relative growth rates could be used as they are related to productivity (Law et al., 2012).

These different management strategies need to be considered with the presence of a dy-

namic phytoplankton and zooplankton community included in the ecosystem framework. As phytoplankton undergo seasonal dynamics, such as spring and autumn blooms (Truscott and Brindley, 1994; Winder and Cloern, 2010; Findlay, 2006), their interaction with the fish population could lead to unforeseen consequences.

I will address the issues raised here in **Chapter 4** and **Chapter 5**.

1.5 The importance of body size in marine ecosystems

Body size is a key feature of a marine organism and defines many of its physiological processes (Andersen and Beyer, 2006), thus models of marine ecosystems often incorporate size structure within their framework (Travers et al., 2009; Fennel, 2010). Empirical evidence suggests that organisms tend to feed upon smaller individuals, be fed upon by larger individuals and hence grow depending on its size (Blanchard et al., 2009; Cohen et al., 1993). An observation within marine ecosystems of a linear relationship between abundance and body size on a logarithmic scale with a slope close to -1, known as a size spectrum (Sheldon et al., 1972; Quinones, 2003), led to the development of population models of marine ecosystems where the organisms have a size-dependent diet preference.

There have been huge advances in the field of size-structured modelling over the last few decades. Platt and Denman (1977) developed a model which incorporated a weight-dependent growth and metabolic rate within it, and this model gave rise to a power-law steady state which, when parameterised for the Sargasso Sea, agreed with empirical data. Size-spectra have also been commonly studied using a variant of the McKendrick-von Foerster partial differential equation (MvF PDE), an equation originally used to investigate population modelling with age distribution. The MvF PDE incorporates size-dependent growth and mortality rates into its framework, and relates these population-level rates to the changes in abundance within the population (Benoît and Rochet, 2004; Datta et al., 2010). Further details of the MvF PDE will be provided in **Chapter 2**.

End-to-end models commonly use a size-structured modelling approach to represent the HTL organisms. For example, Travers et al. (2009) used the OSMOSE framework within their E2E framework (Shin and Cury, 2001). Maury (2010) couples a size-structured pelagic model, which uses the dynamic energy budget theory (Nisbet et al., 2010) to account for the uptake and use of energy for vital processes, such as growth, maintenance and reproduction to the biogeochemical PISCES model.

A size-structured modelling approach is particularly useful in the context of E2E modelling,

as it improves model simplicity (important for understanding cause-and-effect feedbacks within the ecosystem, as well as reducing the computational resources required) and reduces the amount of parameters required for the model while leading to empirically observable effects (Dickie et al., 1987). It also provides a useful indicator for measuring the effects of fishing on the ecosystem (Pope et al., 2006), as size-at-entry fishing tends to lead a steeper slope of the size-spectrum as fishing pressure increases (Rice, 1996; Bianchi, 2000).

1.6 Thesis structure

The aim of this thesis is to contribute to the understanding of the development and dynamics of end-to-end models. In particular, the consequences of coupling together submodels which differ in structure and resolution are explored in the context of some of the major influences currently shaping marine ecosystems.

In **Chapter 2**, I explore the consequences of the choice of size resolution in the numerical methods used to simulate size-structured models. To address this issue, I use a size-structured fish community model, with a non-dynamic plankton spectrum representing the LTL organisms. I derive a numerical stability condition for this model, and examine the effect of size resolution upon the slope and stability of size spectrum solutions. In **Chapter 3**, I investigate the ramifications of coupling together submodels which differ significantly in their structure and resolution. I develop a two-way coupled end-to-end model, using a box framework of phytoplankton and zooplankton to represent the LTLs and the size-structured fish community model to represent the HTLs. I explore the effect that the choice of the zooplankton's functional response has upon the E2E model, and compare it against the original size-structured fish community model. In **Chapter 4**, I use the dynamic E2E model to investigate the effects of global warming across the marine ecosystem, and in particular, the effect of a warming climate upon the seasonal dynamics of phytoplankton. Temperature is incorporated directly into the E2E model through the phytoplankton's growth rate, and the abundances and dynamics of the marine organisms are focussed upon to understand the consequences of increased sea surface temperatures. In **Chapter 5**, I study the impact of fishing upon the dynamics of the marine ecosystem, and in particular, whether the interactions between fish and lower-trophic-level organisms leads to a major shift in the dynamics of the phytoplankton. I compare the effect of two different fishing strategies upon the marine ecosystem, specifically, the size-at-entry and balanced harvest strategies. I study the disruption caused to the marine ecosystem by either strategy, whilst considering the potentially achieved yield. The thesis ends with a General Discussion in **Chapter 6**, where I debate the limitations of the method used and future directions for this work.

Chapter 2

Continuous or discrete: consequences of model choice for size-structured ecosystems

Abstract

Size structure is a key feature of marine ecosystems, where organisms tend to grow by feeding upon smaller individuals. It can be incorporated into models in various ways, from smooth continuous variation, to a small number of discrete size classes. Models of marine ecosystems are important in understanding fundamental ecological mechanisms and predicting system-level changes, such as those brought about by over-fishing or climate change. Here we develop a mathematical framework to quantify how the large-scale behaviour of an ecosystem model can vary according to how finely its size structure is resolved. Explicitly, we show that both the slope and stability of size spectrum solutions to a size-based McKendrick-von Foerster model can vary dramatically depending on the choice of size resolution of the model. When evaluating possible ecosystem responses to changes, predictions based on coarsely resolved size-structured models should be treated with caution. In coarsely discretised models the properties of, and departures from, stable steady states can appear as artefacts of model choice, rather than reflecting ecological reality.

Keywords

McKendrick-von Foerster equation; size spectrum; finite difference approximation; stability; marine ecosystem

2.1 Introduction

Models for the dynamics of marine ecosystems often incorporate size structure, on the grounds that body size is a key feature of a marine organism, defining many of its biological processes (Andersen and Beyer, 2006). Empirical evidence shows that organisms tend to feed upon smaller individuals, are fed upon by larger individuals and grow depending on their size (Blanchard et al., 2009; Cohen et al., 1993). The data collected tends to show an approximately linear log(mass)-log(abundance) relationship, known as a size spectrum (Quinones, 2003; Sheldon et al., 1972).

The dynamics of size-structured populations have been modelled in many ways, including individual based modelling (Shin and Cury, 2001), matrix methods (Hughes, 1984; de Roos et al., 1992), stage-based approaches (de Roos et al., 2008; Rudolf, 2007), ordinary differential equations (Fennel, 2010; Armstrong, 1999; Pahl-wostl, 1997) and through the use of partial differential equations (PDEs) (Silvert and Platt, 1978; Benoît and Rochet, 2004). A commonly favoured method for modelling size-structure in ecosystems is through the use of a PDE known as the McKendrick-von Foerster PDE (MvF PDE), in which the abundance of the population is dependent on size and time (Benoît and Rochet, 2004; Andersen and Beyer, 2006; Law et al., 2009; Datta et al., 2011). Regardless of the mathematical framework, there are two paradigms for modelling size spectra: where the species identity of individuals is not considered, such as in a community size spectrum (Benoît and Rochet, 2004; Law et al., 2009) or where individuals are assigned a species identity and each species is size-structured (Andersen and Beyer, 2006; Hartvig et al., 2010; Rossberg, 2012). This chapter is concerned with modelling a community size spectrum.

In general, PDEs are challenging for formal analysis, and are usually studied using numerical integrations instead. This can lead to issues with stability and convergence of the numerical approximation, as well as being computationally expensive (Lax, 1965). The stability and convergence of the numerical approximation depends upon the discretised step sizes, in this case, the time step size (Δt) and the log(mass) step size (Δx). It is possible to analyse mathematically the MvF PDE (Datta et al., 2011; Capitán, 2010; Rossberg, 2012). However, this requires certain assumptions to be made; Datta et al. (2011) assumed that the steady state was a power-law and that the model had an infinite range of sizes. Numerical simulations are still required when studying the MvF PDE as there are a finite number of species in the marine ecosystem, and this allows exploration of different scenarios such as fishing management strategies.

When numerically simulating the MvF PDE, the numerical discretisation is typically chosen to be very fine, i.e. the step sizes are very small, but this leads to a computationally expensive

model. Ackleh and Ito (1997) discretised a nonlinear size-structured population model, similar to the MvF PDE, using an implicit finite difference approximation. From this numerical scheme, they derived conditions for uniqueness and proved convergence of the numerical approximation to the solution.

Benoît and Rochet (2004) used a fourth order Runge-Kutta method to solve the MvF PDE, with $\Delta x = 0.5$, where x is log weight and dimensionless. The mass and time steps were determined through trial and error and chosen small enough so that patterns were independent of the value of the steps, yet large enough for a reasonable computational time.

Another example is Fennel (2009), where a coupled nutrient-phytoplankton-zooplankton-detritus (NPZD) and fish model is studied. The fish compartment is not explicitly modelled using the MvF PDE, rather, it is comprised of three size-structured species (with size-structured interactions), where there are five classes for planktivorous sprat, six classes for herring and seven classes for cod. Each size-class for each species is then modelled using ordinary differential equations for biomass concentration and abundance.

These three examples illustrate that the level of discretisation varies between different studies. The question is what is the optimum level of discretisation, or 'best' trade-off between accuracy and computability, required for numerically integrating the McKendrick-von Foerster PDE?

In this study, we apply an upwind, finite-differencing discretisation to the McKendrick-von Foerster PDE (Lax, 1965; Press et al., 2007), in other words, the individuals in discrete size-classes grow depending on the individuals in smaller size-classes. This paper addresses two points:

1. Reliable integration of discretised size-spectrum dynamics
2. Effects of discretisation on steady-state properties

The importance of these results to marine ecosystem models is discussed in the final section.

2.2 Methods and Results

2.2.1 The McKendrick-von Foerster equation

The McKendrick-von Foerster PDE was originally used to model the population dynamics of an age-structured population. It was adapted into a size-structured model by Silvert and Platt (1978), where abundance is a function of body mass and time, and is given by:

$$\frac{\partial U(w,t)}{\partial t} = -M(w,t)U(w,t) - \frac{\partial (G(w,t)U(w,t))}{\partial w} \tag{2.1}$$

where $U(w,t)$ is the density of organisms of mass w per unit volume, $G(w,t)$ is the growth function and $M(w,t)$ is the mortality function of organisms of mass w at time t (Silvert and Platt, 1978; Blanchard et al., 2009; Datta et al., 2010; Law et al., 2009; Andersen and Beyer, 2006; Arino et al., 2004; Calsina and Saldafia, 1995; de Roos et al., 2008; Farkas and Hagen, 2007; Hartvig et al., 2010; Rossberg, 2012).

The size-spectra PDE, Eq.(2.1), is transformed to depend on the natural logarithm of weight, since the sizes of organisms making up the marine community can span many orders of magnitude. The co-ordinate transformation is $w = w_0 e^x$ where w_0 is a reference weight, and x is a dimensionless variable. This leads to the logarithmically transformed size-spectra PDE:

$$\frac{\partial u(x,t)}{\partial t} = -\mu(x,t)u(x,t) - \frac{\partial (g(x,t)u(x,t))}{\partial x} \tag{2.2}$$

The mortality and growth rates of the size-spectra equation

In the size-spectra PDE, mortality consists of predation, intrinsic mortality and senescent mortality. Predation is upon smaller organisms with a preference towards prey which are a predator-prey mass ratio (PPMR) apart from themselves (determined by a Gaussian feeding kernel, $\phi(x,x') = (1/\sigma\sqrt{2\pi})exp\{-(x-x'-\beta)^2/2\sigma^2\}$ where β is the log(PPMR) and σ is the feeding kernel width) (Law et al., 2009). The intrinsic mortality accounts for death which is not caused by predation, and is assumed to be a constant rate $\tilde{k}$. As there are no top-class

predators in this modelling framework, a senescent mortality of $\mu_s e^{\rho(x-x_s)}$ is introduced once organisms reach a certain log(mass) x_s, where μ_s is the senescent mortality rate and ρ is the senescent mortality exponent (Law et al., 2009; Benoît and Rochet, 2004). The growth rate is determined by the assimilation of mass gained by consumption.

The boundary conditions for the size-spectra PDE needs to be defined. For the left hand boundary, small organisms require resources to feed upon in order to grow. This is implemented into the model by assuming that there is a fixed resource spectrum of phytoplankton. As reproduction is not accounted for in this model, the newborn size-class is also fixed. For the right hand boundary, it is assumed that there is a maximum log(mass) $x_{\max}$ for the fish community, and that there are no organisms within the model which are greater than this $x_{\max}$.

In other words, the PDE model is:

$$\frac{\partial u(x,t)}{\partial t} = -\left[\overbrace{\tilde{k}}^{\text{intrinsic mortality}} + \overbrace{\mu_s e^{\rho(x-x_s)}}^{\text{senescent mortality}} + \overbrace{\mu(x,t)}^{\text{predation}}\right] u(x,t) - \frac{\partial\left\{\left[\overbrace{g(x,t)}^{\text{growth}}\right] u(x,t)\right\}}{\partial x} \tag{2.3}$$

$$\text{Initial condition: } u(x,0) = u^0(x) \text{ for } x \in [x_{\min}, x_{\max}]$$
$$\text{Boundary conditions: } u(x_{\min},t) = u_1 \text{ where } u_1 \text{ is a constant value}$$
$$u(x,t) = 0 \text{ for } x > x_{\max}$$

where $\mu(x,t) = \gamma \int (w_0 \exp(x'))^q \phi(x',x) u(x',t) dx'$ and
$g(x,t) = \alpha\gamma w_0^q \exp(x(q-1)) \int \exp(x') \phi(x,x') u(x',t) dx'$, $x_{\min}$ is the minimum log(mass) of the fish community and $x_{\max}$ is the maximum log(mass) of the fish community. See Table 2.1 for the parameter definitions.

Table 2.1: Parameter values

		Parameter value		
Term	Parameter description	Fig.2.1	Fig.2.2	Fig.2.3
Discretisation terms				
Δx	log(mass) step-size	0.1	see figure	see figure
Δt	time step-size	see figure	≤ 0.001	≤ 0.001
Feeding terms				
γ	volume searched per unit time per unit mass^q ($m^3 \cdot yr^{-1} \cdot g^{-q}$)	600	600	600
q	search volume exponent	0.8	0.8	0.8
α	mass conversion efficiency	0.2	0.2	0.2
ϕ	feeding-kernel function			
β	log(preferred predator:prey mass ratio)	4	4	4
σ	feeding-kernel width	2	2	2
Mortality terms				
$\tilde{k}$	intrinsic mortality rate (yr^{-1})	0.1	0.1	0.1
μ_s	senescent mortality rate (yr^{-1})	0.5	0.5	0.5
ρ	senescent mortality exponent	1.5	1.5	1.5
Initial conditions				
w_0	reference weight (g)	4.54×10^{-8}	4.54×10^{-8}	4.54×10^{-8}
$w_{\min}$	minimum body mass (g)	1×10^{-3}	1×10^{-3}	1×10^{-3}
$w_{\max}$	maximum body mass (g)	3.3×10^{3}	3.3×10^{3}	3.3×10^{3}
p_1	density of the smallest phytoplankton size-class (m^{-3})	2.2×10^{6}	2.2×10^{6}	2.2×10^{6}
λ_p	exponent of the phytoplankton spectrum	-1	-1	-1
u_1	density of the smallest consumer size-class (m^{-3})	100	100	100
λ_u	initial exponent of the consumer spectrum	-1	-1	-1

(Law et al., 2009, see Table 1)

2.2.2 Reliable integration of discretised size-spectrum dynamics

The solutions of partial differential equations can be approximated using numerical methods, one of which is the finite differencing method, where the domain space is partitioned into a mesh and used to approximate the derivatives of the equation through these discrete points (Lax, 1965; Press et al., 2007). The finite-difference method chosen must be numerically stable, i.e. any small errors which are introduced to the numerical scheme should dampen out so that the approximate solution approaches the continuous solution over time. This stability condition often depends on the step sizes chosen for the variables, in this case the time and log(mass) variables.

Discretising the size-spectra equation

An upwind, finite-differencing approach is applied to the transformed size-spectra PDE (Eq.(2.2)) to approximate the continuous PDE with a discrete function. An upwind technique was used as each size-class grows depending on the size-classes below it in the chain, i.e. $u(x,t+1) = \mathbf{f}(u(\bar{x}_{\bar{x}<x},t)$. In order to discretise the size-spectra PDE, the equation first needs to be linearised around the steady-state solution. See Appendix 2.4.1 for the steps involved in linearising and discretising the size-spectra PDE. Linearising about the steady-state solution by assuming that $u(x,t) = u^* + \varepsilon\tilde{u}(x,t)$, where u^* is the steady-state solution and ε is small, and discretising the subsequent equation yields the discretised size-spectra PDE:

$$\begin{aligned}\frac{\tilde{u}_j^{l+1} - \tilde{u}_j^l}{\Delta t} = &-\gamma\sum_{i>j}(w_0 e^{x_i})^q \phi(x_i,x_j)\tilde{u}_i^l \Delta x u_j^{*l} - \mu_j^{*l}\tilde{u}_j^l - \frac{g_j^{*l}\tilde{u}_j^l - g_{j-1}^{*l}\tilde{u}_{j-1}^{*l}}{\Delta x} \\ &- (1-\kappa)\alpha\gamma w_0^q e^{x_j(q-1)}\sum_{i<j} e^{x_i}\phi(x_j,x_i)\tilde{u}_i^l u_j^{*l} \\ &+ (1-\kappa)\alpha\gamma w_0^q e^{x_{j-1}(q-1)}\sum_{i<j-1} e^{x_i}\phi(x_{j-1},x_i)\tilde{u}_i^l u_{j-1}^{*l}\end{aligned} \tag{2.4}$$

where $\tilde{u}(x_j,t_l) := \tilde{u}_j^l, u^*(x_j,t_l) := u_j^{*l}, g_j^{*l} = g(x_j,t_l)|_{u_j^{*l}}$ and $\mu_j^{*l} := \mu(x_j,t_l)|_{u_j^{*l}}$.

Kelley (1995, Chapter 1) shows that if the finite-difference approximation can be re-written into the general form of $\underline{u}^{l+1} = \mathbf{M}\underline{u}^l + \underline{c}$, where $\mathbf{M}$ is known as the iteration matrix, then the iteration of the numerical approximation is numerically stable if $\xi(\mathbf{M}) < 1$. $\xi(\mathbf{M})$ is the spectral radius of the iteration matrix, i.e. the value of the maximum absolute eigenvalue of

M. The finite-difference approximation of the size-spectra PDE can be written in the form $\underline{\tilde{u}}^{l+1} = \mathbf{M}\underline{\tilde{u}}^{l} + \underline{c}$. See Eq.(2.9) in Appendix 2.4.1 for the iteration matrix of the linearised size-spectra PDE.

The iteration matrix of the size-spectra PDE is too complex to derive analytical forms for its eigenvalues. However, the numerical method can be applied to the time-independent size-spectrum solution to illustrate the importance that the choices of Δt and Δx has upon the numerical approximation of the size-spectra PDE. Furthermore, we will demonstrate that if Δx is kept constant, then numerical stability of the finite-differencing method can be achived by decreasing Δt.

Illustration of reliable and unreliable integration

Figure 2.1a and c shows the time-independent size-spectrum solution for four different time steps, while Figure 2.1b and d shows the stability condition for these time steps. Figure 2.1 shows that the finite-difference approximation of Eq.(2.3) is numerically stable if Δt is small enough. When $\Delta t = 0.001$, Figure 2.1a shows that the approximation is numerically stable. This is verified by the eigenvalues of the iteration matrix which are plotted in Figure 2.1b, and shows that the spectral radius of the iteration matrix is always less than 1. Note that these solutions are all very close to each other as, for each time step, the numerical approximation is approaching the continuous solution. Hence, the solutions are fairly indistinguishable from each other.

However, increasing the time step-size is all that is required for the finite-difference approximation to become numerically unstable. Figure 2.1c shows that if $\Delta t = 0.004$, and all other parameters are kept the same, the time-independent size-spectrum solution becomes numerically unstable. As can be seen in Figure 2.1c, the numerical approximation is no longer tending towards the continuous time-independent size-spectrum solution, but instead, the density of individuals of about 0.01g is increasing exponentially. This is verified by Figure 2.1d, which shows that at when time=0.16year, the spectral radius of the iteration matrix is greater than 1.

2.2.3 Effects of discretisation on steady-state properties

The previous section shows that the MvF PDE can be numerically solved using a finite-difference approximation. This numerical approximation remains numerically stable for all log(mass) step sizes, as long as the time step-size is small enough and an appropriate ini-

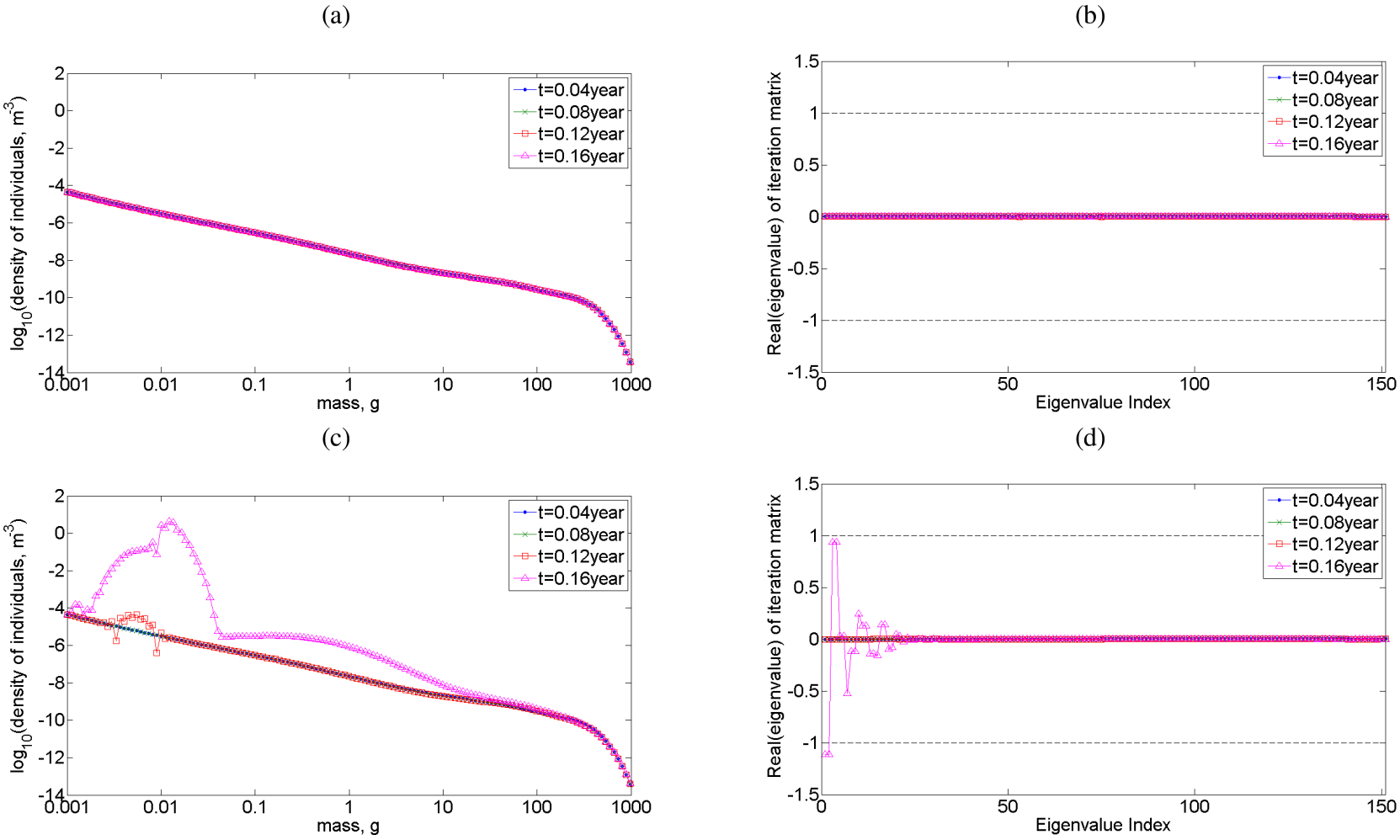

Figure 2.1: The numerical stability of the finite-difference approximation is dependent on the step-sizes, Δx and Δt. The size-spectrum solution and its stability condition are plotted for different time steps, time = 0.04year, 0.08year, 0.12year and 0.16year. (a) and (c) show the size-spectrum solution over time while (b) and (d) show the eigenvalues of the iteration matrix at different time steps. If each eigenvalue is between the values of -1 and 1, then the finite-differencing method is numerically stable. Otherwise, the finite-differencing method is numerically unstable. (a) and (b) use a small time step ($\Delta t = 0.001$) and shows a numerically stable solution. (c) and (d) use a larger time step ($\Delta t = 0.004$) and shows a numerically unstable solution.

tial population abundance is chosen. Hence, the MvF PDE can be coarsely discretised and remain numerically stable.

Is the solution to the coarsely discretised model consistent with that of the finely discretised model? We investigate this question by gradually increasing Δx and comparing the stable steady-state solutions. The McKendrick-von Foerster equation is numerically solved using the finite-differencing method outlined in Eq.(2.4) for the mathematically stable steady-state solutions.

Figure 2.2a shows the stable steady-state solution of the McKendrick-von Foerster equation for different levels of discretisation. Although each discretisation of the McKendrick-von Foerster equation leads to an approximately linear size-spectrum as the stable steady-state solution, the gradient of the size-spectrum varies depending on the discretisation. As the discretisation becomes more coarse, the gradient of the size-spectrum increases (Figure 2.2b). Note that the straight line is only a visual guide; formal regression is inappropriate because the plotted points are from numerical analysis of the model and not experimental data.

The stability of the steady-state solution is also studied by analysing the return times to equilibrium after perturbation. Return times are defined as:

$$\text{return time} := -\frac{1}{\text{real}(\lambda_{\max})} \text{ where } \lambda_{\max} < 0 \tag{2.5}$$

where λ_{max} is the least negative eigenvalue, where the eigenvalues are determined from the Jacobian matrix evaluated at equilibrium.

Figure 2.3 shows that as the coarseness of the discretisation increases, the relative return times decrease. This is due to the number of equations that need to be solved decreasing as the coarseness of the discretisation increases. (See Appendix 2.4.3 for more details.)

The results also show that as the discretisation becomes finer, the return time increases exponentially. Thus, the mathematical stability of the discretised MvF PDE is affected by the choice of the resolution of the numerical discretisation. This is shown by the shaded grey region of Figure 2.3. Plank and Law (2011) show that different combinations of the predator-prey mass ratio and the feeding kernel can lead to a stable steady state, or an unstable steady state, and find that stability requires the feeding kernel width to be at least 2/5 of the predator-prey mass ratio. This chapter has shown that the mathematical stability of the MvF PDE is also dependent upon the level of discretisation chosen to numerically approximate it.

(a)

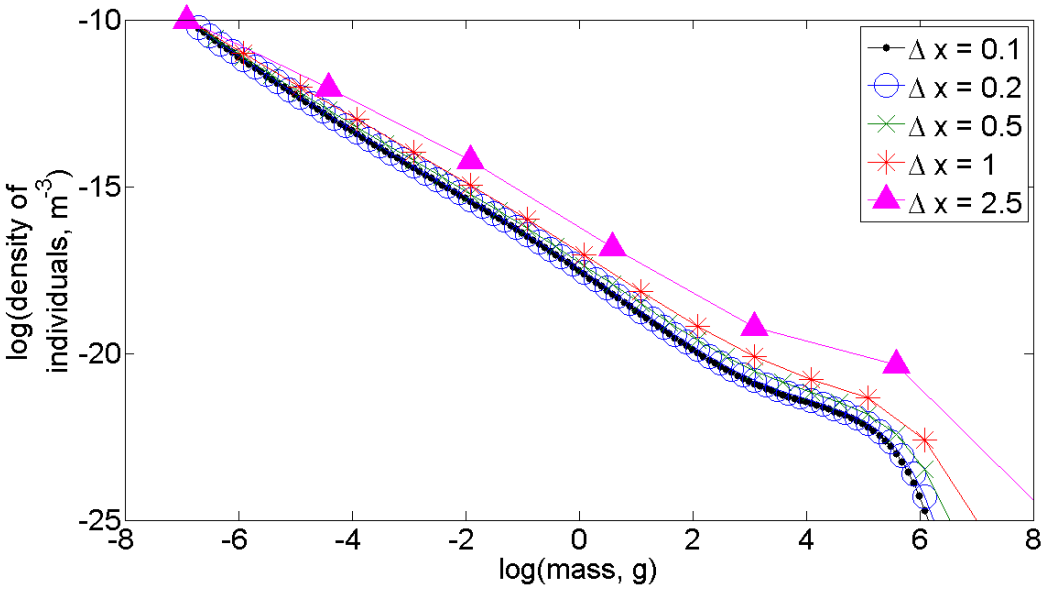

(b)

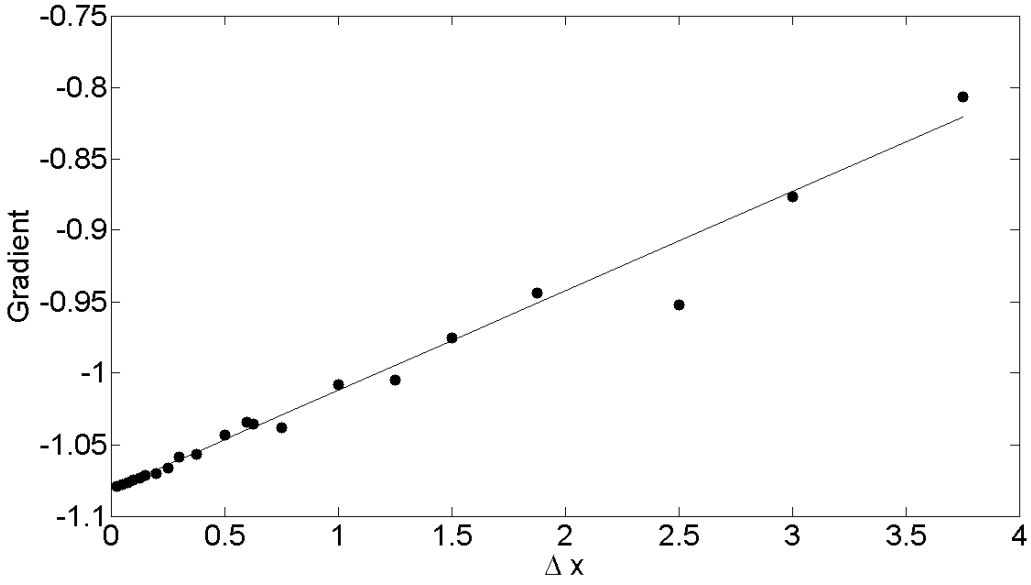

Figure 2.2: The gradient of the size-spectrum solution increases as Δx increases from a fine discretisation to a coarse discretisation. (a) The stable size-spectrum solution for varying values of Δx (b) The gradient of the size-spectrum for different values of Δx

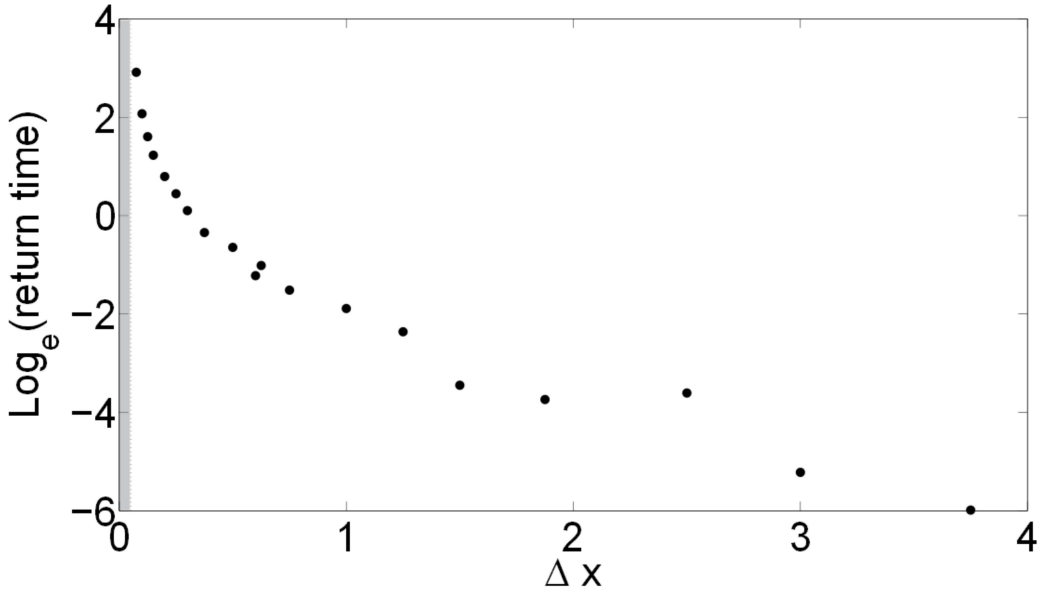

Figure 2.3: The return time to equilibrium decreases as Δx increases. The shaded grey region shows that if Δx crosses a threshold on the fine scale, the steady-state solution crosses from stable to unstable.

2.3 Discussion

Modelling the Size Spectrum

The McKendrick-von Foerster partial differential equation, which is used for modelling size-spectra, can be solved using numerical approximations. However, care must be taken when solving the MvF PDE with a finite-differencing method, as different levels of discretisation lead to different results. The results show that as the level of discretisation becomes more coarse, although the general behaviour remains consistent with the fine discretisation (i.e. an approximately linear size-spectrum solution), it does not capture the full behaviour of the model (see Figure 2.2).

Baird and Suthers (2007) developed a size-resolved pelagic ecosystem model and studied the error in the discretisation of the size-classes. They compared simulations with 17, 32, 62, 123 and 245 size-classes, showing that the results for the two coarsest scales (17 and 32) are very different from the finer scales (62, 123 and 245). They identified the major source of error as the model's ability to resolve the appropriate range of prey sizes for a particular predator species. For example, at the coarsest level of discretisation, the predator of radius 7.7cm has two prey "species" to feed upon whereas at the finest level of discretisation, the same predator has 38 prey species. As the discretisation becomes finer, the prey ranges converge so that they are almost identical. Hence, the discrepancy in results between the coarsely

and finely discretised MvF PDE could be due to the implementation of the Gaussian feeding kernel. The results of the MvF PDE equation could be more consistent if the feeding kernel spanned the same number of size-classes for all levels of discretisation.

The differences in the stable steady-state solution for varying levels of discretisation could also be due to a trade-off between two types of errors (Picard et al., 2010). One error is known as the 'distribution error', which is the difference between the discrete and continuous distribution, and arises due to large size-classes combining individuals of different sizes and averaging the result. The second error is known as the 'sample error', the mean of the standardised variances of the estimator of the transition rates, and is due to highly variable transition rates with very small size-classes. Picard et al. (2010) show that the optimal size-class width is a trade-off between the 'distribution error' and the 'sample error' . They apply their algorithm to a data set on a tree species of a tropical rainforest in French Guiana and show that the optimal number of size-classes is 8 classes of 11.4cm in width. Hence the differences in stable steady-states between the coarsely and finely discretised models, shown in Figure 2.2, could be due to the 'distribution error' growing as Δx increases.

Empirical Size Spectra

Han (1998) showed that the construction of a continuous spectrum based on empirical data is dependent on the size-class intervals used. An error results from the effect of the choice of size-class interval, as logarithmically equal size-class intervals correspond to linearly unequal size-class intervals. When constructing discrete models of biomass spectra (Kerr, 1974; Sheldon et al., 1977), only when the choice of size-class intervals is small does the discrete model for size-spectra become close to accurate. However, the error can be corrected by applying the coefficient of the effect of size-intervals to the size-spectra models.

In light of Han's results, should empirical data be used to inform the discretisation level of size-structured models? Mancinelli et al. (2008) collected the dry mass of benthic macroinvertebrates over two seasons, and varied the logarithmic bases into which the data was sorted, leading to size spectra of varied resolutions. The data was allocated to 19 different size frequency distributions, and ranged from having approximately 100 finely discretised size-classes to only 12 coarsely discretised size-classes. Their study showed that site- or season-specific multivariate effects on size spectra are strongly dependent on the resolution of the size spectrum. With a fine discretisation, there was an increase in the noise of the data. However, with a coarse discretisation, the size structure originally present in the data is lost. As with the algorithm determined by Picard et al. (2010), there is a trade-off between fine and coarse discretisation.

Thus, when developing size-structured models, analysis of the effect of discretisation on the model should be carried out. Figure 2.2b indicates that there is a linear relationship between the discrete step size for log(mass) and the slope of the size-spectrum. This relationship could be used as a correction factor when modelling at a coarse scale, in order to determine the gradient of the size-spectrum solution at finer scales.

Stability of the Size-Structured Model

The mathematical stability of the steady-state solution was analysed by studying the return times to equilibrium after perturbation. For this study, I have taken the return time to be a function of the least negative eigenvalue (Eq.(3.1)). However, simulations using different perturbations to the model (changing the slope of the static phytoplankton spectrum, changing the abundance of newborns in the consumer spectrum) led to similar results obtained from Eq.(3.1) (see Appendix 2.4.2 for more details).

Plank and Law (2011, Figure 4) show that stability occurs roughly when $\sigma \geq 2/5\beta$ (where σ is the width of the feeding kernel and β is the log(preferred predator-prey mass ratio). Figure 2.3 shows that the steady-state transitions from stable to unstable as Δx decreases for

the MvF PDE. This transition of stability is a numerical artefact of the finite differencing scheme used to approximate the MvF PDE. Hence, the mathematical stability of the MvF PDE depends on the width of the feeding kernel, the preferred predator-prey mass ratio and the choice of the discretisation of the numerical scheme.

As shown by Rossberg (2012), using a naïve implementation of the backward differencing approximation can lead to negative real eigenvalues, which arise due to the boundary assumption that the largest individuals in the model do not grow. Hence, the stability of the forward differencing scheme could also be due to boundary conditions affecting the numerical analysis.

Size-based Indicators

One of the main drivers behind developing size-spectra models is for the use of size-based metrics in assessment and management of marine ecosystems. One such metric could be a comparison of the slope of the size-spectrum in an unexploited state against that of an exploited state (Jennings and Dulvy, 2005). However, the size composition of catches differs significantly from that of the actual community due to fishing gear selectivity. Jennings and Dulvy (2005) suggest that to avoid misleading comparisons, size-based metrics should be expressed as relative indices rather than absolute. One way of using a relative size-based index is by looking at the departure of the size-spectrum from a linear solution, or its nonlinearity.

As a more coarsely discretised size-spectra model yields a more positive slope than a finely discretised size-spectra model, a more fair comparison between the two models would be to look at the relative change of the slope after exploitation. Initial investigations show that the coarsely discretised and finely discretised models behave in the same qualitative way under increased fishing pressure, but further work is needed to investigate the relative changes in behaviour. Hence, coarsely discretised models could be valid when restricted to analysing relative change, which is difficult when comparing model outputs to empirical data as data collected before exploitation are rarely available.

As this study has shown, not only does the empirical size-spectrum need to be carefully summarised, but the discretisation of size-spectra models also need to be carefully chosen. As Han (1998) show, empirical data provides discrete size-spectra and hence requires appropriately discretised size-structured models to understand the data. The resolution of the size spectrum, both empirically and in models, affects the outputs in ways which are, generally, unaccounted for. This study has shown the effect of the resolution of the size spectrum upon the steady state solutions, and the stability of those solutions. However, short term dynamics, such as seasonal phytoplankton blooms, could affect the size-structured model, its steady-state solutions and the stability. Rigorous analysis on the numerical method used to model

an ecological ecosystem is needed to ensure that patterns observed are emergent from the model, and not numerical artefacts.

Acknowledgements

We would like to thank Gustav Delius and Jamie Wood for helpful discussion, Axel Rossberg for valuable comments on the manuscript, Michael J.Plank for his help with the computer code for this research and Richard Law for his insights. The research was supported by a joint studentship to CW from the Centre for Environment Fisheries and Aquaculture Science UK and the University of York UK. CW was awarded a travel grant from the Fisheries Society of the British Isles to participate in the *Body size, food webs and ecosystem dynamics workshop* at the University of Canterbury, New Zealand.

2.4 Appendix

2.4.1 Deriving the iteration matrix for the discretised size-spectra equation

Recall the size-spectra PDE is

$$\frac{\partial u(x,t)}{\partial t} = -\mu(x,t)u(x,t) - \frac{\partial}{\partial x}\left(g(x,t)u(x,t)\right)$$

where

$$\begin{aligned}\mu(x,t) =& \underbrace{\tilde{k} + \mu_s e^{\rho(x-x_s)}}_{M_1(x,t)} + \underbrace{\gamma \int (w_0 e^{x'})^q \phi(x',x) u(x',t) dx'}_{M_2(x,t)} \\ g(x,t) =& (1-\kappa)\alpha\gamma w_0^q e^{x(q-1)} \int e^{x'} \phi(x,x') u(x',t) dx'\end{aligned} \tag{2.6}$$

Linearise the size-spectra equation

To analyse the numerical stability of the size-spectra PDE, it needs to be linearised around the steady-state solution. Assume $u(x,t) = u^* + \varepsilon\tilde{u}(x,t)$ where u^* is the steady-state solution and ε is small. Then the mortality and growth functions which were defined in Eq.(2.6) can be written as

$$\begin{aligned}\mu(x,t) =& M_1(x,t) + \gamma \int (w_0 e^{x'})^q \phi(x',x)(u^* + \varepsilon\tilde{u}(x,t)) dx' \\ & M_1(x,t) + M_2^*(x,t) + \varepsilon\tilde{M}_2(x,t) \\ g(x,t) =& g^* + \varepsilon\tilde{g}(x,t)\end{aligned}$$

where $M_2^*(x,t) := M_2(x.t)|_{u^*}, \tilde{M}_2(x,t) := M_2(x,t)|_{\tilde{u}(x,t)}, g^* := g(x,t)|_{u^*}$ and $\tilde{g}(x,t) := g(x,t)|_{\tilde{u}(x,t)}$.

Then the size-spectra PDE can be re-written as

$$\begin{aligned}\frac{\partial \tilde{u}(x,t)}{\partial t} =& -\tilde{M}_2(x,t)u^* - \mu^*\tilde{u}(x,t) - \varepsilon\tilde{M}_2(x,t)\tilde{u}(x,t) - \frac{\partial}{\partial x}\left(g^*\tilde{u}(x,t)\right) \\ & - \frac{\partial}{\partial x}\left(\tilde{g}(x,t)u^*\right) - \varepsilon\frac{\partial}{\partial x}\left(\tilde{g}(x,t)\tilde{u}(x,t)\right)\end{aligned}$$

Letting $\varepsilon \to 0$ yields the linearised size-spectra PDE:

$$\frac{\partial \tilde{u}(x,t)}{\partial t} = -\tilde{M}_2(x,t)u^* - \mu^*\tilde{u}(x,t) - \frac{\partial}{\partial x}\left(g^*\tilde{u}(x,t)\right) - \frac{\partial}{\partial x}\left(\tilde{g}(x,t)u^*\right) \tag{2.7}$$

Discretise the linearised size-spectra equation

Eq.(2.7) is discretised using an upwind finite-differencing method. To simplify notation, define $\tilde{u}(x_j,t_l) := \tilde{u}^l_j, \tilde{\mu}(x_j,t_l) := \tilde{\mu}^l_j, \tilde{g}(x_j,t_l) := \tilde{g}^l_j$. Then the discretsation of the linearised size-spectra PDE is

$$\begin{aligned}\frac{\tilde{u}^{l+1}_j - \tilde{u}^l_j}{\Delta t} =& -\gamma\sum_{i>j}(w_0 e^{x_i})^q \phi(x_i,x_j)\tilde{u}^l_i \Delta x u^{*l}_j - \mu^{*l}_j\tilde{u}^l_j - \frac{g^{*l}_j\tilde{u}^l_j - g^{*l}_{j-1}\tilde{u}^{*l}_{j-1}}{\Delta x} \\ & - (1-\kappa)\alpha\gamma w_0^q e^{x_j(q-1)}\sum_{i<j} e^{x_i}\phi(x_j,x_i)\tilde{u}^l_i u^{*l}_j \\ & + (1-\kappa)\alpha\gamma w_0^q e^{x_{j-1}(q-1)}\sum_{i<j-1} e^{x_i}\phi(x_{j-1},x_i)\tilde{u}^l_i u^{*l}_{j-1}\end{aligned}$$

This can be re-written as

$$\begin{aligned}\tilde{u}^{l+1}_j =& D^{*l}_j\tilde{u}^l_j + \left\{\frac{\Delta t}{\Delta x}g^{*l}_{j-1} - \Delta t(A^*_2)^l_j e^{x_{j-1}}\phi(x_j,x_{j-1})\right\}\tilde{u}^l_{j-1} \\ & - \Delta t\Delta x(A^*_1)^l_j\left\{e^{x_{j+1}q}\phi(x_{j+1},x_j)\tilde{u}^l_{j+1} + e^{x_{j+2}q}\phi(x_{j+2},x_j)\tilde{u}^l_{j+2} + ...\right\} \\ & + \Delta t e^{x_{j-2}}\phi(x_j,x_{j-2})\left\{(A^*_2)^l_{j-1} - (A^*_2)^l_j\right\}\tilde{u}^l_{j-2} \\ & + \Delta t e^{x_{j-3}}\phi(x_j,x_{j-3})\left\{(A^*_2)^l_{j-2} - (A^*_2)^l_{j-1}\right\}\tilde{u}^l_{j-3} + ...\end{aligned} \tag{2.8}$$

where

$$
\begin{aligned}
D_j^{*l} &= 1 - \Delta t \mu_j^{*l} - \frac{\Delta t}{\Delta x} g_j^{*l} \\
(A_1^*)_j^l &= \gamma w_0^q u_j^{*l} \\
(A_2^*)_j^l &= (1-\kappa)\alpha\gamma w_0^q e^{x_j(q-1)} u_j^{*l}
\end{aligned}
$$

Write the discretised approximation into the general form with an iteration matrix

The finite-difference approximation can be written in the form $\underline{\tilde{u}}^{l+1} = \mathbf{M}\underline{\tilde{u}}^l + \underline{c}$ where

$$\underline{\tilde{u}}^l = \begin{pmatrix} \tilde{u}_1^l \\ \tilde{u}_2^l \\ \vdots \\ \tilde{u}_j^l \\ \vdots \\ \tilde{u}_N^l \end{pmatrix} \qquad \underline{c} = \begin{pmatrix} 0 \\ 0 \\ \vdots \\ 0 \\ \vdots \\ 0 \end{pmatrix}$$

$$M = \begin{pmatrix} 1 & 0 & 0 & 0 & \cdots & 0 \\ \ddots & \ddots & \ddots & \ddots & \ddots & \cdots \\ \cdots & +\frac{\Delta t}{\Delta x} g_{j-2}^{*l} - \Delta t (A_2^*)_{j-1}^l e^{x_{j-2}} \phi(x_{j-1,j-2}) & +D_{j-1}^{*l} & -\Delta t \Delta x (A_1)_{j-1}^{*l} e^{x_j q} \phi(x_j, x_{j-1}) & -\Delta t \Delta x (A_1^*)_{j-1}^l e^{x_{j+1} q} \phi(x_{j+1}, x_j) & \cdots \\ \cdots & +\Delta t e^{x_{j-2}} \phi(x_j, x_{j-2}) \{ (A_2^*)_{j-1}^l - (A_2^*)_j^l \} & +\frac{\Delta t}{\Delta x} g_{j-1}^{*l} - \Delta t (A_2^*)_j^l e^{x_{j-1}} \phi(x_j, x_{j-1}) & +D_j^{*l} & -\Delta t \Delta x (A_1^*)_j^l e^{x_{j+1} q} \phi(x_{j+1}, x_j) & \cdots \\ \cdots & \ddots & \ddots & \ddots & \ddots & \cdots \\ \cdots & \ddots & \ddots & \ddots & \ddots & D_N^{*l} \end{pmatrix} \tag{2.9}$$

2.4.2 The return times of the steady-state solutions for continuous and discrete models

In Section 2.2.3, the stability of the steady-state solution for the discretised McKendrick-von Foerster equation was studied by analysing the return time to equilibrium after perturbation. The return time is also a function of the least negative eigenvalue, and in Section 2.2.3, is defined as:

$$\text{return time } := -\frac{1}{\text{real}(\lambda_{\max})} \text{ where } \lambda_{\max} < 0$$

How accurate is this definition for the return time? We perturb the system in two different ways and measure the time for the system to return to its original equilibrium state. We perturb the system in two different ways:

1. Changing the gradient of the static phytoplankton spectrum
2. Changing the fixed abundance of newborns (u_1)

The perturbations are implemented into the model for one year, before the parameters are returned to the original set in Table 2.1. The model is then allowed to continue integrating forwards in time, using a standard Euler's method, until it has reached the original equilibrium state (assuming that the perturbed state is equal to the equilibrium state when $|u_{\text{perturbed}} - u_{\text{equilibrium}}| < 1e-6$.

Figure 2.4 shows that the definition for return times as a function of the largest eigenvalue leads to a result which is qualitatively similar to perturbing the system and waiting for the perturbed state to return to the equilibrium state. The main difference is that the defined return time leads to a result which appears to be exponentially decreasing much more rapidly as Δx increases than the perturbed systems.

2.4.3 Size-class intervals and number of size-classes

The range of log(mass) is chosen between some minimum and maximum size, i.e. $[x_{min}, x_{max}]$. When partitioning the log(mass) domain space, the number of size-classes, N_C depend on the step-size chosen:

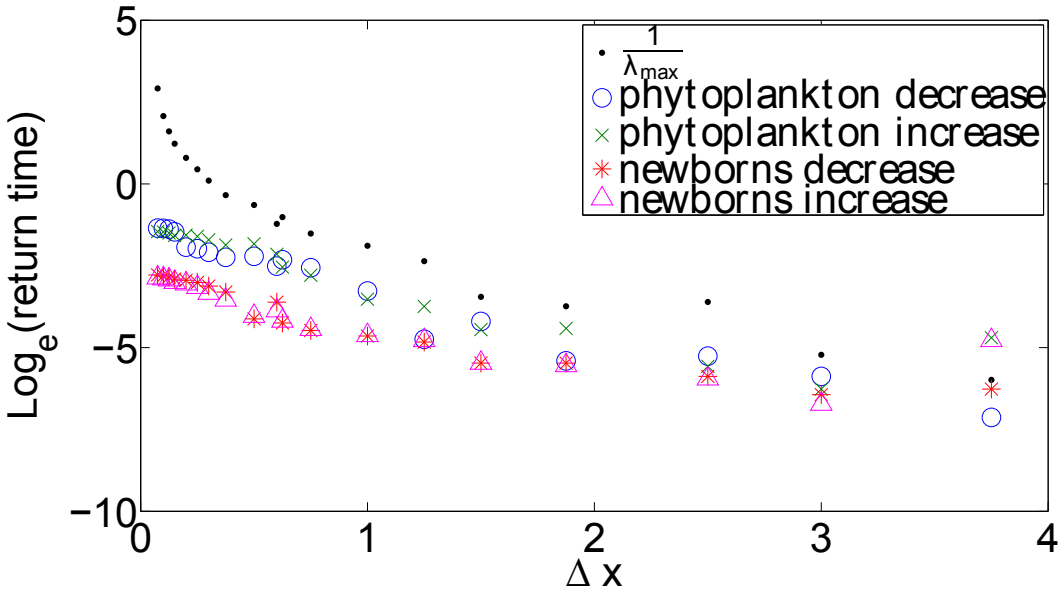

Figure 2.4: As the log(mass) interval, Δx, increases, the return time to equilibrium after perturbation decreases. Defining return time as $-\frac{1}{\lambda_{max}}$ leads to a qualitative similar result to perturbing the system and waiting for the state to return to equilibrium. (Black, filled circle marker, $\bullet$) return time $:= -\frac{1}{\lambda_{max}}$ (Blue, circle marker, $\circ$) the gradient of the phytoplankton size-spectrum was decreased to -1.5 (Green, cross marker, $\times$) the gradient of the phytoplankton spectrum was increased to -0.5 (Red, star marker, $*$) the abundance of the newborn size-class, u_1, was decreased by a factor of 0.5 (Pink, triangle marker,$\triangle$) the abundance of the newborn size-class, u_1, was increased by a factor of 1.5

$$N_C = \left| \frac{x_{max} - x_{min}}{\Delta x} \right|$$

When N_C is an integer value, then x_{max} is unaffected by the discretisation. However, when N_C is not an integer value, it is rounded down so that the new maximum size, $\tilde{x}_{max}$ is less than x_{max}. For example, when $x_{min} = 10, x_{max} = 25, \Delta x = 0.1$, $N_C = 150$ and $\tilde{x}_{max} = x_{max} = 25$. However, when $\Delta x = 0.7$, then $N_C = 21.43$ which leads to $24.7 = \tilde{x}_{max} < x_{max} = 25$. This leads to ranges of Δx where the number of size-classes remains the same, despite an increasing log(mass) step-size. This can lead to numerical artefacts in the results.

These numerical artefacts need to be removed from results before analysis. Figure 2.3 shows the results when the maximum log(mass) size was taken into account and controlled for. The discretisations chosen were to ensure that the consumer spectrum always has the same largest size-class (about $x = 8$, or $w = 3270g$). Figure 2.3 shows that the return time to steady-state after perturbation decreases as the coarseness of the discretisation increases. When all possible discretisations are chosen without taking this consideration into account,

the result is not as clear to understand.

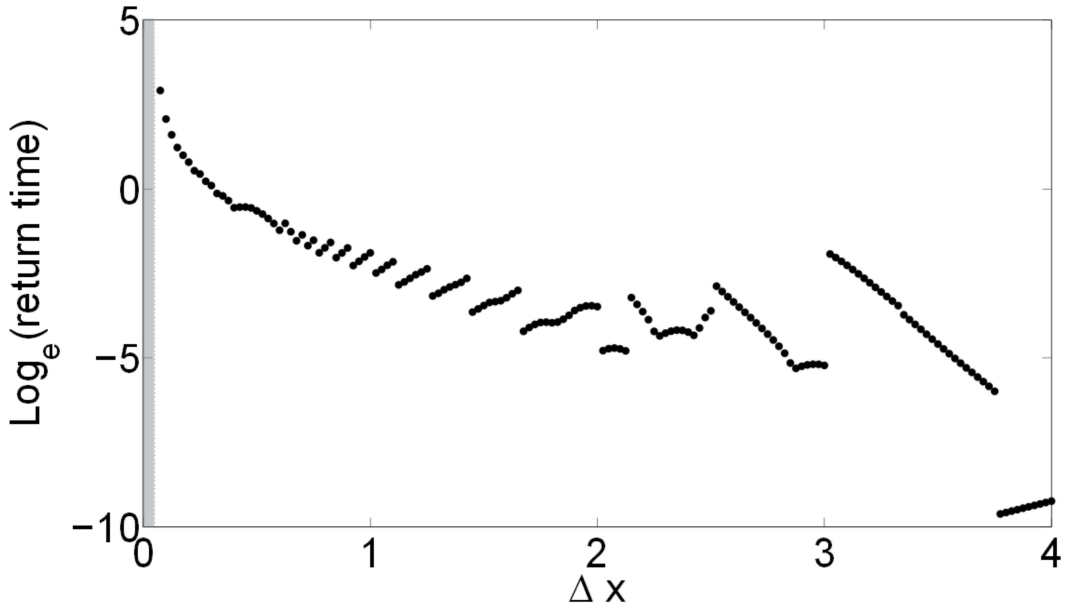

Figure 2.5: The return time to equilibrium decreases as Δx increases. The shaded grey region shows that if Δx crosses a threshold on the fine scale, the steady-state solution crosses from stable to unstable.

As can be seen in Figure 2.5, the return time to equilibrium continues to decrease as Δx increases, but there are jumps in the results. The jumps, where the return time momentarily increases as Δx increases, are due to the numerical discretisation of the McKendrick-von Foerster equation. During these jumps, the log(mass) step-size is increasing yet the number of size-classes is staying the same. This is due to the numerical implementation of the code only allowing a maximum log(mass) of 8. Hence the return time seems to be closely related to the number of size-classes used as well as the coarseness of the discretisation. However, the general trend stated in Section 2.2.3 remains true - as the discretisation becomes more coarse, the return time decreases.

Chapter 3

Development of an end-to-end model: exploring the importance of the structure of the zooplankton link

Abstract

End-to-end models of marine ecosystems couple biogeochemical models of lower-trophic-level organisms, and population dynamic models of higher-trophic-level organisms into a single modelling framework. Models of lower-trophic-level organisms tend to use a functional group approach with minimal size-structure within these groups, whereas models of higher-trophic-level organisms are species-centric with each species' life history described using a finely resolved age- or size-structure. The difference between the "structure" and "resolution" of these coupled models could lead to numerical artefacts being misinterpreted as ecosystem-scale dynamics. Here, we develop a new end-to-end model which couples together a phytoplankton population, zooplankton population and a size-structured fish community. With this minimal framework, we investigate the effect of model architecture upon the interpretation of steady-state results of a marine ecosystem, and in particular, focus on the importance of the dynamics of the zooplankton population. The model shows that large-scale steady-state behaviours of the system (e.g. the size-spectra and associated slopes) are comparable with previous models and empirical observations of marine ecosystems. However, the underlying structure of the model can lead to significant differences in the individual life histories within the fish community and in particular, lead to vastly different growth rates for larval fish under different assumptions of the representation of the lower-trophic-level organisms.

3.1 Introduction

In traditional models of marine ecosystems, the population dynamics of lower trophic level organisms (LTLs), such as phytoplankton and zooplankton, and the higher trophic level organisms (HTLs), such as targeted fish stocks, have been modelled independently of each other (Libralato and Solidoro, 2009; Rose et al., 2010; Travers et al., 2007).

The LTL population dynamics are commonly described using biogeochemical models, which capture the way nutrients are utilised by the biological organisms at this trophic level. The LTLs have been most commonly modelled using box compartments which represent the concentrations of nutrients, phytoplankton and zooplankton (and detritus), with the dynamics within each box defined by ordinary differential equations. This genre of models has become known as NPZD-type models (Franks et al., 1986). In the last two decades, these models have been extended in several ways. One method has been to increase the number of functional types within the modelling framework. The European Regional Seas Ecosystem Model (ERSEM) separates the NPZD components into several functional types: for example, the phytoplankton module is divided into diatom, flagellate, picoplankton, dinoflagellate and coccolithorpe (Baretta, 1995). The other commonly used method has been to impose a simple size-structure on the components of the NPZD model. The NEMURO model increases the complexity of the NPZD model through size-structure: the phytoplankton group is divided into small and large, whilst the zooplankton group is divided into small, large and predatory (Kishi et al., 2007).

Due to the strong dependence of the nutrient component upon climatic factors, hydrodynamic models and biogeochemical models have been coupled together (Franks, 2002; Fasham et al., 1990). ERSEM has been coupled to several different hydrodynamic models, for examle, a 1d General Ocean Turbulence Model (GOTM) (Blackford, 2004) and a three-dimensional baroclinic model known as POLCOMS (Lewis and Allen, 2009), whilst Travers et al. (2009) coupled together the Regional Ocean Modelling System (ROMS) with a size-structured NPZD model, known as $N_2P_2Z_2D_2$ (so named as each model was divided into two size-structured components of large and small).

These LTL models use a 'closure' term to represent the predation of fish on the LTL organisms, by assuming that the dynamics of the fish community is so slow when compared to the dynamics of the LTL organisms that their influence upon these organisms are essentially constant. The choice of 'closure' term can have an important effect upon the dynamics of the LTL model (Steele and Henderson, 1992; Edwards and Yool, 2000).

Models for the population dynamics of HTL organisms have been developed from the per-

spective of fisheries management (Travers et al., 2007), and tend to target commercially important fish stocks, such as cod (Beaugrand and Kirby, 2010), herring (Megrey et al., 2007) and salmon (Shiomoto et al., 1997). These models structure the fish population through some individual-based trait, such as age (Mellin et al., 2009; Kamioka, 2005), stages (de Roos et al., 2008) or size (Datta et al., 2010; Law et al., 2009; Benoît and Rochet, 2004). These HTL models use a 'closure' term to represent the LTL organisms, either through an assumption of a constant 'pool' of plankton (Law et al., 2009; Benoît and Rochet, 2004) or by assuming a 'carrying capacity' parameter (Travers et al., 2007).

Over the last five years, the importance of the relationship between climate, LTL and HTL organisms have become apparent. LTL organisms such as phytoplankton are directly affected by climate variability, by the physical and chemical properties of the ocean. Zooplankton is one of the primary food sources of larval fish and planktivores, and so have a direct impact on HTL population dynamics (Carlotti and Poggiale, 2010; Daewel et al., 2007; Field et al., 2006; Rose et al., 2010). This has led to the development of end-to-end (E2E) models, which couple together submodels of the higher and lower trophic level organisms into one framework (Libralato and Solidoro, 2009; Rose et al., 2010; Travers et al., 2009).

One of the current approaches to studying E2E models is to couple together existing submodels, as demonstrated by Travers et al. (2009), where the ROMS-$N_2P_2Z_2D_2$ was used to model the LTLs and OSMOSE (an individual-based model of size-structured schools of organisms) for the HTLs. Aydin et al. (2005) used the NEMURO model together with Ecopath with Ecosim (EwE) to model the growth rates of Pacific salmon. Libralato and Solidoro (2009) coupled together a Trophic-Diffusive model for the LTLs with EwE to create an E2E model. The main issue when coupling together existing submodels is that each model was developed with a different intention in mind. Models of LTL organisms have been developed to improve our understanding of biogeochemical cycles (Edwards and Yool, 2000), whilst models of HTL organisms have been developed to understand the life histories of fish and support decisions in fisheries management. As these three examples of E2E models have shown, the framework for modelling the LTL organisms differs greatly from that used to model the HTL organisms.

As can be seen from existing E2E models, functional groups which have been coarsely size-structured tend to be used for models of LTLs (Kishi et al., 2007; Travers et al., 2009) whereas a species-based approach is commonly used for models of HTLs. Hence, the "structure" of the coupled models differ significantly. There is also a considerable difference in the "resolutions" used in LTL and HTL models. In general, there are at most 1-3 compartments of zooplankton which can be used as a resource for 35 commercially important fish species (Steele et al., 2007) or 11 size-structured fish populations (Travers et al., 2009). Shin et al. (2010) state that effects such as trophic cascades can be difficult to observe in E2E models

due to the effects cancelling each other out when the LTL compartments are aggregated. The variation in "structure" and "resolution" in the coupled models could lead to numerical artefacts due to model architecture, with these artefacts being mistaken for ecosystem effects.

In this chapter, we study the impact of coupling together models which differ in "structure" and "resolution". Two models will be compared, where the first model, known as the SR-Fish model, will use the size-structured fish community model discussed in Chapter 2, with the assumption of a static resource spectrum representing the LTL organisms. The second model will be the PZ-Fish model, a novel dynamic E2E model which couples together a phytoplankton-zooplankton model (PZ model) (Truscott and Brindley, 1994) to the size-structured fish community discussed in Chapter 2. With these two modelling frameworks, we investigate the plausibility of an E2E model, whose submodels differ significantly in their compositions, and the importance of the zooplankton dynamics within the marine ecosystem. In particular, we explore the effect that the choice of functional response for the zooplankton's grazing rate upon phytoplankton has upon the dynamics of the PZ-Fish model.

3.2 Methods

3.2.1 The SR-Fish Model

The Static Resource-Fish model (SR-Fish) is a size-structured fish community model which assumes a static resource (i.e. plankton) spectrum for small fish to feed upon. The population density of the fish community is modelled using a variant of the McKendrick-von Foerster PDE (MvF PDE) (Benoît and Rochet, 2004; Law et al., 2009; Datta et al., 2010; Datta, 2011), where the density of individuals is a function of body mass and time, and is given by:

$$\frac{\partial u(x,t)}{\partial t} = -\mu(x,t)u(x,t) - \frac{\partial(g_{SR}(x,t)u(x,t))}{\partial x} \tag{3.1}$$

with initial condition $u(x,0) = u^0(x)$ for $x \in [x_{\min}, x_{\max}]$ and boundary conditions

1. $g(0,t)u(0,t) = \kappa \int g_{SR}(x,t)u(x,t)e^{x-x_{\min}}dx$
2. $u(x,t) = 0$ for $x > x_{\max}$

where $u(x,t)$ is the density of individuals of log(mass) x per unit volume, $x_{\min}$ is the minimum log(mass) of the fish community, $x_{\max}$ is the maximum log(mass) of the fish community and the population dynamics are governed by size-dependent mortality and growth rates, $\mu(x,t)$ and $g_{SR}(x,t)$, respectively.

Mortality consists of predation, intrinsic mortality and senescent mortality. Predation is upon smaller organisms, with the strongest preference towards individuals which are a log(predator-prey mass ratio) (log(PPMR)) smaller than themselves. This is determined by a Gaussian feeding kernel, $\phi(x',x) = (1/\sigma\sqrt{2\pi})\exp\{-(x'-x-\beta)^2/2\sigma^2\}$ where β is the log(PPMR) and the width is proportional to σ. An intrinsic mortality rate represents death which is not caused by predation, and is assumed to be a constant rate $\tilde{k}$. To ensure that there is no accumulation of unrealistically large organisms due to the absence of top-class predators in this model, a senescent mortality rate of $\mu_s e^{\rho(x-x_s)}$ is introduced once organisms reach a certain log(mass) x_s, where μ_s is the mortality rate and ρ is the senescent mortality exponent (Law et al., 2009; Benoît and Rochet, 2004).

The size-dependent mortality rate can then be written as

$$\mu(x,t) = \tilde{k} + \mu_s e^{\rho(x-x_s)} + \gamma w_0^q \int e^{x'q}\phi(x',x)u(x',t)dx' \tag{3.2}$$

where γ is the volume search rate (with units g^{-q} year^{-1} m^3), q is the volume search exponent (as the rate at which a predator searches its environment for prey scales with body size) (Benoît and Rochet, 2004; Law et al., 2009) and w_0 is the reference weight derived from the co-ordinate transform $w = w_0 e^x$ where w is the body mass in g of the individual.

Growth is through the assimilation of mass gained by consumption. It is assumed that upon ingestion, a fraction of that energy gained (κ) is used for reproduction and the rest of the energy is used for somatic growth ($1-\kappa$). The size-dependent growth rate can be written as

$$\begin{aligned} g_{SR}(x,t) &= (1-\kappa)\alpha\gamma w_0^q e^{x(q-1)} B_{SR}(x) \\ &\text{where} \\ B_{SR}(x) &= \int e^{x'}\phi(x,x')u(x',t)dx' \end{aligned} \tag{3.3}$$

The reproduction term to the larval fish class can then be written as

$$R_{SR} = \kappa\alpha\gamma \int e^{x'(q-1)} B_{SR}(x') e^{x'-x_{\min}} u(x',t) dx' \tag{3.4}$$

where $x_{\min}$ is the size-class denoting the larval fish (see Section 3.2.4 for more details).

A static resource spectrum is assumed within this model to provide food for the small size-classes of fish, and has a range in body mass of $[w_{SR,min}, w_{SR,max}]$. The size-classes of this static resource spectrum are distributed according to a power law $p_1 w_{SR}^{\lambda_P}$ (Law et al., 2009), where p_1 is the abundance of phytoplankton of mass $w_{SR,min}$, w_{SR} is the mass of the phytoplankton and λ_P is the exponent of the resource spectrum.

3.2.2 The PZ-Fish Model

We develop a new dynamic end-to-end model, henceforth known as the Phytoplankton Zooplankton-Fish (PZ-Fish) model, which represents the lower trophic level organisms as two populations of phytoplankton (P, density of individuals of log(mass) x_P per m^{-3}) and zooplankton (Z, density of individuals of log(mass) x_Z per m^{-3}), while the dynamics of the size-structured fish community are modelled as described in Section 3.2.1. Within this model, the phytoplankton population density grows logistically in the absence of predators with a maximum growth rate of r_P and a carrying capacity of $P_{\max}$, is preyed upon by Z at some grazing rate $f(P)$ and is also preyed upon by fish at a rate of $A_P(u)$. Z grows according to its consumption of P at a rate $\alpha_Z f(P)$, dies at some intrinsic mortality rate μ_Z and is preyed upon by fish at a rate of $A_Z(u)$.

To account for the predation of fish on the phytoplankton populations, it is assumed that fish which are a PPMR bigger than the phytoplankton have the strongest feeding preference upon them. This feeding preference is determined using the Gaussian function described in Section 3.2.1. In other words, if phytoplankton has a log(mass) of x_P, then $\phi_P(x) = 1/(\sigma\sqrt{2\pi})\exp\{-(x - x_P - \beta)^2/2\sigma^2\}$ is the function representing the feeding preference of the fish community for phytoplankton. β and σ have been kept identical to the values chosen for the SR-Fish model to allow for comparison between these models, i.e. we are assuming that the phytoplankton class is identical to the size-class of the static-resource spectrum with body mass $9.12 \times 10^{-7} g$. An alternative assumption would be to assume that the feeding kernel of the fish upon the phytoplankton is distributed over a wider range of size-classes, but this chapter is aiming to investigate the challenges involved when fish feed upon one phytoplankton class, and one zooplankton class. The feeding kernel for fish feeding on zooplankton can be determined in the same way, assuming that zooplankton has a log(mass)

of x_Z.

Figure 3.1 displays $\phi_P(x)$ and $\phi_Z(x)$, and shows that the fish community does not have a strong feeding preference for phytoplankton, and that the fish of about mass 0.005g has the strongest preference for feeding on zooplankton. Fish which are bigger than 1g have grown beyond the body size in which they have a preference for feeding on zooplankton; at this point, they begin feeding upon small, larval fish.

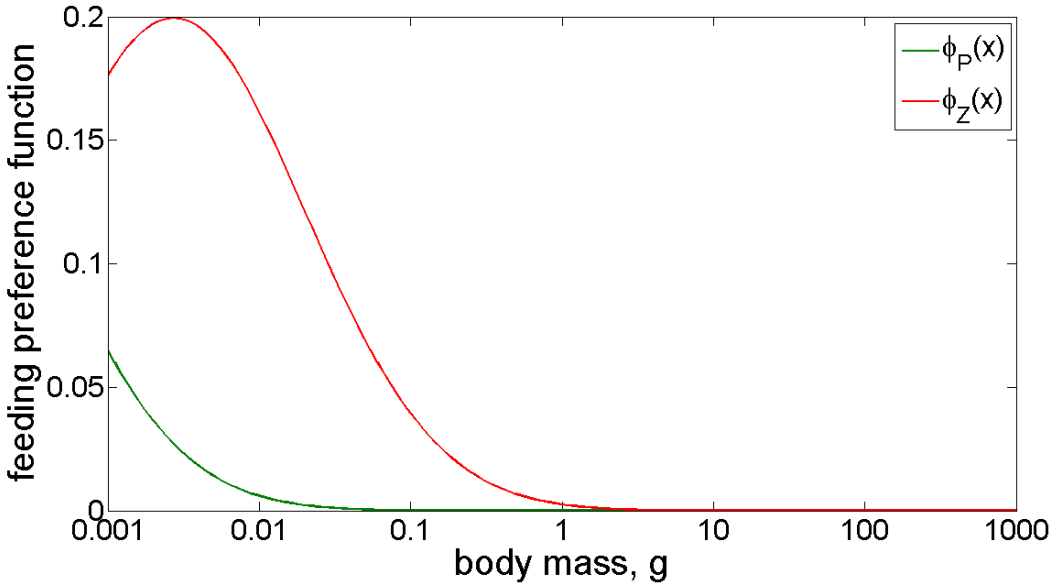

Figure 3.1: The feeding kernel functions representing the fish community feeding on phytoplankton ($\phi_P(x)$, the solid green line) and zooplankton ($\phi_Z(x)$, the solid red line) where $w_P = 9.12 \times 10^{-7}$g and $w_Z = 4.98 \times 10^{-5}$g.

The predation of fish upon phytoplankton ($A_P(u)$) and zooplankton ($A_Z(u)$) can be written as

$$A_P(u) = \gamma w_0^q \int e^{x'q} \phi_P(x') u(x',t) dx' \tag{3.5}$$

$$A_Z(u) = \gamma w_0^q \int e^{x'q} \phi_Z(x') u(x',t) dx' \tag{3.6}$$

The PZ-Fish model can be summarised as

$$\frac{dP}{dt} = r_P P\left(1 - \frac{P}{P_{\max}}\right) - f(P)Z - A_P(u)P \tag{3.7}$$

$$\frac{dZ}{dt} = \alpha_Z f(P)Z - \mu_Z Z - A_Z(u)Z$$

$$\frac{\partial u(x,t)}{\partial t} = -\mu(x,t)u(x,t) - \frac{\partial(g_{PZ}(x,t)u(x,t))}{\partial x} \tag{3.8}$$

where

$$g_{PZ}(x,t) = (1-\kappa)\alpha\gamma w_0^q e^{x(q-1)} B_{PZ}(x)$$

where

$$B_{PZ}(x) = \int e^{x'}\phi(x,x')u(x',t)dx' + \int e^{x_P}\phi_P(x)P(x_P)dx_P + \int e^{x_Z}\phi_Z(x)Z(x_Z)dx_Z$$

and

$$R_{PZ} = \kappa\alpha\gamma \int e^{x'(q-1)} B_{PZ}(x') e^{x'-x_{\min}} u(x',t)dx' \tag{3.9}$$

where g_{PZ} is the size-dependent growth rate and R_{PZ} is the reproductive rate for the fish community in the PZ-Fish model. The growth of individual fish in the size-structured community now accounts for consumption upon dynamic populations of phytoplankton and zooplankton. The reproductive rate also accounts for the consumption of phytoplankton and zooplankton in the same way.

See Table 3.2 for a definition of all the parameters used in this model and in the SR-Fish model.

3.2.3 Functional responses

The representation of the zooplankton's grazing rate upon the phytoplankton population (i.e. the formulation of the functional response) can have a profound influence on the dynamics of planktonic models, leading to oscillating or constant population densities (Gentleman and Neuheimer, 2008). Most expressions of functional responses have a satiating response to increasing prey availability as well as grazing thresholds and varying degrees of nonlinearity (Franks, 2002). The most common functional responses are characterised by Holling Type (Holling, 1959). Type I responses increase linearly with food:

$$f(P) = r_Z P$$

where r_Z is the zooplankton's maximum grazing rate. Type II responses assume that the consumer is limited by its capacity to process food, and thus satiates when there are high densities of prey available:

$$f(P) = \frac{r_Z P}{C_{II} + P}$$

where C_{II} is the half-saturation coefficient. Finally, Type III responses have a sigmoidal form: at low prey densities, the grazing rate accelerates and then decelerates as it approaches satiation. It can be written as:

$$f(P) = \frac{r_Z P^2}{C_{III}^2 + P^2}$$

where C_{III} is a parameter describing the nonlinearity in the zooplankton's feeding response to prey abundance.

In this chapter, we investigate the effect that the choice of functional response has upon a dynamic end-to-end model. The PZ-Fish model represents the effect of fish predation on phytoplankton and zooplankton through a dynamic, linear response. When the PZ-Fish model is at equilibrium (or steady-state), i.e. the populations of phytoplankton, zooplankton and fish remain constant over time, then the values of $A_P(u)$ and $A_Z(u)$ are constant and the steady-state solutions of the PZ submodel can be studied. Let $A_P(u) = A_P$ and $A_Z(u) = A_Z$ when the PZ-Fish model is at equilibrium.

Table 3.1 shows the analytical steady-state solutions and the associated Jacobian matrix (the matrix of first-order partial derivatives of the system) for the PZ submodel. For each functional response, there are three possible steady-state solutions: (0,0), (P^*,0) and (P^*, Z^*). The stability of those steady-states (the ability of the populations to return to the steady-state solution under small perturbations) can be determined by studying the associated Jacobian matrix. The Routh-Hurwitz stability criterion can be applied to determine the stability of the steady-state, where the solution is stable if the trace of the Jacobian matrix is negative

and the determinant of the Jacobian matrix is positive. However, even with a simple 2×2 matrix, the derivation for the conditions required for stability can be complex and difficult to analyse, in which case, stability can be determined by direct calculation of the Jacobian's eigenvalues.

3.2.4 Numerical methods

Numerical methods are necessary to study the dynamics of the SR-Fish and PZ-Fish models. This requires a discretisation method to be chosen, where the domain space is partitioned into a mesh and used to approximate the differential equations (Lax, 1965; Press et al., 2007) (see Chapter 2 for a thorough investigation into the effect of discretisation upon size-structured models). The boundary conditions for the discretised SR-Fish and PZ-Fish models are

$$\begin{aligned}
\frac{du(x_{\min},t)}{dt} &= -\mu(x_{\min},t)u(x_{\min},t) - \frac{g(x_{\min},t)u(x_{\min},t)}{\Delta x} + \frac{g(0,t)u(0,t)}{\Delta x} \\
&= -\mu(x_{\min},t)u(x_{\min},t) - \frac{g(x_{\min},t)u(x_{\min},t)}{\partial x} + \frac{R}{\Delta x} \\
\frac{du(x_{\max},t)}{dt} &= -(\tilde{k}+\mu_s e^{\rho(x-x_s)})u(x_{\max},t) - \frac{g(x_{\max},t)u(x_{\max},t)}{\Delta x} + \frac{g(x_{\max-1},t)u(x_{\max-1},t)}{\Delta x}
\end{aligned}$$

where g_{SR} or g_{PZ} is used for the size-dependent growth rate $g(x,t)$ and R_{SR} or R_{PZ} is used for the reproductive rate R, depending on whether the SR-Fish or PZ-Fish model is being studied.

Parameters

The parameter values used within the numerical simulations, as well as their full definitions and units, for the SR-Fish and PZ-Fish models can be found in Table 3.2. The size-structured fish community model uses parameter values from Law et al. (2009)[Table 1]. The only exception is the fraction of consumed biomass which is allocated to reproduction, κ. A value of 0.75 was chosen to ensure co-existence of the full phytoplankton-zooplankton-fish community. An empirical value for this parameter cannot be found, as the model aggregates species into a single community of fish. Therefore, the parameters for explicit life histories of the constituent species cannot be used within this modelling framework.

The P growth rate, r_P, and the Z mass conversion efficiency, α_Z, parameter values were taken from Truscott and Brindley (1994). The Z Holling Type II half-saturation coefficient

Table 3.1: Table showing the steady-state solutions and the associated Jacobian matrix for that solution

Functional Response	Steady state	Jacobian
Holling Type I	$(0,0)$	$\begin{pmatrix} r_P - A_P & 0 \\ 0 & -\mu_Z - A_Z \end{pmatrix}$
	$\left(\frac{(r_P - A_P)P_{\max}}{r_P}, 0\right)$	$\begin{pmatrix} -r_P + A_P & \frac{-r_Z(r_P - A_P)P_{\max}}{r_P} \\ 0 & \frac{\alpha_Z r_Z (r_P - A_P)P_{\max}}{r_Z} - \mu_Z - A_Z \end{pmatrix}$
	$\left(\frac{\mu_Z + A_Z}{\alpha_Z r_Z}, \frac{1}{r_Z}\left[r_P(1 - \frac{P^*}{P_{\max}}) - A_P\right]\right)$	$\begin{pmatrix} r_P - \frac{2r_P P^*}{P_{\max}} - r_Z Z^* - A_P & -r_Z P^* \\ \alpha_Z r_Z Z^* & 0 \end{pmatrix}$
Holling Type II	$(0,0)$	$\begin{pmatrix} r_P - A_P & 0 \\ 0 & -\mu_z - A_Z \end{pmatrix}$
	$\left(\frac{(r_P - A_P)P_{\max}}{r_P}, 0\right)$	$\begin{pmatrix} -r_P + A_P & \frac{r_Z(r_P - A_P)P_{\max}}{r_P C_{II} + (r_P - A_P)P_{\max}} \\ 0 & \frac{\alpha_Z r_Z (r_P - A_P)P_{\max}}{r_P C_{II} + (r_P - A_P)P_{\max}} - \mu_Z - A_Z \end{pmatrix}$
	$\left(\frac{(\mu_Z + A_Z)C_{II}}{\alpha_Z r_Z - \mu_Z - A_Z}, \frac{1}{r_Z}\left[r_P(1 - \frac{P^*}{P_{\max}}) - A_P\right][C_{II} + P^*]\right)$	$\begin{pmatrix} r_P - \frac{2r_P P^*}{P_{\max}} - \frac{r_Z C_{II} Z^*}{(C_{II} + P^*)^2} - A_P & \frac{-r_Z P^*}{C_{II} + P^*} \\ \frac{\alpha_Z r_Z C_{II} P^*}{(C_{II} + P^*)^2} & 0 \end{pmatrix}$
Holling Type III	$(0,0)$	$\begin{pmatrix} r_P - A_P & 0 \\ 0 & -\mu_Z - A_Z \end{pmatrix}$
	$\left(\frac{(r_P - A_P)P_{\max}}{r_P}, 0\right)$	$\begin{pmatrix} -r_P + A_P & \frac{-r_Z P^{*2}}{C_{III}^2 + P^{*2}} \\ 0 & \frac{\alpha_Z r_Z (r_P - A_P)^2 P_{\max}^2}{r_P^2 C_{III}^2 + (r_P - A_P)^2 P_{\max}^2} - \mu_Z - A_Z \end{pmatrix}$
	$\left(\frac{(\mu_Z + A_Z)C_{III}^2}{\alpha_Z r_Z - \mu_Z - A_Z}, \frac{1}{r_Z P^*}\left[r_P(1 - \frac{P^*}{P_{\max}}) - A_P\right][C_{III}^2 + P^{*2}]\right)$	$\begin{pmatrix} r_P - \frac{2r_P P^*}{P_{\max}} - \frac{2r_Z C_{III}^2 P^* Z^*}{(C_{III}^2 + P^{*2})^2} - g_P & \frac{r_Z P^{*2}}{C_{III}^2 + P^{*2}} \\ \frac{2\alpha_Z r_Z C_{III}^2 P^* Z^*}{(C_{III}^2 + P^{*2})^2} & \frac{\alpha_Z r_Z P^{*2}}{C_{III}^2 + P^{*2}} - \mu_Z - g_Z \end{pmatrix}$

Note: for the non-trivial steady-state solutions (P^*, Z^*), the zooplankton's steady-state is written as a function of the phytoplankton's steady-state, i.e. $Z^* = F(P^*)$.

value ranges between 9.22×10^3 and 4.45×10^5 m^{-3} (Fasham et al., 1990; Stock et al., 2008), and a value of 9.22×10^3 m^3 chosen for this study. The Z Holling Type III switching parameter was converted from the value used in Edwards and Brindley (1999). The value of P carrying capacity, $P_{\max}$, was chosen to be 2.2×10^5 m^{-3}. The Z grazing rate, r_Z, was varied, depending on the choice of functional response (see Section 3.2.3): 2.74×10^5 $year^{-1}$ for Type I, 365 $year^{-1}$ for Type II (Fasham et al., 1990; Stock et al., 2008) and 548 $year^{-1}$ for Type III (Edwards and Brindley, 1999). The Z intrinsic mortality rate, μ_Z, was assumed to be 0.1 $year^{-1}$ as this is the intrinsic mortality rate assumed for the fish community.

The slope of the static-resource spectrum λ_P, was determined by using the stable steady-state solutions for the PZ-Fish model (for each of the Holling Type functional responses), and using trial and error to find a value for the slope of the static-resource spectrum, which yielded a steady-state solution for the SR-Fish model which was comparable to those of the PZ-Fish model.

Table 3.2: Parameter definitions for the SR-Fish and PZ-Fish models.

Parameter	Description	Unit	Parameter Value
Static resource spectrum			
$w_{SR,min}$	minimum body mass of the resource spectrum	g	9.12×10^{-7}
$w_{SR,max}$	maximum body mass of the resource spectrum	g	2.72×10^{-3}
p_1	abundance of phytoplankton of mass $w_{SR,min}$	m^{-3}	1.45×10^2
λ_p	exponent of the resource spectrum	-	-0.13
PZ sub-model			
r_P	P growth rate[a]	$year^{-1}$	109.5
$P_{\max}$	P carrying capacity	m^{-3}	2.2×10^5
r_Z	Z grazing rate	$year^{-1}$	various (see Figure 3.4)
C_{II}	Z Holling type II half-saturation constant[b]	m^{-3}	9.2×10^3
C_{III}	Z Holling type III switching parameter[c]	m^{-3}	5.2×10^3
α_Z	Z mass conversion efficiency[a]	-	0.05
μ_Z	Z intrinsic mortality rate	$year^{-1}$	0.1
ϕ_P	predation kernel on P	-	
ϕ_Z	predation kernel on Z	-	
w_P	P mass	g	9.12×10^{-7}
w_Z	Z mass	g	4.98×10^{-5}

Table 3.2: Parameter definitions for the SR-Fish and PZ-Fish models.

Parameter	Description	Unit	Parameter Value
Fish sub-model			
$w_{\min}$	minimum body mass	g	1×10^{-3}
$w_{\max}$	maximum body mass	g	3.3×10^{3}
w_0	reference weight, $w = w_0 e^x$	g	4.54×10^{-8}
Feeding terms			
γ	volume searched per unit time per unit mass$^{q\ d}$	$m^3\ year^{-1}\ g^{-q}$	600
q	search volume exponent^d	-	0.8
α	mass conversion efficiency^d	-	0.2
ϕ	feeding-kernel function	-	
β	log(preferred predator:prey mass ratio^d	-	4
σ	feeding-kernel width^d	-	2
κ	fraction of ingested energy allocated to reproduction	-	0.75
Mortality terms			
$\tilde{k}$	intrinsic mortality rate^d	$year^{-1}$	0.1
μ_s	senescent mortality rate^d	$year^{-1}$	0.5
ρ	senescent mortality exponent^d	-	1.5
x_s	size-class at which senescent mortality is introduced^d	-	log(60)

[a] Truscott and Brindley (1994)

[b] Murray (2001)

[c] Edwards and Brindley (1999)

[d] Law et al. (2009)

3.3 Results

In this section, the dynamic PZ-Fish model is compared to the SR-Fish model, and they are measured against each other in various ways. Firstly, we investigate the effect that the choice of functional response for the zooplankton's grazing upon phytoplankton has upon the stability of the PZ-Fish model. We then compare the PZ-Fish model against the SR-Fish model, for each functional response, and use the following measures:

1. Total biomass in the fish community
2. The slope of the size-spectrum
3. Stability of the steady-state solution
4. Growth of a cohort of fish over five years

Note that the slope of the size-spectrum, and the associated R^2, is calculated using Matlab's *polyfit* function, which uses a least squares method to fit the coefficients to a linear polynomial. These measures were chosen in order to see if the dynamic PZ-Fish model can give comparable results to the well-studied SR-Fish model.

3.3.1 Stability due to the choice of functional response

In this section, we study the stability of the (P^*, Z^*) steady-state solutions for each Holling Type functional response, under different predation pressures by the fish community (i.e. (A_P, A_Z)-parameter space). We only study the non-trivial steady-state solution here, as we are interested in a marine ecosystem which allows for co-existence of all the species within it. Figure 3.2 shows the regions where the (P^*, Z^*) steady-state solution is non-negative, the stability of the solution and also marks the predation pressure that a size-structured fish community would exert upon the phytoplankton and zooplankton populations.

The PZ submodel is a 2×2 system, and the associated Jacobian matrix can be used to determine the two associated eigenvalues at the steady-state. These eigenvalues can be used to determine the stability of the steady-state solutions. Eigenvalues are generally complex numbers, but the real part of the eigenvalue can be used to determine stability of the steady-state. If both real parts of the eigenvalue are negative, then the steady-state is stable (i.e. the system returns to the steady-state solution after a small perturbation). If either of the real

parts of the eigenvalue are positive, then the steady-state is unstable (i.e. the system does not return to the steady-state solution after a small perturbation).

Figure 3.2 shows the stability of the (P^*, Z^*) steady-state solution when a Holling Type I, II or III functional response is assumed. The marker indicates the predation pressures exerted upon the phytoplankton and zooplankton populations by a size-structured fish community.

Figure 3.2a shows that when a Holling Type I functional response is used in the PZ-submodel, then the (P^*, Z^*) steady-solution is stable if it is non-negative. Otherwise, the extinction of P and Z is the stable solution to the system. When comparing the Holling Type I functional response to the Type II and Type III responses, the Holling Type I remains stable under much more intensive predation pressures from the fish community - only when the predation pressure of the fish upon the phytoplankton population (A_P) exceeds the phytoplankton growth rate (r_P), do the phytoplankton and zooplankton populations crash and become extinct. This is the case for each Holling Type functional response, however, the existence and stability of the steady-state solutions are more sensitive to the predation pressure of the fish upon the zooplankton community (A_Z) for Holling Type II and III functional responses.

The existence of the (P^*, Z^*) steady-state solution when a Holling Type II functional response is assumed, is highly dependent on the predation of fish on the zooplankton population (see Figure 3.2b). When $A_Z > 18$ year^{-1}, then the zooplankton population has been grazed to extinction. When $(P^*, Z^*) > 0$, it is most commonly an unstable solution, and the phytoplankton and zooplankton populations oscillate over time (see Figure 3.3a). As can be seen in Figure 3.2b, there is only a small region of (A_P, A_Z)-parameter space in which the (P^*, Z^*) steady-state solution is stable.

When a Holling Type III functional response is assumed, the (P^*, Z^*) steady-state solution is non-negative under higher predation pressures than when a Type II functional response is assumed, with $A_Z > 28$ year^{-1} before the zooplankton is grazed to extinction (see Figure 3.2c). There is also a much larger region of (A_P, A_Z)-parameter space in which the steady-state solution is stable, compared to when a Type II functional response is assumed. The marker in Figure 3.2c also shows that when a size-structured fish community is assumed to be feeding on the phytoplankton and zooplankton populations, the predation pressures exerted upon the lower trophic level organisms means that the (P^*, Z^*) steady-state solution is on the cusp of stability, and it would only require a small change in the predation pressures to lead to an unstable solution. Thus, in an end-to-end model where the PZ model is coupled to a size-structured fish community, a Type III functional response could lead to the system being easily destabilised under environmental influences, such as fishing.

(a)

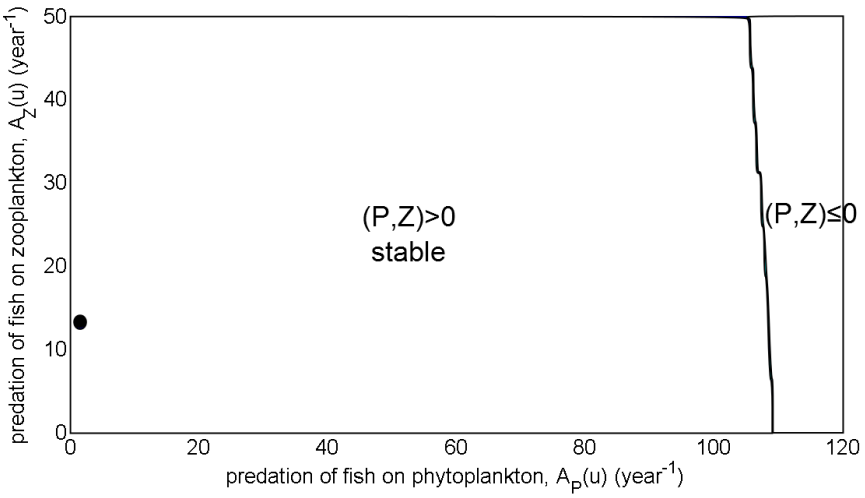

(b)

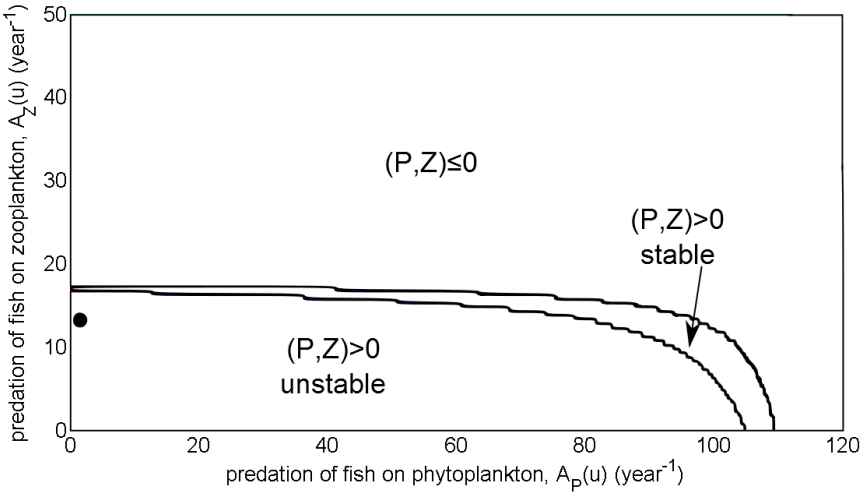

(c)

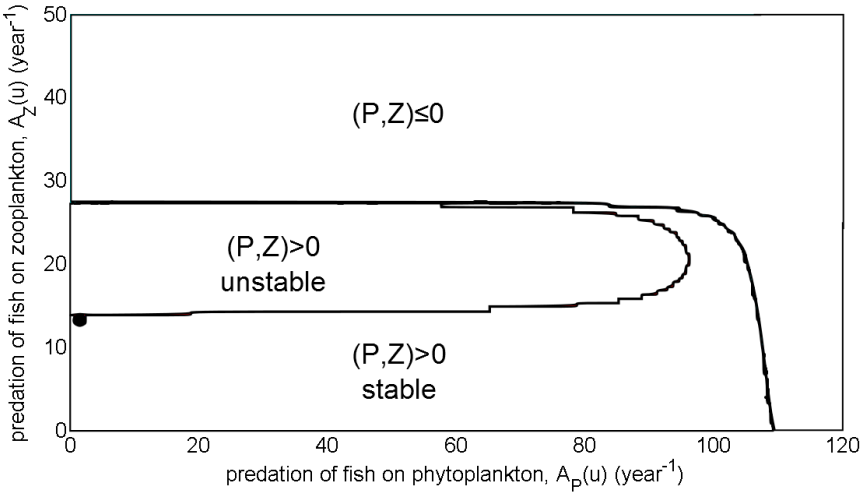

Figure 3.2: The stability of the (P^*, Z^*) steady-state solutions for the three functional responses used to represent the zooplankton's grazing on the phytoplankton. The marker represents the predation pressures of a size-structured fish community upon the phytoplankton and zooplankton populations (determined using the steady-state solution of the SR-Fish model and calculating Eq.(3.6) at this steady-state). The functional responses used are (a) Holling Type I (b) Holling Type II and (c) Holling Type III.

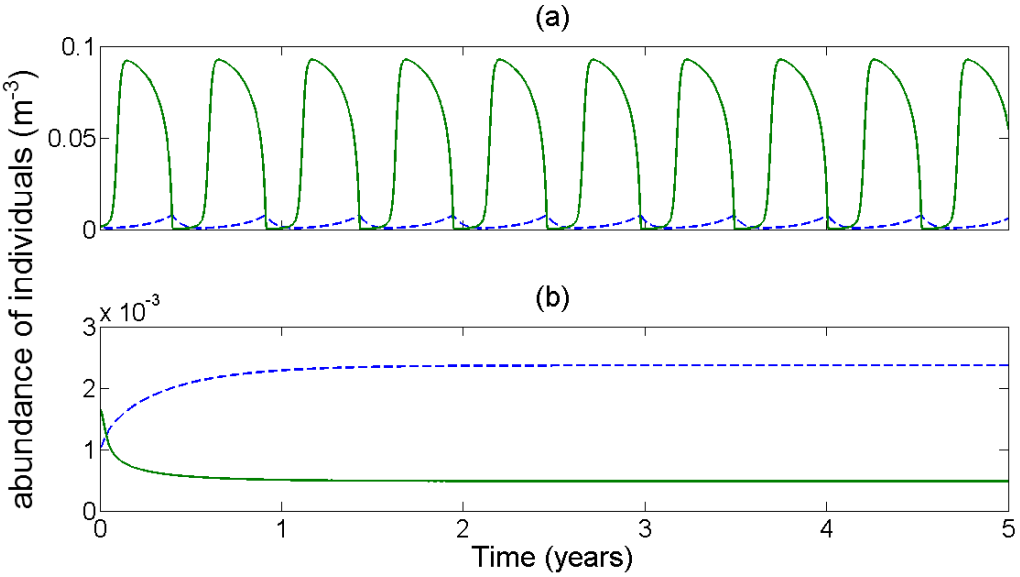

Figure 3.3: An illustration of the dynamic behaviours of the (P^*, Z^*) steady-state solution, which are either (a) unstable, where the phytoplankton and zooplankton populations oscillate over time or (b) stable. In this example, a Holling Type III functional response is assumed, but similar behaviour occurs under a Type II response.

3.3.2 Comparing the steady-state solutions

In this section, we compare the SR-Fish model against the PZ-Fish model (with the three different functional responses), and analyse the steady-state solutions of the entire marine ecosystem. We investigate whether a dynamic PZ-Fish model can yield comparable results to the previously well-studied SR-Fish model, and so whether it is a valid framework for an end-to-end model.

The steady-state solutions

Figure 3.4 compares the steady-state solutions of the SR-Fish model against those of the PZ-Fish model, for each functional response. The static resource spectrum of the SR-Fish model was chosen to ensure that the abundance of the size-structured fish community was similar to that obtained when using the dynamic PZ-Fish model. As can be seen, when the static resource spectrum is amalgamated into two boxes of phytoplankton and zooplankton, the density of these boxes are larger than that of the static resource spectrum. When a Holling Type II functional response is used within the PZ-Fish model, the density of the steady-state solution is much larger than those obtained when using a Holling Type I or III response. See Appendix 3.5.1 for an analysis using phase-planes to understand the differences between the steady-state solutions.

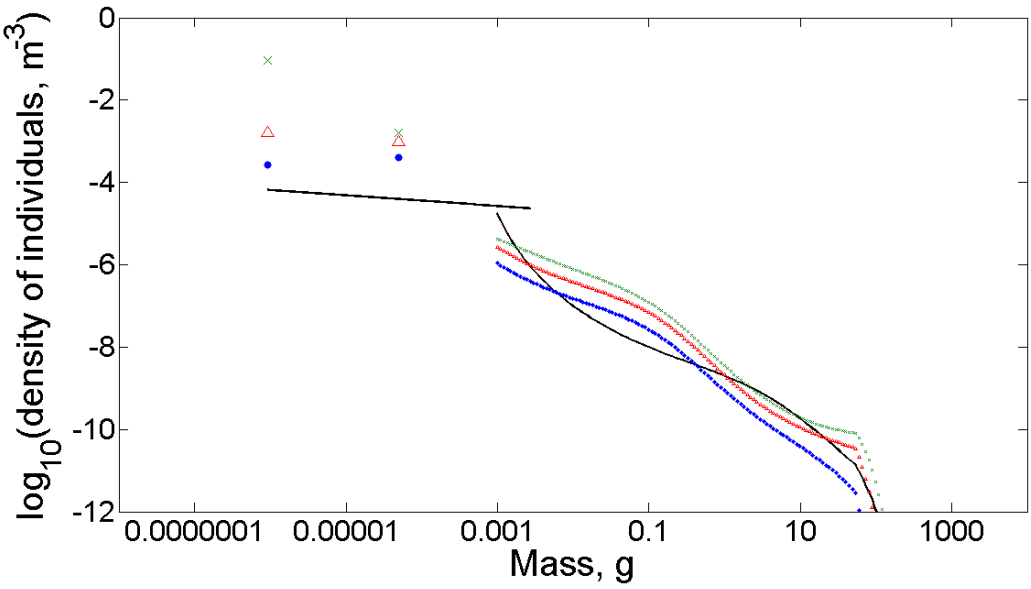

Figure 3.4: The steady-state size-spectra for the SR-Fish model (black, solid line), the PZ-Fish model with Type I response (blue $-\bullet-$), the PZ-Fish model with Type II response (green $-\times-$) and the PZ-Fish model with Type III response (red $-\triangle-$). The zooplankton grazing rate, r_Z, varies for each functional response, with $r_Z = 2.74 \times 10^5$ year^{-1} for a Type I response, $r_Z = 365$ year^{-1} for a Type II response and $r_Z = 548$ year^{-1} for a Type III response.

The biomass of the marine ecosystem

Figure 3.5 compares the total biomass of the steady-state solutions, where the green shaded areas are the biomasses obtained from the lower trophic level organisms (either the static resource spectrum or the P and Z components) and the biomasses obtained from the fish community are shaded in black. As can be seen, when a Type II functional response is assumed within the PZ-Fish model, under these parameters, the biomass within the marine ecosystem is greater than the other model choices. This is due to the large proportion of biomass obtained from the phytoplankton population, which is almost at its carrying capacity. The Type III functional response also has a larger proportion of its biomass obtained from the phytoplankton and zooplankton populations than under a Type I or static-resource spectrum assumption.

If analysing the biomass obtained from the fish community only, apart from the Type II model choice, the PZ-Fish model yields a comparable amount of biomass to the SR-Fish model.

Slope of the size-spectrum

Empirical size-spectra tend to exhibit a slope with a gradient close to -1 (Quinones, 2003). Figure 3.6 shows that the SR-Fish model has a gradient at about -1.05. The PZ-Fish model

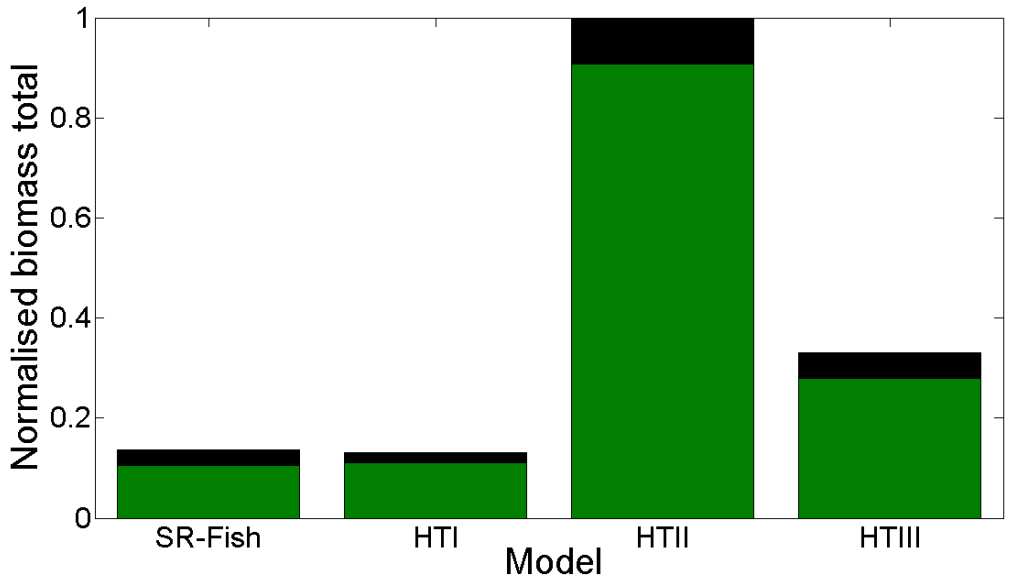

Figure 3.5: The biomass of the marine ecosystem, with the lower trophic level organisms (either a static resource or the P and Z components) represented by the green bar and the size-structured fish community represented by the black bar. The mode types are the SR-Fish model and the PZ-Fish model with either a Holling Type I, II or III functional response assumed. The zooplankton grazing rate, r_Z, varies for each functional response, with $r_Z = 2.74 \times 10^5$ year^{-1} for a Type I response, $r_Z = 365$ year^{-1} for a Type II response and $r_Z = 548$ year^{-1} for a Type III response.

has a more negative slope than the SR-Fish model, regardless of the choice of functional response, with gradients between -1.2 and -1.1. However, the difference is not of a great magnitude, and the PZ-Fish model yields size-spectra which are comparable to empirical size-spectra.

Stability of the marine ecosystem

The stability of the SR-Fish and PZ-Fish models are studied by using Matlab's *fsolve* function to determine the Jacobian matrix of the E2E models at steady-state. From the Jacobian matrix, the associated eigenvalues (and thus the stability) of the E2E models can be determined. If all of the real parts of the eigenvalues are negative, then the E2E model is stable and if any of the real parts of the eigenvalues are positive, then the E2E model is unstable. Whilst each of the models are stable, Figure 3.7 shows that the largest eigenvalues of the PZ-Fish model are less negative than the SR-Fish model, i.e. the PZ-Fish model has steady-state solutions which are "less stable" than the SR-Fish model. This means that when the system is perturbed slightly, the PZ-Fish system takes longer to return to steady-state than the SR-Fish model, which could have implications when considering potential scenarios such as climate change and fishing strategies.

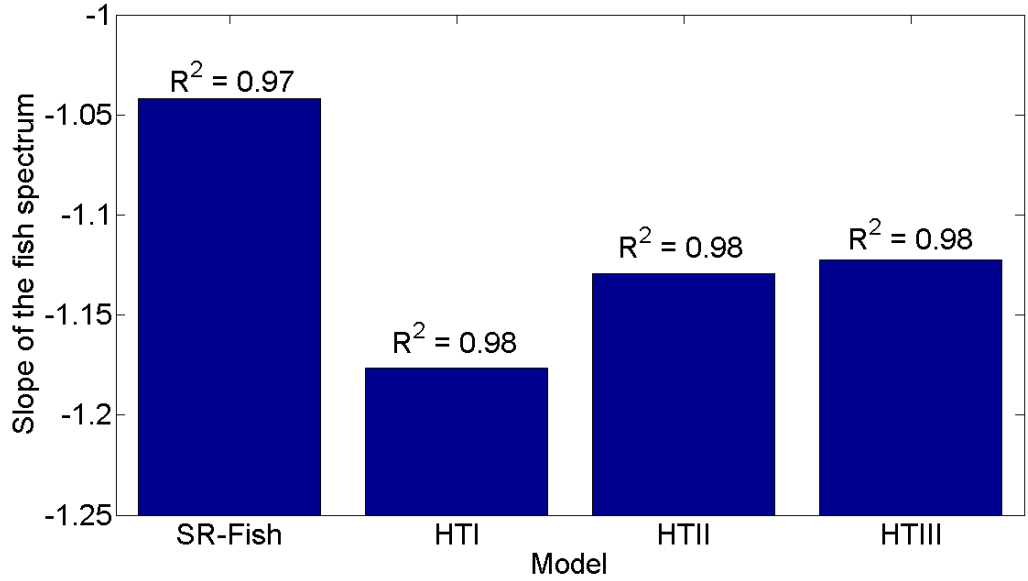

Figure 3.6: The slope of the size-spectrum for the fish community for each model type, i.e. the SR-Fish model or the PZ-Fish model with either a Holling Type I, II or III functional response assumed. The zooplankton grazing rate, r_Z, varies for each functional response, with $r_Z = 2.74 \times 10^5$ year^{-1} for a Type I response, $r_Z = 365$ year^{-1} for a Type II response and $r_Z = 548$ year^{-1} for a Type III response.

The difference in stability between the PZ-Fish and SR-Fish models are likely due to model architecture. In the SR-Fish model, the static resource spectrum has no dynamics within it, whereas the PZ-Fish model must account for two dynamic populations of phytoplankton and zooplankton. Thus, the added complexity within the PZ-Fish model is likely to affect the stability of the ecosystem, and make it more susceptible to environmental changes.

Growth of a larval fish

The growth of a cohort of fish can be determined by the solution of $dx/dt = g(x,t)$, where $g(x,t)$ comes from Equation 3.3 for the SR-Fish model or Equation 3.9 for the PZ-Fish model (Law et al., 2009). Figure 3.8 shows the growth of a cohort fish over five years for each model. A cohort from the SR-Fish model grows from 0.001g to about 5g over five years. However, a cohort from the PZ-Fish model does not grow as fast as in the SR-Fish model: when a Holling Type II functional response is assumed, the larval fish only grows to 0.1g over five years.

The growth of the cohort of fish within the PZ-Fish model is the fundamental way in which the PZ-Fish model differs from the SR-Fish model. The growth of a fish is dependent on the prey it consumes, whether that is a spectrum of resources or two boxes of phytoplankton and zooplankton. In the SR-Fish model, the larval fish has a high density of prey on which it can feed upon - it can feed on resources from $< 1 \times 10^{-5}$g to 0.001g. As the SR-Fish

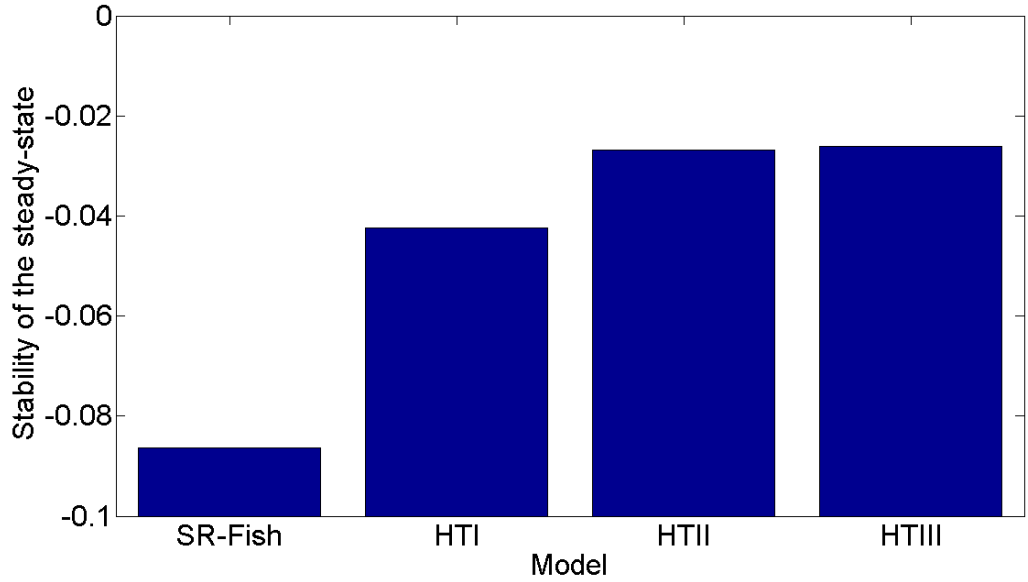

Figure 3.7: The stability of the marine ecosystem for each model type, i.e. the SR-Fish model or the PZ-Fish model with either a Holling Type I, II or III functional response assumed. The zooplankton grazing rate, r_Z, varies for each functional response, with $r_Z = 2.74 \times 10^5$ year^{-1} for a Type I response, $r_Z = 365$ year^{-1} for a Type II response and $r_Z = 548$ year^{-1} for a Type III response.

model assumes a spectrum of resources, the larval fish have much more prey available to it than under the PZ-Fish model assumption. In the PZ-Fish model, the larval fish have only two boxes of phytoplankton and zooplankton to feed upon. Thus, the larval fish within the PZ-Fish model have a limited supply of prey available to them, and cannot grow as quickly or as large as the fish within the SR-Fish model.

3.4 Discussion

The most common method for developing end-to-end models of marine ecosystems is to couple together existing submodels of higher and lower trophic level organisms into one framework. The difference between the "structure" and "resolution" of these modelling frameworks can have a significant impact upon the dynamics of an end-to-end model, and could lead to the misinterpretation of ecosystem-scale effects which are due to model architecture, rather than being a consequence of biological processes. In this modelling study, we develop an E2E model with one phytoplankton population, one zooplankton population and a size-structured fish community and show that the differences in submodel structure can lead to steady-state solutions of the marine ecosystem which appear plausible, but which have underlying faults which need more consideration. In particular, we highlight the importance of the zooplankton link when coupling together end-to-end models.

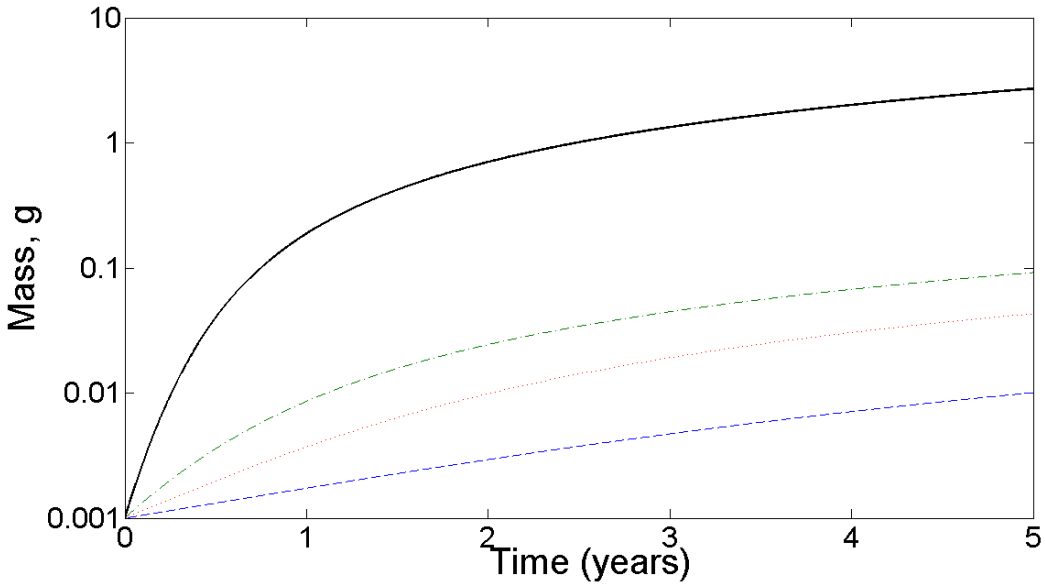

Figure 3.8: The growth of a cohort of fish over five years for the SR-Fish model (black, solid line), the PZ-Fish model with Type I response (blue $-\bullet-$), the PZ-Fish model with Type II response (green $-\times-$) and the PZ-Fish model with Type III response (red $-\triangle-$). The zooplankton grazing rate, r_Z, varies for each functional response, with $r_Z = 2.74 \times 10^5$ year^{-1} for a Type I response, $r_Z = 365$ year^{-1} for a Type II response and $r_Z = 548$ year^{-1} for a Type III response.

Travers et al. (2009) developed an E2E model which coupled the ROMS-$N_2P_2Z_2D_2$ (describing the dynamics of lower trophic levels) and OSMOSE (describing the dynamics of higher trophic levels) into one framework, and compared this dynamic model to a one-way forcing of the fish model where the mortality rates of plankton groups were kept constant. They show that a dynamic E2E model predicts different food web structures in the Benguela upwelling ecosystem and that this is due to changes in the food chain supported by plankton. Their study shows the importance of the plankton dynamics and the feedback of these dynamics up through the food chain in an ecosystem.

The results shown in Figure 3.4, 3.5, 3.6, 3.7 and 3.8 show that an E2E model which couples together two submodels which have differing "structures" and "resolutions" can lead to steady-state solutions which are comparable to the results obtained from the isolated submodels. Taking measurements of the steady-state solution does not allow for an understanding of the dynamics that drive the system. As we saw, steady-state properties such as the total biomass within the ecosystem and the slopes of the size-spectra cannot be used to distinguish between different choices of functional responses within the zooplankton's described dynamics, or even between the choice of representing the LTL organisms by a static resource spectrum or as two dynamic compartments of phytoplankton and zooplankton. Thus, data collected regarding these types of steady-state properties cannot be used to discern the dynamics of the marine ecosystem. The underlying differences between the sub-

models can yield significant changes in the dynamical behaviour of the fish community, such as in the growth trajectories of larval fish. Aggregating the LTL organisms into two compartments of phytoplankton and zooplankton leads to a much slower growth rate for larval fish, than when a size-spectra of primary producers (of the same resolution of the size-structured fish community) is assumed. It is only through studying the dynamical properties of the marine ecosystem, such as responses to perturbations to investigate stability or measuring the growth rates of fish, that a deeper understanding of the impact that interactions between species across different trophic levels has upon the ecosystem can be gained.

To examine the question of whether it is the difference in resolutions between the submodels that leads to different dynamical properties of the marine ecosystem, there are two possible routes for investigation. Firstly, the zooplankton population could be modelled at a finer resolution, either through increasing the number of functional groups within the modelling framework or by using a size-structured approach for modelling their dynamics. Fuchs and Franks (2010) developed an NPZ model where plankton size was continuous to explore the potential impacts of climate change on planktonic ecosystems. However, their modelling framework did not account for growth in the zooplankton population, which is a key feature of the MvF PDE. A similar continuous size-structured approach for the zooplankton population, which incorporates size-dependent growth through the population, could be adopted within this framework.

Another alternative, which would maintain the minimal framework (and the tractability that it provides), would be to distribute the feeding kernels of the fish upon the phytoplankton and zooplankton populations over a wider range of size-classes. The key issue within this modelling framework is the method in which fish feed upon the plankton: the fish have a single preference for phytoplankton of size x_P and zooplankton of size x_Z. However, if the phytoplankton are distributed over a range of size-classes, $[x_P, x_P + \Delta x_P]$, then the fish would have a large range of plankton to feed upon than a single size-class.

This study has also shown the importance of the zooplankton population in the modelling of marine ecosystems. The choice of functional response to represent the zooplankton's grazing rate upon phytoplankton can have a significant impact upon the stability of the PZ submodel, and this could then influence the dynamics of the marine ecosystem. Gentleman and Neuheimer (2008) show that the choice of functional response can have profound implications for ecological stability of planktonic ecosystem.

Many current E2E models assume a satiating response of the zooplankton when feeding upon phytoplankton, i.e. a Type II functional response (Fennel, 2009; Kishi et al., 2007; Scheffer and Rinaldi, 2000; Travers et al., 2009). We have shown that whilst the stability of the PZ submodel may be highly sensitive to the choice of functional response (see Figure

3.2), when the PZ submodel is coupled to the size-structured fish community, the stability of the marine ecosystem exhibits less susceptibility to the choice of functional response (see Figure 3.7).

In conclusion, we have shown that an end-to-end model which couples together submodels of differing structures and resolutions can yield steady-state solutions which appear to be comparable to the isolated submodels, but that the amalgamation of several plankton functional types into one size-class can have significant consequences to the underlying dynamics of the model. The implications of aggregated functional types to the dynamics of marine ecosystems under key scenarios, such as climate change and fishing strategies, need to be better understood, so that ecosystem-scale effects and artefacts due to model architecture can be distinguished from each other. The PZ-Fish model is a useful tool for understanding the feedbacks that occur between the HTLs and LTLs, but should not be used to predict specific outcomes for the fish community until it has been further developed.

3.5 Appendix

3.5.1 Phase plane analysis of the choice of functional responses

Figure 3.4 shows that the Holling Type II functional response leads to a steady-state solution which is significantly different from that obtained with the Holling Type I or III responses. This is due to the parameters chosen within the model, leading to a different 'type' of solution for the Type II response and can be understood using a phase plane analysis of the PZ submodel.

The nullclines of the phytoplankton and zooplankton dynamics are the abundances at which the phytoplankton or zooplankton populations do not change over time, or when $\frac{dP}{dt} = 0$ and $\frac{dZ}{dt} = 0$, respectively. The point at which these two nullclines intersect is known as the steady-state of the solution. Figure 3.9 shows the phase planes for the PZ submodel, when a Type I, II or III functional response is assumed for the zooplankton's grazing upon the phytoplankton. As can be seen, the structures of each of the phase planes differs, but has fundamental similarities.

A Type I functional response has only two possible steady-state solutions: $(0,0)$ or (P^*,Z^*). Figure 3.9a shows a steady-state solution with a low phytoplankton and low zooplankton abundance for the Type I functional response.

However, when a Type II response is assumed, the phytoplankton's nullcline is now a parabola, and the (P^*,Z^*) steady-state solution can occur either before or after the peak of the parabola. For the parameters chosen, the steady-state solution occurs after the peak of the parabola (see Figure 3.9b). This means that the steady-state solution has a very high phytoplankton abundance, close to the carrying capacity $P_{\max}$, and a low zooplankton abundance.

Figure 3.9c shows the phase plane for a Type III functional response. The phytoplankton nullcline is now a sigmoidal function, and the (P^*,Z^*) steady-state solution can occur in three regions: before the minimum turning point, between the minimum and maximum turning points or after the maximum turning point. For these parameters, the (P^*,Z^*) steady-state solution occurs before the minimum turning point, yielding a low phytoplankton-low zooplankton abundance for the steady-state solution which is comparable to the Type I response.

As Figure 3.9 shows, the parameter set used for the Type II functional response leads to a steady-state solution which differs fundamentally from the Type I or III responses, and thus yields significantly different results within the end-to-end PZ-Fish model.

(a)

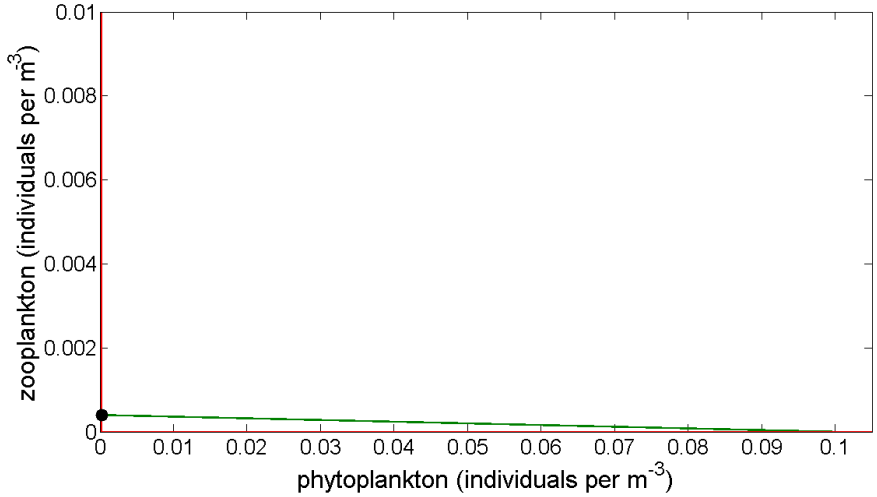

(b)

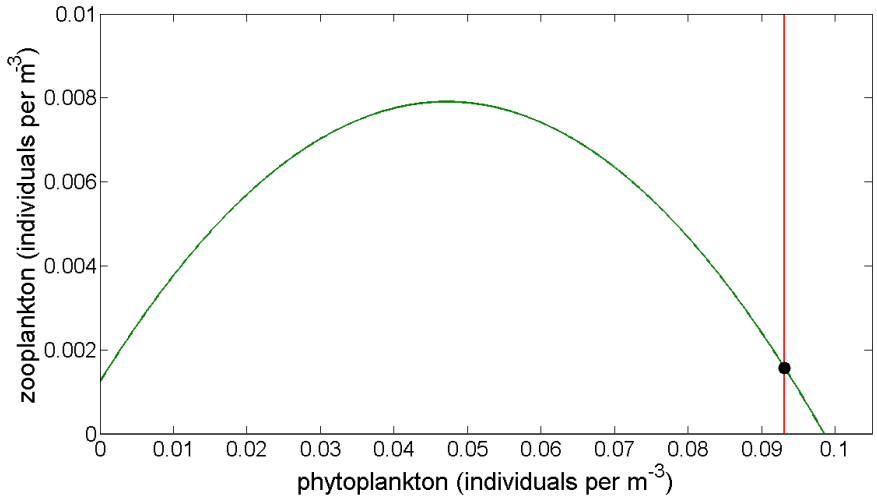

(c)

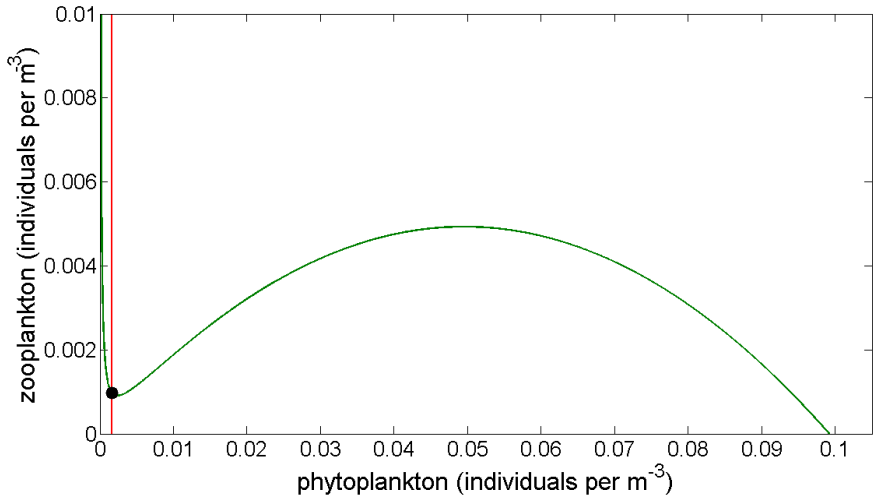

Figure 3.9: The phase planes of each functional response used within the PZ submodel, where phytoplankton nullclines are the green lines and the zooplankton nullcines are the red lines. The steady-state solution occurs at the intersection of the phytoplankton and zooplankton nullcines. The functional responses used are (a) Holling Type I (b) Holling Type II and (c) Holling Type III.

Chapter 4

The impact of a warming climate upon the seasonal dynamics of phytoplankton, and the consequences to the marine ecosystem

Abstract

Climate change models predict an increase in sea surface temperatures of $1-6^{\circ}$C over the next 100 years. Temperature is a key environmental factor in the occurrence of spring phytoplankton blooms in marine ecosystems, as warmer spring temperatures lead to an increased phytoplankton growth rate. Thus, a warming climate would have a direct effect upon the seasonal dynamics of phytoplankton, and an indirect effect upon the zooplankton and fish communities that feed upon it. Here, we develop a new end-to-end model, which couples together phytoplankton, zooplankton and a size-structured fish community. We use this model to investigate the effects of a future ocean warming scenario across the marine ecosystem. The model shows that increased temperatures lead to an earlier occurrence and longer durations of the spring phytoplankton bloom and predicts the loss of the autumn phytoplankton bloom.

Keywords

End-to-end model; climate change; phytoplankton blooms; size-structured fish model

4.1 Introduction

Plankton is the primary resource for higher trophic levels (HTLs) such as fish, either as a direct food source or indirectly as food for zooplankton populations that fish feed upon (Townsend et al., 1994). A key feature of phytoplankton population dynamics in temperate oceans is rapid growth in the population biomass followed by an equally rapid decline, known as a seasonal phytoplankton bloom. This phenomenon typically occurs in the spring months, with a smaller bloom often occurring in the autumn months (Truscott and Brindley, 1994; Winder and Cloern, 2010; Findlay, 2006). It can persist for a few weeks to months (Elliott et al., 2006; Thomas et al., 2003; Winder and Cloern, 2010). The seasonal dynamics of primary production is of major importance to global carbon dynamics and in providing the raw material upon which the entire marine ecosystem is based.

There are a number of important factors which can lead to the occurrence of a spring bloom: increased nutrient availability, light intensity, the thermal stratification of the water column and temperature (McCauley and Murdoch, 1987; Moisan et al., 2002; Townsend et al., 1994). Temperature is a key influence because phytoplankton growth rates are temperature dependent (Moisan et al., 2002); with warmer temperatures leading to a greater phytoplankton growth rate.

One expected consequence of global warming is an increase in the sea surface temperature. Climate change models predict that sea surface temperatures will increase between 1.1°C to 6.4°C over the next 100 years (Huertas et al., 2011). The sensitivity of phytoplankton growth rates to water temperature means that global warming will impact the spring blooms. Data from the Continuous Plankton Recorder (CPR) has been studied by Reid et al. (1998), and in particular, the extent to which the observed variability in plankton populations is linked to climate change. Reid et al. (1998) note that there has been a regime shift in the North Sea ecosystem after 1987, and that this is regime shift coincided with a consistently high North Atlantic Oscillation (NAO) between 1988 and 1995. Elliott et al. (2006) showed that in a temperate lake, increasing the water temperature led to an earlier occurrence of the spring blooms, and a later occurrence of summer blooms. Similarly, Peeters et al. (2007) showed that warmer air temperatures and low wind speeds led to an earlier occurrence of the spring bloom.

The changes in the spring phytoplankton bloom will have a direct effect on the fish populations, and in particular, upon the survival of the fish larvae. Cushing (1975) proposed the 'match-mismatch' hypothesis, in which the timing of spawning fish and the timing of the spring phytoplankton bloom must overlap in order for the fish larvae to optimise their growth, and hence increase their survival rate. An earlier seasonal phytoplankton bloom could lead to

a ‘mismatch’ if the fish are unable to adapt their spawning times, and thus negatively impact the fish stocks. These potential consequences need to be considered to understand better how to manage fisheries in a way that is sensitive to environmental change.

Mathematical models are useful tools for understanding and predicting how effects of different climate warming scenarios may influence phytoplankton and dependent HTLs. In many existing such models, organisms at lower trophic level (LTLs), such as phytoplankton and zooplankton, are modelled using hydrodynamic models, which capture elements of the physical environment of the ocean, and biogeochemical models that represent how nutrients are utilised by these LTL biological components (Libralato and Solidoro, 2009; Carlotti and Poggiale, 2010). These models use a ‘closure’ term to represent the predation of fish on the phytoplankton and zooplankton. The functional form chosen for this ‘closure’ term can influence the dynamics of the LTL model (Steele and Henderson, 1992; Edwards and Yool, 2000). Where a ‘closure’ term is used, it effectively assumes that there is no interaction between the HTLs and the LTLs, so the feedbacks that occur between these trophic levels cannot be studied.

Over the last ten years, there has been considerable interest in developing ‘end-to-end’ (E2E) models, where the biogeochemical processes are coupled together with the lower and higher trophic level organisms into one framework (Rose et al., 2010; Fulton, 2010). An E2E approach allows models to capture how organisms within the marine ecosystem interact with each other. This allows ecosystem-scale questions to be addressed, such as the impact of climate warming on the marine ecosystem.

Here, we use an E2E model which couples a phytoplankton-zooplankton model (PZ model) (Truscott and Brindley, 1994) to a size-structured fish community model, henceforth called the PZ-Fish model. This modelling framework is simple and tractable - the PZ model is a predator-prey model which has been well studied in the past (Truscott and Brindley, 1994; Freund et al., 2006; James et al., 2003). It has a non-trivial stable fixed point and also allows for the occurrence of a phytoplankton bloom. The size-structured fish community model allows for a reduction in parameters due to allometric scaling laws. By using this minimal E2E framework, where the key factors and their interrelationships are explicitly modelled, we are able to understand the effect of the phytoplankton blooms upon the ecosystem dynamics.

We use this model to address an ecosystem-scale question: what is the likely effect of a warming climate upon the seasonal dynamics of phytoplankton, and what will be the consequences for the wider marine ecosystem?

4.2 Methods

4.2.1 A PZ-Fish model

We define a dynamic model that couples phytoplankton and zooplankton to a size-structured fish community model (the PZ-Fish model). Figure 4.1 is a schematic diagram showing the flow of biomass through this modelled marine ecosystem. The phytoplankton population is predated upon by zooplankton and fish; the zooplankton is predated upon by fish; and the fish of log(mass) x are predated upon by larger fish, and grow larger by eating smaller fish. The sub-models of phytoplankton-zooplankton and the size-structured fish community are explained in further detail in Subsection 4.2.2 and Subsection 4.2.3.

4.2.2 The phytoplankton and zooplankton dynamics

An excitable model for phytoplankton and zooplankton was first proposed by Truscott and Brindley (1994). Within this model, the phytoplankton population density, P (density of individuals of log(mass) x_P per m^{-3}), grows logistically in the absence of predators with a maximum growth rate of r_P and a carrying capacity of $P_{\max}$, and is preyed upon by the zooplankton population density, Z (density of individuals of log(mass) x_Z per m^{-3}), at some grazing rate $f(P)$. We assume a Holling Type III functional response for the zooplankton's grazing upon phytoplankton, i.e. $f(P) = \frac{r_Z P^2}{C^2+P^2}$, where r_Z is the zooplankton's maximum grazing rate and C is a parameter describing the nonlinearity in the zooplankton's feeding response to prey abundance.

Z grows according to predation on P, at a rate $\alpha_Z f(P)$ where $0 < \alpha_Z < 1$ is the zooplankton's conversion efficiency, and dies at some intrinsic death rate μ_Z. We extend the Truscott and Brindley (1994) model to include predation by the size-structured fish community, with predation rates $A_P(u)$ and $A_Z(u)$, for the phytoplankton and zooplankton respectively, where u (density of individuals per m^{-3}) represents the density of the fish community.

To account for the predation of fish on the phytoplankton and zooplankton populations, a feeding kernel function, $\phi(x,x')$ (where x,x' represent log(body mass)), is needed to measure the preference of fish of log(body mass) x to feed on a prey item of log(body mass) x'. It is assumed that a predator has the strongest feeding preference for prey items which are a fixed predator-prey mass ratio (PPMR) smaller than itself (Andersen and Beyer, 2006; Law et al., 2009; Datta, 2011), but will also feed on prey close to this PPMR. This feeding preference is

Table 4.1: Parameter definitions for the PZ-Fish model.

Parameter	Description	Unit	Parameter Value
PZ sub-model			
$\tilde{r}_P$	P growth rate[a]	day^{-1}	0.3
P_{max}	P carrying capacity	m^{-3}	2.2×10^5
r_Z	Z grazing rate	day^{-1}	1.5
C	Z Holling type III switching parameter[b]	m^{-3}	5.2×10^3
α_Z	Z mass conversion efficiency[a]	-	0.05
μ_Z	Z intrinsic mortality rate	day^{-1}	2.74×10^{-4}
ϕ_P	predation kernel on P	-	
ϕ_Z	predation kernel on Z	-	
w_P	P mass	g	9.12×10^{-7}
w_Z	Z mass	g	4.98×10^{-5}
Fish sub-model			
w_{min}	minimum body mass	g	1×10^{-3}
w_{max}	maximum body mass	g	3.3×10^3
w_0	reference weight from $w = w_0 e^x$	g	4.54×10^{-8}
Feeding terms			
γ	volume searched per unit time per unit mass^{q} [c]	$m^3\ day^{-1}\ g^{-q}$	1.64
q	search volume exponent[c]	-	0.8
α	mass conversion efficiency[c]	-	0.2
ϕ	feeding-kernel function	-	
β	log(preferred predator:prey mass ratio[c]	-	4
σ	feeding-kernel width[c]	-	2
κ	fraction of ingested energy allocated to reproduction	-	0.75
Mortality terms			
$\tilde{k}$	intrinsic mortality rate[c]	day^{-1}	2.74×10^{-4}
μ_s	senescent mortality rate[c]	day^{-1}	1.37×10^{-3}
ρ	senescent mortality exponent[c]	-	1.5
x_s	size-class at which senescent mortality is introduced[c]	-	log(60)

[a] Truscott and Brindley (1994)
[b] Edwards and Brindley (1999)
[c] Law et al. (2009)

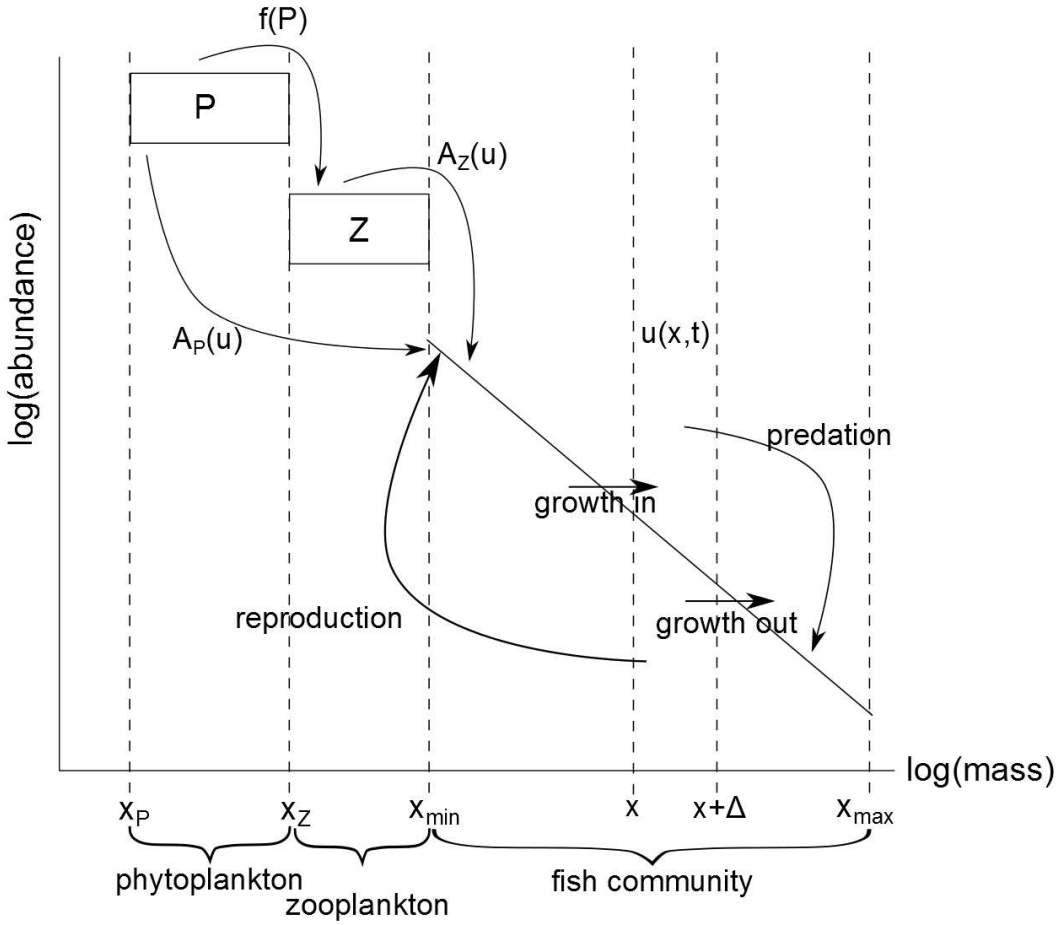

Figure 4.1: Schematic diagram showing the flow of biomass through the phytoplankton (P), zooplankton (Z) and size-structured fish community ($u(x,t)$). Phytoplankton are eaten at predation rates $f(P)$ by zooplankton and $A_P(u)$ by fish. Zooplankton are eaten at predation rate $A_Z(u)$ by fish. The abundance of fish of size x change by being predated upon by larger fish, growing larger by eating smaller fish and by smaller fish growing larger. The consumed biomass for a fish of size x is allocated either to its own growth, or to reproduction.

determined using a Gaussian function, $\phi(x,x') = 1/(\sigma\sqrt{2\pi})exp\{-(x-x'-\beta)^2/2\sigma^2\}$, where β is the log(PPMR) and the width is proportional to σ (Benoît and Rochet, 2004; Law et al., 2009).

In other words, if phytoplankton has a log(mass) of x_P, then $\phi_P(x) = 1/(\sigma\sqrt{2\pi})exp\{-(x-x_P-\beta)^2/2\sigma^2\}$ is the function representing the feeding preference of the fish community for phytoplankton. Similarly the feeding kernel for fish feeding upon zooplankton is $\phi_Z(x) = 1/(\sigma\sqrt{2\pi})exp\{-(x-x_Z-\beta)^2/2\sigma^2\}$ where x_Z is the log(mass) of Z. Thus the predation of fish upon phytoplankton ($A_P(u)$) and zooplankton ($A_Z(u)$) can be written as

$$A_P(u) = \gamma \int_{x_{\min}}^{x_{\max}} e^{x'q}\phi_P(x')u(x',t)dx' \tag{4.1}$$

$$A_Z(u) = \gamma \int_{x_{\min}}^{x_{\max}} e^{x'q}\phi_Z(x')u(x',t)dx' \tag{4.2}$$

where γ is the volume search rate and q is the volume search exponent (as the rate at which a predator searches its environment for prey scales with body size), $x_{\min}$ and $x_{\max}$ are the minimum and maximum log(mass) size-classes for the fish community (Benoît and Rochet, 2004; Law et al., 2009).

4.2.3 The size-structured fish community dynamics

The fish community is modelled using the McKendrick-von Foerster partial differential equation (MvF PDE) (Datta, 2011; Law et al., 2009; Benoît and Rochet, 2004). According to the MvF PDE, the abundance of fish is a function of body mass, w (g), and time, t (days). The change of abundance of fish is due to a size-dependent growth rate and a size-dependent mortality rate. As the spectra usually span many orders of magnitude the MvF PDE is often studied using log-transformed mass, x (Benoît and Rochet, 2004; Law et al., 2009). Thus, the abundance of fish, of size x and at time t, is represented by $u(x,t)$, and increases and decreases according to some size-dependent rates $g(x,t)$ and $\mu(x,t)$, respectively.

Death

The size-dependent mortality rate has three components to it: predation by larger size-classes of fish, an intrinsic mortality rate and a senescent mortality rate. Predation is determined by the Gaussian feeding kernel, $\phi(x,x')$, described previously (see Section 4.2.2). Note that this feeding kernel is the interaction between the size-classes of the fish community only,

whereas $\phi_P(x)$ is the interaction of the fish community with phytoplankton, and similarly $\phi_Z(x)$ for zooplankton.

An intrinsic mortality rate accounts for death not caused by predation, and is assumed to be a constant rate $\tilde{k}$. Finally, a senescent mortality rate, $\mu_s e^{\rho(x-x_s)}$, prevents a high abundance of large size-classes in the absence of top-class predators in this model. Here μ_s is the mortality rate, ρ is the senescent mortality exponent and x_s is the size-class at which senescent mortality is introduced (Benoît and Rochet, 2004; Law et al., 2009).

Thus the combined size-dependent mortality rate can be written as

$$\mu(x,t) = \tilde{k} + \mu_s e^{\rho(x-x_s)} + \gamma w_0^q \int_x^{x_{max}} e^{x'q} \phi(x',x) u(x',t) dx'$$

Growth

The size-dependent growth rate assumes that growth is a result of mass gained by consumption. In other words, a fish in size-class x predates upon smaller fish (or phytoplankton and zooplankton) and converts the prey biomass into energy which is used for somatic growth and reproduction. The size-dependent growth rate can be written as

$$g(x,t) = (1-\kappa)\alpha\gamma w_0^q e^{x(q-1)} B(x)$$

where

$$B(x) = \int_{x_{min}}^{x} e^{x'} \phi(x,x') u(x',t) dx' + \int_{x_{P_{\min}}}^{x_{P_{\max}}} e^{x_P} \phi_P(x) P(x_P) dx_P + \int_{x_{Z_{\min}}}^{x_{Z_{\max}}} e^{x_Z} \phi_Z(x) Z(x_Z) dx_Z$$

where $0 < \kappa < 1$ is the fraction of converted biomass allocated to reproduction, $0 < \alpha < 1$ is the conversion efficiency.

Reproduction

As mentioned previously, upon consuming a prey's biomass, the predator allocates a fraction of that converted biomass to reproduction (κ) and the remainder to growth (1-κ) (Perrin and Sibly, 1993; Thygesen et al., 2005; Hartvig et al., 2010). The reproduction term to the larval fish class can be written as

$$R = \kappa\alpha\gamma w_0^q \int_{x_{\min}}^{x_{\max}} e^{x'(q-1)} B(x') e^{x'-x_1} u(x',t) dx'$$

where $x_{\min}$ is the size-class denoting the larval fish.

The E2E model: the PZ-Fish model

The full E2E model, which we call the PZ-Fish model, can be summarised as:

$$\begin{aligned}
\frac{dP}{dt} &= r_P P\left(1 - \frac{P}{P_{\max}}\right) - f(P)Z - A_P(u)P \\
\frac{dZ}{dt} &= \alpha_Z f(P)Z - \mu_Z Z - A_Z(u)Z \\
\frac{\partial u(x,t)}{\partial t} &= -\mu(x,t)u(x,t) - \frac{\partial(g(x,t)u(x,t))}{\partial x}
\end{aligned} \tag{4.3}$$

with initial condition $P(0) = P^0, Z(0) = Z^0$ and $u(x,0) = u^0(x)$ for $x \in [x_{\min}, x_{\max}]$ and boundary conditions

1. $g(0,t)u(0,t) = \kappa \int g(x,t)u(x,t)e^{x-x_{\min}} dx$
2. $u(x,t) = 0$ for $x > x_{\max}$

Numerical methods are required to learn about the dynamics of this model. This requires a discretisation method to be chosen, where the domain space is partitioned into a mesh and used to approximate the derivatives of the equation through these discrete points (Press et al., 2007). If $x_{\min}$ and $x_{\max}$ are the smallest and largest size-classes of the discretized fish community (respectively), then the lower and upper boundary conditions for the fish community can be written as

$$\begin{aligned}
\frac{du(x_{\min},t)}{dt} &= -\mu(x_{\min},t)u(x_{\min},t) - \frac{g(x_{\min},t)u(x_{\min},t)}{\partial x} + \frac{R}{\Delta x} \\
\frac{du(x_{\max},t)}{dt} &= -(\tilde{k} + \mu_s e^{\rho(x-x_s)})u(x_{\max},t) - \frac{g(x_{\max},t)u(x_{\max},t)}{\Delta x} + \frac{g(x_{\max-1},t)u(x_{\max-1},t)}{\Delta x}
\end{aligned}$$

We use a finite difference method for the numerical simulations, with log(mass) x discretised with step size $\Delta x = 0.1$ and time t discretised with step size $\Delta t = 0.1$.

Parameters

The full definitions and units of the parameters used to formulate the PZ-Fish model can be found in Table 4.1, together with the default value used for the numerical simulations.

The PZ sub-model

The P growth rate, $\tilde{r}_P$, and the Z mass conversion efficiency, α_Z, parameter values were taken from Truscott and Brindley (1994). The Z grazing half saturation coefficient was taken from Edwards and Brindley (1999). The units used by Edwards and Brindley (1999) were $\mathrm{m}^{-3}\mathrm{gC}$, so we assumed that the measured mass of plankton in this model was carbon and re-scaled the parameter into m^{-3}. This was done by dividing the empirical parameter by the body mass of P.

The value of P carrying capacity, $P_{\max}$, was chosen to be $2.2 \times 10^5 \mathrm{m}^{-3}$, together with the Z grazing rate, r_Z, as a value of 1.5 day^{-1}, as these choices allowed for a strong seasonal phytoplankton bloom. A value of 1.5 day^{-1} is within the empirical range of 0.6-1.4 day^{-1} reported by Edwards and Brindley (1999). Finally, the Z intrinsic mortality rate, μ_Z, was assumed to be 2.74×10^{-4} day^{-1}, as this is the intrinsic mortality rate assumed on the fish community.

The size-structured fish model

The majority of the parameters used for the size-structured fish model were taken from Law et al. (2009)[Table 1]. The exception is the fraction of consumed biomass which is allocated to reproduction, κ. A value of 0.75 had to be used, as smaller values did not permit co-existence of the full phytoplankton-zooplankton-fish community. Choosing an empirical value for this parameter is difficult, because the model has to aggregate many different species into a single community of fish. It is therefore not possible to use parameters for explicit life histories of the constituent species. The assumption of a constant fraction of incoming biomass to reproduction simply assumes that reproduction is taking place at all body sizes within the community as a whole.

4.2.4 Seasonal phytoplankton blooms

To investigate the impact of global warming on the seasonal dynamics of phytoplankton, we focus on the long-term systematic temperature changes, where $T(t)$ is the temperature over time and its impact upon the nutrients of the ecosystem $N(t)$. We assume that phytoplankton is directly and indirectly affected by global warming by incorporating a temperature- and nutrient-dependent phytoplankton growth rate into the modelling framework. We consider a scenario of climate change where there is an increase of 3°C of the mean temperature over the next 100 years. Figure 4.2a shows the mean, minimum and maximum temperatures used for the 100 year simulation.

To mimic the rapid warming of ocean waters, and thereby to predict its effect on ecosystem dynamics, we use a sawtooth temperature profile:

$$T(t) = \begin{cases} (T_0 - \Delta T) + \left(\frac{2\Delta T \cdot 100}{365-20}\right) - \left(\frac{2\Delta T}{365-20}\right) \cdot t & \text{for } 0 \leq t < 100 \text{ days} \\ (T_0 - \Delta T) - \left(\frac{2\Delta T \cdot 100}{20}\right) + \left(\frac{2\Delta T}{20}\right) \cdot t & \text{for } 100 \leq t < 120 \text{ days} \\ (T_0 + \Delta T) + \left(\frac{2\Delta T \cdot (120)}{365-20}\right) - \left(\frac{2\Delta T}{365-20}\right) \cdot t & \text{for } 120 \leq t < 365 \text{ days} \end{cases} \tag{4.4}$$

where $T_0 = 10°\text{C}$ is the mean temperature, $\Delta T = 6°\text{C}$ is the maximum change in temperature from the mean temperature over the year, the seasonal forcing occurs on day 100 and lasts for 20 days. Figure 4.2b shows this sawtooth temperature profile over one year.

We assume the phytoplankton growth rate is represented as a function of temperature, $T(t)$, and nutrients, $N(t)$, i.e. $r_P = r_P(t, T(t), N(t))$. If these are independent effects, then the phytoplankton growth rate becomes a product of the temperature dependent component, $J(t, T(t))$, and the nutrient limitation factor, $L(t, T(t))$ (Fasham et al., 1990). Thus, r_P becomes:

$$r_P = r_P(t, T, N) = J(t, T(t)) \cdot L(t, T(t)). \tag{4.5}$$

The Van't Hoff rule describes the effect of changing temperature on reaction rates, and following the method described by Freund et al. (2006) for implementing the Van't Hoff rule into the temperature-dependent component of the growth rate gives

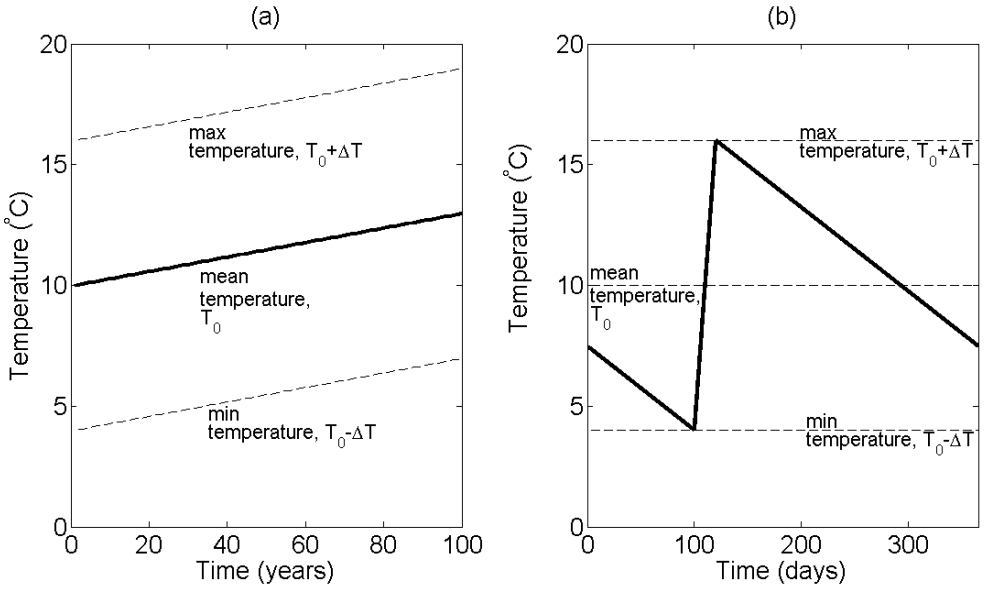

Figure 4.2: (a) The temperature profile for 100 years uses a sawtooth temperature profile each year, where there is an increase of 3°C in the mean temperature over 100 years. (b) The sawtooth temperature profile for one year, with $T_0 = 10$°C and $\Delta T = 6$°C, where the forcing occurs at day 100 and ends on day 120 (see Equation 4.4).

$$J(t,T(t)) = (Q_{10})^{(T(t)-T_0)/10}\tilde{r}_P. \tag{4.6}$$

The Van't Hoff rule says that a change of temperature by 10°C will multiply the reaction rate at mean temperature by a factor of Q_{10}, where $\tilde{r}_P$ is the initially chosen phytoplankton growth rate. As with Freund et al. (2006), we choose a value of $Q_{10} = 2$. Figure 4.3a (the dotted-dashed black line) shows the temperature dependent growth rate, $J(t,T(t))$, over the course of one year.

Once the phytoplankton bloom has been initiated, it is controlled via the decreasing nutrient concentrations (Fasham, 1993; Findlay, 2006). We assume that the nutrient concentration is a function of total new production following the onset of stratification (where the water column forms layers that prevents water mixing due to warmer temperatures) in early spring, and model the nutrient limitation factor by:

$$L(t,T(t)) = \max\left(1 - \delta\int_0^t J(t',T(t'))L(t',T(t'))P(t')\left(1-\frac{P(t')}{P_{\max}}\right)dt', 0.1\right) \tag{4.7}$$

where $0 < \delta < 1$ is chosen to account for the flux of nutrients out of the upper mixed layer as they are taken up by phytoplankton. We fix a minimum value of 0.1 for $Q(t,N)$ to account for the continual supply of nutrients mixing into the upper mixed layer from deeper waters. We also allow the nutrient concentration to slowly increase to its maximum value between day 270 and 365. If we did not allow this, there would be an artificial bloom induced at day 0 every year, caused by the sudden increase in nutrient concentration.

Figure 4.3a (the dotted red line) shows the nutrient limitation factor, $Q(t,N)$, over the course of one year. Figure 4.3b (the dashed green line) shows the phytoplankton growth rate that is obtained by multiplying together the temperature dependent component and the nutrient limitation factor for one year.

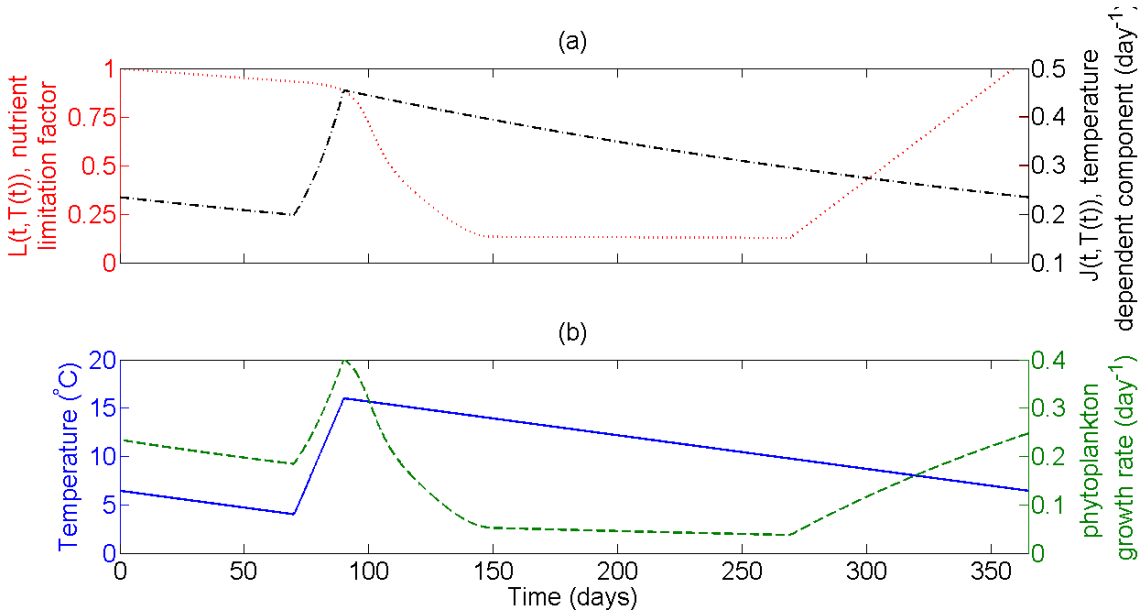

Figure 4.3: The effect of temperature on the phytoplankton growth rate, $r_P(t,T(t),N(t))$, for one year. (a) The two independent components of the phytoplankton growth rate, the nutrient limitation factor, $L(t,T(t))$ (dotted red line) against the temperature-dependent component, $J(t,T(t))$ (dash-dotted black line). These factors are multiplied together to determine $r_P(t,T(t),N(t))$. (b) Sawtooth temperature profile, $T(t)$ (solid blue line) against the phytoplankton growth rate, $r_P(t,T(t),N(t))$ (dashed green line).

4.3 Results

4.3.1 The effect of warming on the timing and duration of the phytoplankton bloom

In this section, we analyse the effect of climate warming upon three large-scale characteristics of the ecosystem over the course of the 100 years of numerical simulation. We examine 1) the time at which the bloom occurs, which is measured as the first peak in phytoplankton abundance after the seasonal forcing at day 100, 2) the duration of the bloom, which is measured as the time between the first peak to the first trough after the phytoplankton crash and 3) the maximum height that the bloom reaches, which is measured as the relative change in abundance when compared to the steady-state value. (Note, the steady-state value is the point at which there is no change in the phytoplankton, zooplankton or fish populations over time and is determined for the scenario in which there is no seasonal forcing).

The consequences of the warming climate to the fish community is analysed here by looking at only two size-classes - the larval fish (with body mass 0.001g) and small fish (with body mass 0.01g). These two size-classes of fish have a strong feeding preference for phytoplankton and zooplankton, and so are most directly affected by changes in the dynamics of these organisms.

The detailed dynamics which drive these signals are examined in Section 4.3.2.

Timing of the bloom

Figure 4.4a shows how many days after the seasonal forcing a phytoplankton bloom occurs (the green bullets, $-\bullet-$). As can be seen, the blooms occur increasingly early under a warming climate. The change in behaviour is due to the maximum phytoplankton growth rate which occurs as the temperature increases, which allows the phytoplankton's growth to quickly exceed the predation pressures on them.

Although the zooplankton's bloom also occurs earlier under warmer temperatures, their shift in timing is not as large as for the phytoplankton population. The zooplankton's bloom occurs about 4 days earlier after a 3°C increase in the temperature, whereas the phytoplankton bloom occurs about 8 days earlier.

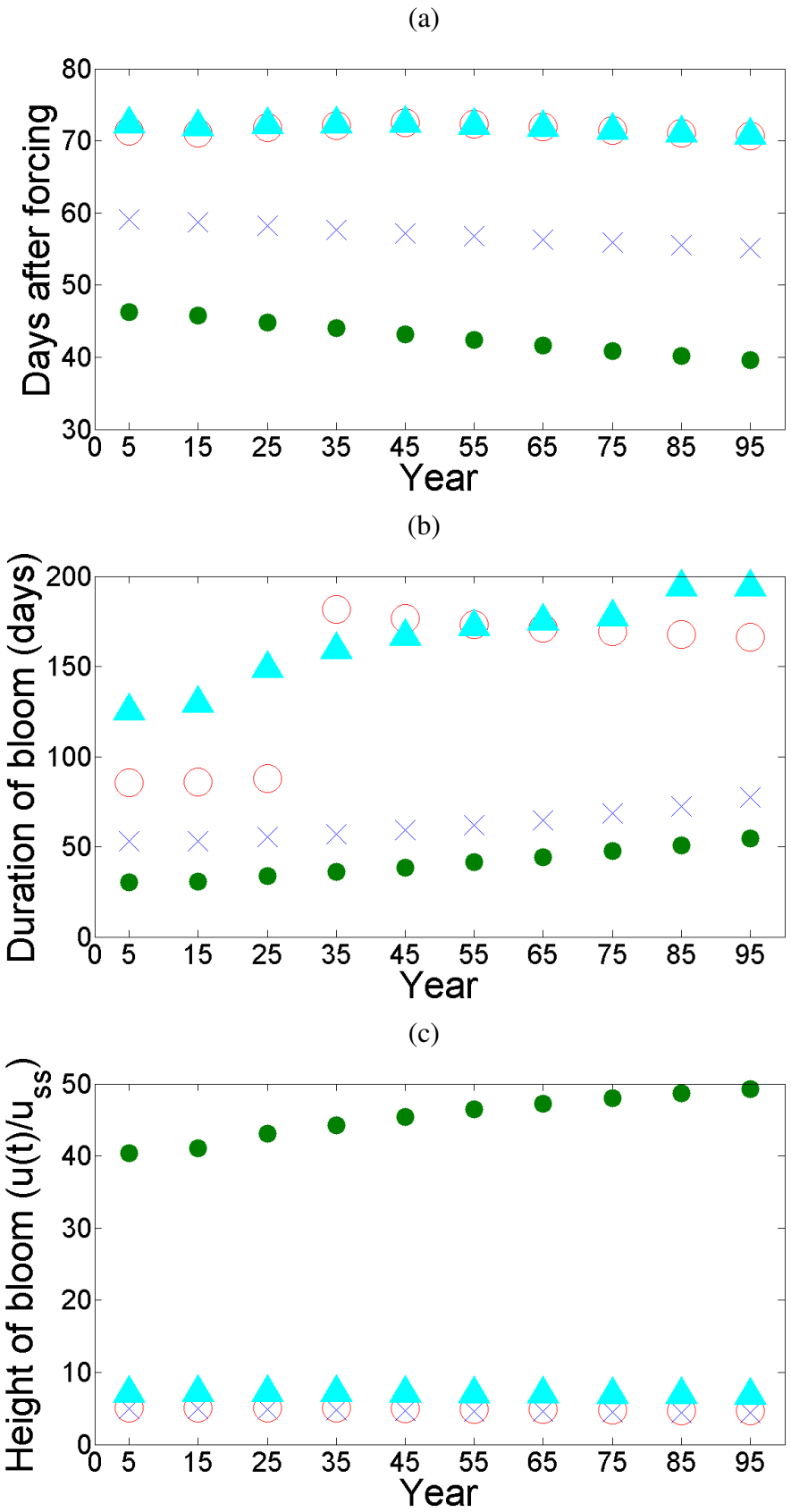

Figure 4.4: The three measured large-scale characteristics of the ecosystem. (a) The number of days after the onset of seasonal forcing in which the peak in abundance occurs, (b) the duration of the bloom (measured between the first peak to the first trough in density) and (c) the height of the maximum peak event for 10 years of the simulated 100 year run, for phytoplankton (green bullets, $-\bullet-$), zooplankton (blue crosses, $-\times-$), larval fish (0.001g) (red circles, $-\circ-$) and small fish (0.01g) (cyan triangles, $-\blacktriangle-$).

There does not appear to be a significant change in the timing of peak density in the fish community.

Duration of the bloom

Figure 4.4b shows the duration of the phytoplankton bloom (the green bullets, $-\bullet-$). The length of the phytoplankton bloom increases with increasing temperature, as the effect on the phytoplankton growth rate allows the phytoplankton to escape the pressures of predation for longer. This pattern of behaviour can also be seen in the zooplankton and small fish.

However, the larval fish show a switch in their reaction to the phytoplankton's bloom duration between year 25 and year 35. This can be understood through Figure 4.5c. Under cooler conditions, there are actually two peaks in the larval fish density due to the spring and autumn phytoplankton blooms. However, as the temperature increases, there is no longer an autumn phytoplankton bloom and there is no secondary peak in the larval fish. Thus, instead of there being a relatively short spring bloom in the larval fish populations, under warmer conditions, there is only one long bloom in the larval fish population.

Magnitude of the bloom

Figure 4.4c shows that there is an increase in the maximum densities reached by the phytoplankton population as temperature increases. As the temperature increases, the combination of the fast phytoplankton growth rate and the high predation pressure on the zooplankton is enough to excite the phytoplankton population to higher densities. See Section 4.3.2 for a full analysis on this occurrence.

4.3.2 The phytoplankton and zooplankton dynamics

The results in Section 4.3.1 reveal potentially important changes to the large-scale behaviour of the ecosystem. The advantage of our E2E model is that it allows us to understand the mechanisms driving these changes in system-level dynamics. To show this, we compare the seasonal dynamics of the PZ-Fish model for two years of the simulation: year 5, when the mean temperature is 10.15°C and year 95, when the mean temperature has increased to 12.85°C.

In year 5, the phytoplankton population undergoes a bloom starting at day 110. This bloom

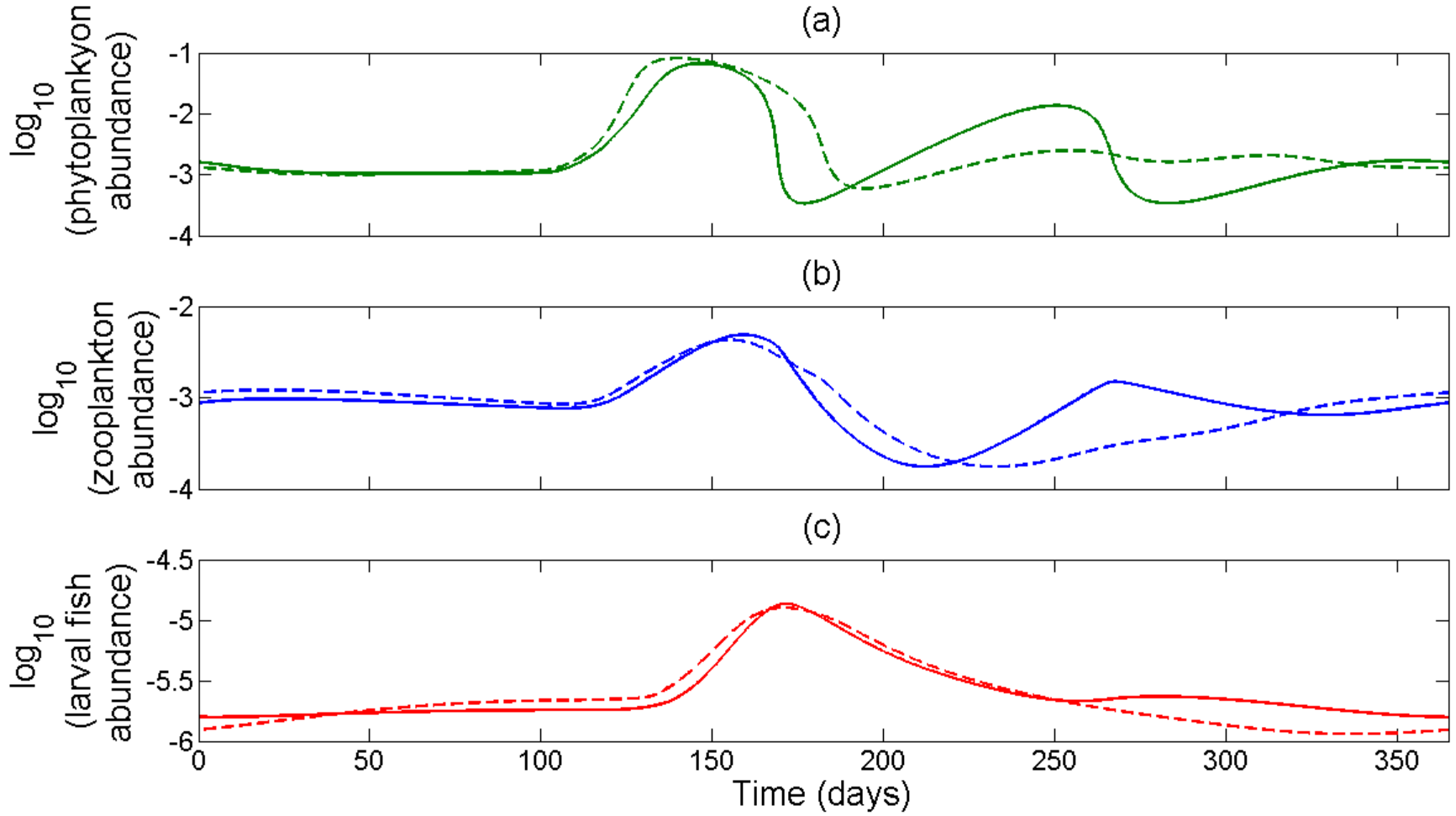

Figure 4.5: The phytoplankton, zooplankton and larval fish densities for one year, in year 5 (the solid lines —) and year 95 (the dashed lines - - -). (a) The phytoplankton density (green lines) (b) the zooplankton density (blue lines) and (c) the larval fish density (red lines).

(a)

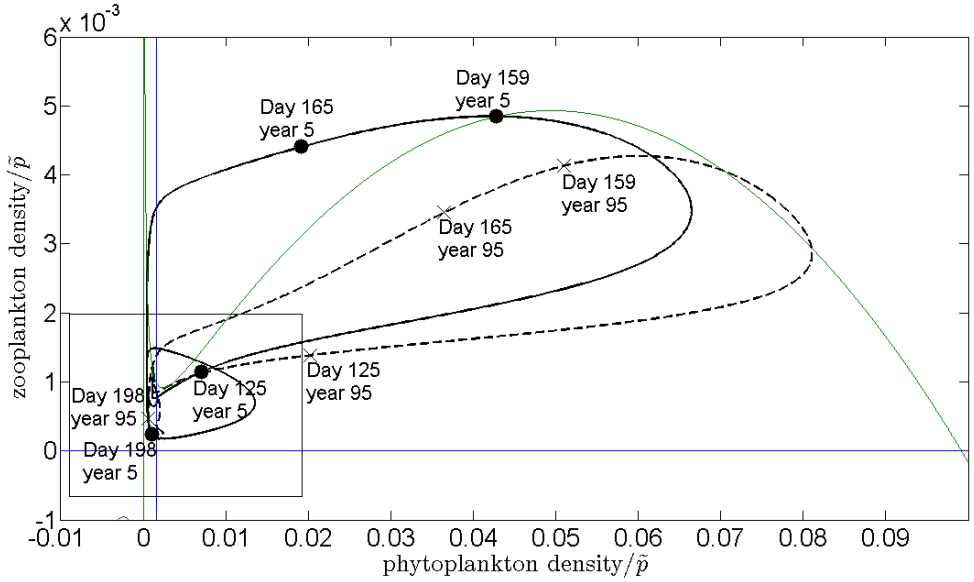

(b)

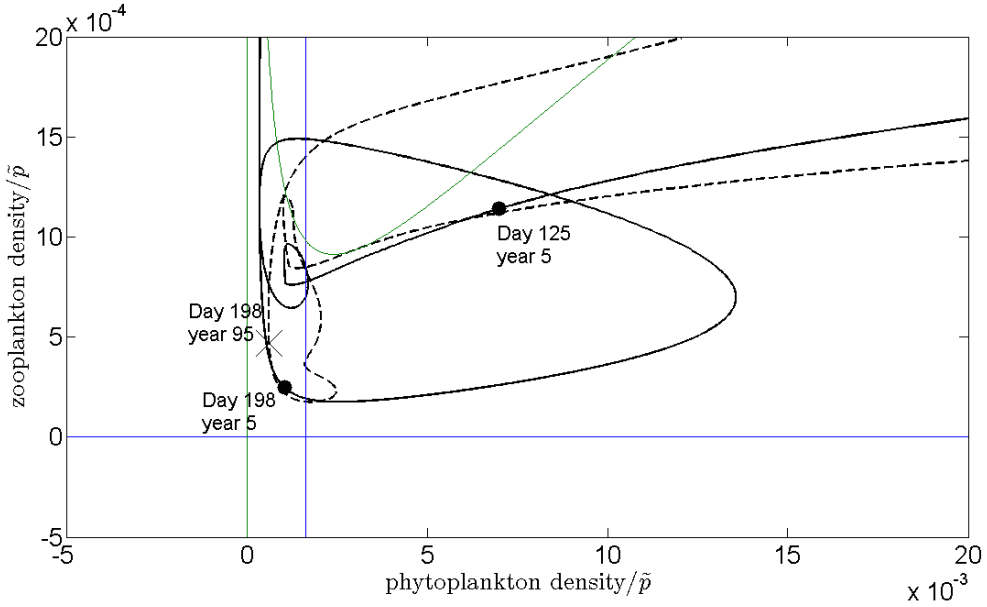

Figure 4.6: Comparing the (P,Z)-phase plane and trajectory for different points of year 5 and year 95. The phytoplankton nullcline is the curved green line and the zooplankton nullcline is the vertical blue line for year 5. These nullclines are dependent upon the predation of the fish community upon the phytoplankton and zooplankton - in particular, the zooplankton nullcline increases as $A_Z(u)$ increases. This allows the phytoplankton population to increase to significantly greater abundances than under the assumption that $A_P(u)$ and $A_Z(u)$ are constant values. (a) The phase plane and trajectories for year 5 (the solid black lines) and year 95 (the dashed black lines). (b) A close-up view of the phase plane and trajectories for year 5 (the solid black lines) and year 95 (the dashed black lines) which are inside the marked box shown in (a).

lasts for about 35 days, before the phytoplankton population drops rapidly in abundance. The phytoplankton population then undergoes a smaller autumn bloom for a further 50 days (Figure 4.5a, solid green line). However, in year 95, the phytoplankton population has only one long bloom, which starts just before day 110 and lasts for almost 55 days before the population drops to its original steady-state abundance (Figure 4.5a, dashed green line).

As is standard in a predator-prey interaction, there is a time delay in the build-up of the zooplankton population (Figure 4.5b). However, the zooplankton population also undergoes an autumn bloom in year 5 (which is absent in year 95) due to the autumn bloom of the phytoplankton.

The increase in zooplankton population means that there is more food for the very small fish to feed upon, which leads to an increase in their growth rates and their contribution to the reproduction term. Figure 4.5c shows the increased density of larval fish, which follows the initial phytoplankton bloom. As these very small fish grow, their diet preferences change: initially, they have a strong preference for feeding on phytoplankton, which leads to an increase in $A_P(u)$, then gradually switch to a preferential zooplankton diet which leads to an increase in $A_Z(u)$.

The increased predation pressure on the phytoplankton and zooplankton populations due to the fish community then leads to a decline in the phytoplankton population, as their growth rate is unable to compensate for the higher predation pressures upon them. This is also due to a decline in the growth rate of the phytoplankton, partly through the temperature dependent growth rate, but also as the lack of available nutrients in the environment limit their growth. Once the phytoplankton population passes a threshold value, the zooplankton population crashes as they are unable to sustain growth under similarly high predation pressures (see Figure 4.6).

However, the difference between the dynamics that occur in year 5 and year 95 are due to the increased grazing pressures upon the zooplankton population. In year 5, the grazing on zooplankton decreases quickly enough that the phytoplankton growth rate is still high enough to induce a second, autumn bloom. In year 95, the extended duration of the spring bloom (due to the high grazing pressure on the zooplankton) is such that the phytoplankton population does not have a high enough growth rate to undergo a second bloom (see Figure 4.6).

4.4 Discussion

The warming climate will have a profound impact on marine organisms - the warmer temperatures will have a direct effect on the growth rate of phytoplankton, and an indirect but potentially significant effect on the survival of fish larvae. This modelling study shows that a warmer temperature led to a shift to an earlier phytoplankton bloom, a longer duration for the phytoplankton bloom and an extinction of the autumn bloom (Figure 4.5).

Timing of the bloom

There have been several empirical studies investigating the effect that the physical environment has on the timing of phytoplankton spring blooms. Edwards et al. (2002) analysed a long term plankton dataset for the North Sea and identified two key periods in that dataset: a cold-boreal event in the 1970s and a warm-temperate event in the 1980s. They showed a clear difference in the timing of the phytoplankton bloom under these two periods, where the bloom occurred earlier in the warm-temperate event by about 2.5 months.

However, a study by Wiltshire and Manly (2004) on the time series dataset at Helgoland Roads in the North Sea showed that an increase of 1.13°C over 40 years has led to a backwards shift in the spring bloom, i.e. it occurs later. These two completely different trends under a warming climate are due to other elements of the environment: Wiltshire and Manly (2004) argued that this backward shift in the spring bloom was due to the persistence of zooplankton during the autumn and winter months, which suppressed the growing biomass needed for a spring phytoplankton bloom, thus causing a delay in the bloom. This was investigated in a later study (by extending the dataset with another 4 years of data), but no significant effect of the zooplankton population upon the start of the bloom was found (Wiltshire et al., 2008). In fact, Wiltshire et al. (2008) show that it is the preceding winter temperature that is the significant effect on the phytoplankton bloom.

A sawtooth temperature profile was used in this study to ensure that the seasonal forcing was strong enough to cause a phytoplankton bloom. Therefore, it is the rapid rate of increase in temperature which triggers a phytoplankton bloom in the PZ-Fish model. A sinusoidal temperature profile was inappropriate for this study as the bloom/non-bloom dynamics are dependent on the initial population of phytoplankton and zooplankton (Freund et al., 2006), whereas they are not for the sawtooth temperature profile.

The earlier timing of the spring bloom is due to the increased phytoplankton growth rate, as it allows the phytoplankton population to grow quicker than it is grazed upon. Therefore, it is the higher growth rates caused by a warmer temperature, not the preceding winter

temperature which affects the timing of the spring blooms in this model.

Duration of the bloom

Our numerical simulations showed a marked increase in the duration of the spring phytoplankton bloom, from 30 days to 55 days, caused by a 2.85°C increase in mean temperature (Figure 4.4b). This result agrees with the modelling results of Kristiansen et al. (2011), which found that warmer ocean temperatures led to longer periods of productivity, and also supports the conclusion by Martens and Beusekom (2008), that global warming will lead to a longer copepod season.

However, Figure 4.4b shows only a small increase in the zooplankton (or copepod) abundances in the ecosystem. This could be due to the single size-class of zooplankton which is used to represent small, large and carnivorous zooplankton groups in the model. Martens and Beusekom (2008) found that the carnivorous zooplankton population gradually increased over a warming climate, and this detail cannot emerge from our current model. Further work is needed to extend the number of size-classes representing the phytoplankton and zooplankton populations, to allow the behaviour of small, large and carnivorous zooplankton populations under different warming scenarios to emerge.

An important consequence of the longer spring bloom is the predicted extinction of the autumn bloom. Figure 4.5a shows that under warmer temperatures, the spring bloom lasts for so long that the system does not allow time for a second bloom in the autumn months. Similar findings are reported by Molen et al. (2012), who used a coupled hydrodynamic-biogeochemical water column model GOTM-ERSEM-BFM to predict that warmer temperatures can lead to a smaller autumn bloom occurring.

It is suggested that the autumn bloom is driven by the deepening of the surface mixed layer at the end of summer, leading to an influx of nutrients to the surface layer as well as a reduction in grazing pressure by predators (Martinez et al., 2011; Findlay, 2006). Martinez et al. (2011) used ocean color time series to study the phytoplankton spring and autumn blooms in the North Atlantic, and found that in the Eastern Atlantic, the autumn bloom was weaker in the 2000s than in the 1980s. They hypothesised that this was due to a delay in the deepening of the mixed layer depth.

Similarly, Song et al. (2010) show that in their model simulations, there is a slight delay in the autumn plankton bloom with high sea surface temperatures. However, their ocean color data shows that the autumn plankton bloom is correlated with sea surface salinity and sea surface temperature. If the effect of salinity is greater than that of temperature, then the autumn plankton bloom will be negatively correlated with temperature (Song et al., 2010).

Thus, their data shows an association of high temperatures with early autumn bloom timing.

Our study shows the importance of the fish community to the dynamics of the phytoplankton population. The delay of the autumn bloom under a warming climate is due to the extended duration of the spring bloom. The spring bloom, in turn, is affected by the increased grazing pressure of the fish community upon the zooplankton population, which decreases the grazing pressure upon the phytoplankton population. If a 'closure' term were used for the phytoplankton-zooplankton submodel, as opposed to a dynamic fish community model, the loss of the autumn bloom under a warming climate is not observed.

Consequences to the fish community

The 'match-mismatch' hypothesis is the proposal that the timing of egg hatching and the timing of the spring phytoplankton bloom must overlap in order for the larval fish larvae to optimise their growth, and increase their survival rate (Cushing, 1975). Kristiansen et al. (2011) showed that the longer period of productivity which is caused by warmer temperatures leads to enhanced survival in the first 30 days of their larval fish.

Our study shows that there is a potential for an increased 'mismatch' under a warming climate: Figure 4.4a shows that while the spring phytoplankton bloom occurs earlier under warmer temperatures, there is no significant change to the timing of the peak of abundance in the larval fish.

To fully explore the consequences of an earlier occurring and longer lasting spring phytoplankton bloom to the fish community, the size-structured fish community model needs adapting. The reproduction function should be annual, not continuous. Currently, the fish community reacts immediately to the earlier onset of the phytoplankton bloom, whereas in reality, spawning is an annual occurrence which would lead to a delayed reaction of the fish community to the seasonal phytoplankton dynamics (Wright and Trippel, 2009).

The amalgamation of several zooplankton functional types into one size-class should also be addressed. The larval fish have only one phytoplankton class and one zooplankton class to feed upon initially. It takes a few days of feeding on these two prey items before the larval fish has enough biomass to grow into the next size-class, and hence extend its feeding range. However, if the zooplankton compartment was extended to more than one size-class, for example small, large and carnivorous zooplankton, there would be potentially more resources for the larval fish to feed upon and use for faster growth and enhanced survival.

Temperature dependence

In this study, we have focused on the impact of increasing the mean sea surface temperature upon a dynamic marine ecosystem. This has been implemented into the model through the phytoplankton growth rate, via the Van't Hoff rule (see Eq.4.6). Temperature also affects other processes, such as optimal growth rates for fish (Peck and Daewel, 2007; Pörtner and Knust, 2007; Gislason et al., 2010) or the hatching times of fish eggs (Pepin et al., 1997; Mooij et al., 2008), which are not currently considered in this modelling framework. These are factors which need to be considered in future work. However, the simplest framework is the suitable starting point for understanding the effect that a changing temperature has upon the complex marine ecosystem.

The variability of the temperature profile is also likely to play an important role in a warming climate. Initial modelling results have shown that decreasing the variance of the temperature profile can lead to a very small spring phytoplankton bloom with no autumn bloom, thus showing the importance of temperature variance in phytoplankton dynamics. Freund et al. (2006) showed that adding fluctuations to the temperature profile induced switching between a bloom and a non-bloom mode. For a comprehensive analysis on the effect of a warming climate on a marine ecosystem, temperature dependent rates should be used for more than just the phytoplankton growth rate, and fluctuations to the temperature profile need to be explored.

Conclusion

Temperature is a strong influence on marine ecosystems, and in order to understand its impact, a whole ecosystem approach is needed. This study shows that such an E2E approach is feasible, and can offer insight and predictions beyond the scope of focussed models. Thus the effect of the spring phytoplankton bloom can help with the understanding of the growth and survival of larval fish, as well as the effect of predation by the fish community upon the phytoplankton and zooplankton populations.

Acknowledgements

We thank Sarah Collings, Simon Croft, Sonja van Leeuwen, Rodney Forster, Liam Fernand, Jamie Wood and Gustav Delius for their helpful insights. This research was supported by a joint studentship to CW from the Centre for Environment Fisheries and Aquaculture Science UK and the University of York UK.

Chapter 5

The consequences of size-selective fishing and balanced harvesting to the seasonal dynamics of phytoplankton

Abstract

The impact of fishing is not restricted solely to the fish community, but also feeds back through the food web to the lower-trophic-level organisms, such as the phytoplankton and zooplankton. We use a dynamic end-to-end model to study two different fishing strategies: size-at-entry and balanced harvesting. With this modelling framework, we explore the direct and indirect effects of these harvesting schemes, and in particular, the impact they have upon the phytoplankton population. We quantify the disruption to the phytoplankton using two measures: 1) the scaled time-averaged Euclidean distance between phytoplankton populations when the fish community is either harvested or not and 2) the periodicity of the phytoplankton dynamics. Our results show that, regardless of the choice of fishing strategy, intensive harvesting upon small fish (of body mass 1g or smaller) can lead to a significant shift in the phytoplankton's dynamics: from stable annual patterns to unpredictable periodic behaviours. Balanced harvesting allows a greater biomass yield of fish to be achieved under low intensity fishing scenarios than a size-at-entry fishing strategy, but can also lead to a greater range of complex dynamics occurring within the phytoplankton population. This has the potential for greater variability in the annual fisheries yield obtained, which could have economic and ecological consequences.

5.1 Introduction

The exploitation of marine resources has been managed in some places for hundreds of years. The traditional approach to fisheries management has been to protect the young and harvest the old, whilst trying to maximise the fished yield (Beverton and Holt, 1993; Law et al., 2012; Garcia et al., 2012; Borrell, 2013). One strategy commonly applied is known as size-at-entry, where fishing only begins upon individuals of a minimum body mass (so as to protect the juveniles), and then the adults are fished with approximately equal intensity (Pope et al., 2006; Jacobsen et al., 2014). This is representative of the current harvesting scheme applied to the North Sea fish stocks (Jacobsen et al., 2014). The impact of this selective fishing strategy has been realised over the last few decades, from stock collapses (such as the decline of the North Sea cod (O'Brien et al., 2000; Hutchinson, 2008)) to evolutionary responses (where fish have begun investing their energy into reaching sexual maturity as early as possible, leading to yields of small-sized fish (Reznick and Ghalambor, 2005; Enberg et al., 2011)).

Over the last few years, a different approach to fisheries management has been suggested, known as balanced harvesting. This approach recommends that the exploitation of the marine ecosystem is distributed across a range of species and sizes in proportion to their natural productivity (Law et al., 2012; Garcia et al., 2012). Law et al. (2012) used a dynamic size-spectrum model to represent a single species of fish, and compared the effects of selective and balanced harvesting upon the yield, resilience and disruption to the fish community. They show that the balanced harvesting strategy can achieve good yields whilst reducing the disruption to the fish community. Jacobsen et al. (2014) used a size- and trait-based model to represent a fish community, and concluded that unselective balanced harvesting is more likely to preserve the structure of fish communities than selective fishing, but the consequence is a significant reduction in the average size of fish obtained.

Mathematical models are useful tools for studying complex systems, for understanding and predicting how the system will react under different scenarios. The conventional means of modelling marine ecosystems have been by representing the system using two independent components: biogeochemical and fish production models (Travers et al., 2009). The representation of the lower trophic level (LTL) organisms, such as phytoplankton and zooplankton, in fish production models has been done implicitly, through some 'carrying capacity' (Travers et al., 2007) or by assuming them to be a static resource (Law et al., 2009). However, the LTL organisms have a direct effect upon the fish community, as they are the primary food source for larval fish and planktivores. The seasonal dynamics of the phytoplankton (which undergo a large spring bloom and smaller autumn bloom in temperate marine ecosystems (Truscott and Brindley, 1994; Winder and Cloern, 2010; Findlay, 2006))

could interact with the fish population in ways which have not yet been explored and lead to unforeseen possibilities.

This has led to a large movement towards the use of ecosystem-scale models in order to account for the potential feedbacks and interactions between different organisms within the marine ecosystem (Gaedke, 1995; Fulton et al., 2003a; Plagányi, 2007). The need to address ecosystem-scale questions has led to the rapid development of 'end-to-end' (E2E) models over the last ten years. E2E models couple together lower and higher trophic level organisms into one framework (Rose et al., 2010; Fulton, 2010), thus allowing for interactions between all organisms within the marine ecosystem.

We use an E2E model which couples together a phytoplankton-zooplankton box component model to a size-structured fish community model, henceforth called the PZ-Fish model (see Chapter 4). This E2E model allows for interactions between the phytoplankton, zooplankton and fish populations, and the minimal framework means that we are able to understand the effect that exploitation of the fish community has upon the dynamics of phytoplankton and zooplankton. We use this model to compare the size-at-entry and balanced harvesting strategies and to investigate the degree of disruption that these fishing schemes have upon the marine ecosystem.

5.2 Methods

A dynamic end-to-end model (the PZ-Fish model) which couples together phytoplankton (P, density of individuals of log(mass) x_P per m^{-3}), zooplankton (Z, density of individuals of log(mass) x_Z per m^{-3}) and a size-structured fish community ($u(x,t)$, density of individuals, of log(mass) x at time t, per m^{-3}) is used to investigate the effect of two different fishing strategies upon a marine ecosystem. The phytoplankton population is predated upon by zooplankton and fish; the zooplankton is predated upon by fish; and the fish of log(mass) x are predated upon by larger fish, and grow larger by eating smaller fish. The PZ-Fish model can be written as:

$$\frac{dP}{dt} = r_P P\left(1 - \frac{P}{P_{\max}}\right) - f(P)Z - A_P(u)P$$
$$\frac{dZ}{dt} = \alpha_Z f(P)Z - \mu_Z Z - A_Z(u)Z$$
$$\frac{\partial u(x,t)}{\partial t} = -\mu(x,t)u(x,t) - \frac{\partial(g(x,t)u(x,t))}{\partial x}$$

with

$$\mu(x,t) = \tilde{k} + \mu_s e^{\rho(x-x_s)} + \gamma w_0^q \int e^{x'q}\phi(x',x)u(x',t)dx'$$
$$g(x,t) = (1-\kappa)\alpha\gamma w_0^q e^{x(q-1)}B(x)$$

where

$$B(x) = \int e^{x'}\phi(x,x')u(x',t)dx' + \int e^{x_P}\phi_P(x)P(x_P)dx_P + \int e^{x_Z}\phi_Z(x)Z(x_Z)dx_Z \qquad (5.1)$$

with initial condition $P(0) = P^0, Z(0) = Z^0$ and $u(x,0) = u^0(x)$ for $x \in [x_{\min}, x_{\max}]$ and boundary conditions

1. $g(0,t)u(0,t) = \kappa \int g(x,t)u(x,t)e^{x-x_{\min}}dx$
2. $u(x,t) = 0$ for $x > x_{\max}$

where r_P is the phytoplankton growth rate (which is temperature- and nutrient-dependent), $P_{\max}$ is the phytoplankton carrying capacity (the maximum population abundance reached in the absence of predators), $f(P)$ is the zooplankton grazing rate upon phytoplankton, $A_P(u)$ is the fish community's grazing rate upon phytoplankton, $0 < \alpha_Z < 1$ is the zooplankton's conversion efficiency, μ_Z is the zooplankton's intrinsic mortality rate, $A_Z(u)$ is the fish community's grazing rate upon zooplankton, $x_{\min}$ is the minimum log(mass) of the fish community, $x_{\max}$ is the maximum log(mass) of the fish community, w_0 is the reference weight derived from the co-ordinate transform $w = w_0 e^x$, $\mu(x,t)$ is the fish community's size-dependent mortality rate (comprising intrinsic mortality, senescent mortality and predation) and $g(x,t)$ is the fish community's size-dependent growth rate (resulting through mass gained by consumption). We assume a Holling Type III functional response for the zooplankton's grazing upon phytoplankton, i.e. $f(P) = \frac{r_Z P^2}{C^2+P^2}$, where r_Z is the zooplankton's maximum grazing rate and C is a parameter describing the nonlinearity in the zooplankton's feeding response to prey abundance.

A sawtooth temperature profile is used to simulate the rapid warming of ocean waters. This has a direct effect on the phytoplankton population, as the phytoplankton growth rate is

assumed to be temperature- and nutrient-dependent. Thus, an increase in temperature leads to a faster phytoplankton growth rate.

This model is identical to the one used to study the impact of a warming climate upon a temperate marine ecosystem in previous work (see Chapter 4 for details). Table 5.1 lists the full definitions and units of the parameters used to formulate the PZ-Fish model, together with the default values used for the numerical simulations. Chapter 4 (Section 2) has details for the reasoning behind most of the default values used. The value of Z grazing rate, r_Z was chosen to be 1 day^{-1}, which is still within the empirical range of 0.6-1.4 day^{-1} reported by Edwards and Brindley (1999). This was due to a change in a parameter within the size-structured fish model, the fraction of consumed biomass which is allocated to reproduction, κ. A value of 0.4 was chosen for this study to try and lie within relatable, empirical ranges. A smaller value of r_Z was used to ensure that bloom dynamics still occurred when seasonally forced, under this new value of κ.

5.2.1 Fishing strategy

In this paper, we compare the effect that two different fishing strategies has upon a temperate marine ecosystem: size-at-entry and balanced harvesting.

Size-at-entry

The size-at-entry strategy assumes that the harvesting of the ecosystem is a fixed mortality rate upon fish larger than some chosen minimum body-size (w_F). In other words:

$$\mu_F^{SAE}(x,t) = \begin{cases} \tilde{\mu}_F & \text{if } x >= x_F \\ 0 & \text{otherwise} \end{cases} \tag{5.2}$$

where x_F is the chosen log(body-size) at which fishing begins and $\tilde{\mu}_F > 0$ is the fixed fishing mortality rate.

Balanced harvesting

Balanced harvesting assumes that fishing intensity is proportional to size-dependent productivity (Law et al., 2012; Jacobsen et al., 2014), where productivity (with units g m^{-3} day^{-1}) is measured as the total rate at which biomass passes through the ecosystem at each body

Table 5.1: Parameter definitions for the PZ-Fish model.

Parameter	Description	Unit	Parameter Value
PZ sub-model			
$\tilde{r}_P$	P growth rate at T=10°C [a]	day^{-1}	0.3
P_{max}	P carrying capacity	m^{-3}	2.2×10^5
r_Z	Z grazing rate	day^{-1}	1.0
C	Z Holling type III switching parameter[b]	m^{-3}	5.2×10^3
α_Z	Z mass conversion efficiency[a]	-	0.05
μ_Z	Z intrinsic mortality rate	day^{-1}	2.74×10^{-4}
ϕ_P	predation kernel on P	-	
ϕ_Z	predation kernel on Z	-	
w_P	P mass	g	9.12×10^{-7}
w_Z	Z mass	g	4.98×10^{-5}
Fish sub-model			
w_{min}	minimum body mass	g	1×10^{-3}
w_{max}	maximum body mass	g	3.3×10^3
w_0	reference weight, $w = w_0 e^x$	g	4.54×10^{-8}
Feeding terms			
γ	volume searched per unit time per unit mass^{q} [c]	$m^3\ day^{-1}\ g^{-q}$	1.64
q	search volume exponent[c]	-	0.8
α	mass conversion efficiency[c]	-	0.2
ϕ	feeding-kernel function	-	
β	log(preferred predator:prey mass ratio[c]	-	4
σ	feeding-kernel width[c]	-	2
κ	fraction of ingested energy allocated to reproduction	-	0.4
Mortality terms			
$\tilde{k}$	intrinsic mortality rate[c]	day^{-1}	2.74×10^{-4}
μ_s	senescent mortality rate[c]	day^{-1}	1.37×10^{-3}
ρ	senescent mortality exponent[c]	-	1.5
x_s	size-class at which senescent mortality is introduced[c]	-	log(60)
Fishing terms			
w_F	minimum body size for entry to the fishery	g	various
$\tilde{\mu}_F$	constant fishing rate	day^{-1}	various

[a] Truscott and Brindley (1994)
[b] Edwards and Brindley (1999)
[c] Law et al. (2009)

size. The productivity can be written as:

$$P(x,t) = w_0 e^x g(x,t) u(x,t)$$

where $g(x,t)$ is the growth dynamics described by Equation 5.1 and $w = w_0 e^x$ is the body mass of the fish (with units g). The fishing rate for the balanced harvesting strategy is thus, simply:

$$\mu_F^{BH}(x,t) = \begin{cases} \frac{\tilde{\mu}_F P(x,t)}{P(x_F,t)} & \text{if } x >= x_F \\ 0 & \text{otherwise} \end{cases} \tag{5.3}$$

The balanced harvesting fishing rate is divided by the productivity at x_F to ensure that the fishing rate is the same as the size-at-entry strategy at this chosen size-class. This it to try and facilitate a qualitative comparison between these two strategies. Jacobsen et al. (2014) scaled these two fishing rates so that the exploitation was the same across all strategies for fish weighing 444g, which is approximately equivalent to assuming a minimum body-size to the fishery of 10g.

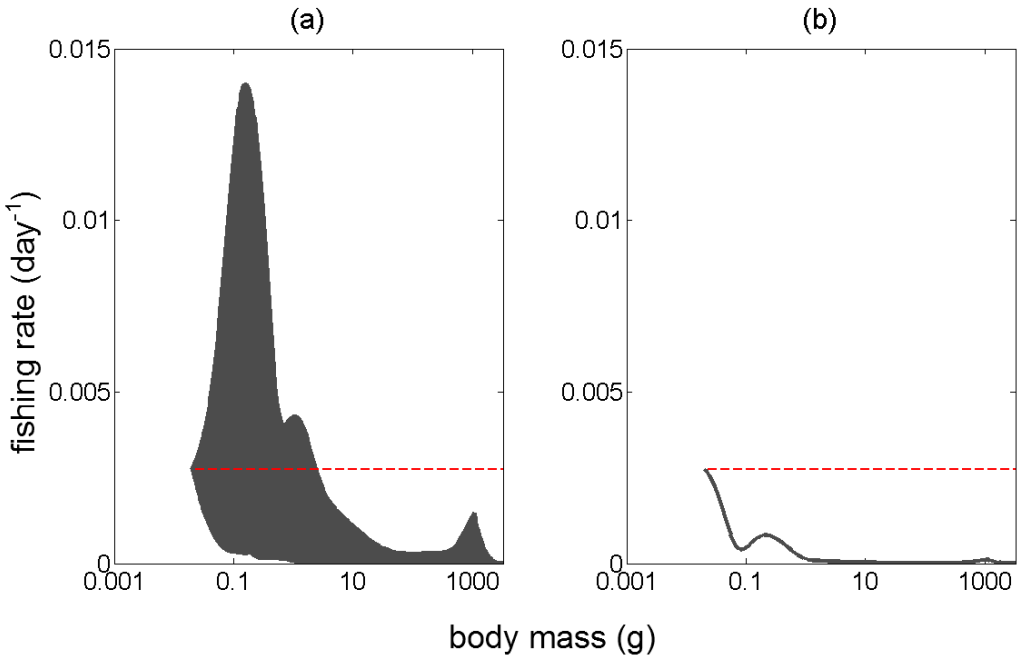

Figure 5.1: Comparing the size-at-entry (dashed red lines) and balanced harvesting strategies (solid grey lines), with $w_F = 0.02$g and $\tilde{\mu}_F = 1$ year^{-1}. (a) The range of fishing intensities over the course of one year and (b) The fishing intensity on day 1 of the year.

Figure 5.1 shows an example of the fishing intensity for each of these strategies over the course of one year, when $w_F = 0.02$g and $\tilde{\mu}_F = 1$ year^{-1}. As the balanced harvesting strategy is dependent on productivity, which varies over time, there is a range of fishing intensities over time for this scenario (see Figure 5.1a).

5.3 Results

Fishing undoubtedly leads to a disturbance of the marine ecosystem, but are some fishing schemes more disruptive than others? Does the benefit of the yield outweigh the cost of the disruption? We investigate this by exploring the effect that the choice of the minimum body size at which harvesting can begin (w_F) and the intensity of that fishing pressure ($\tilde{\mu}_F$) has upon the ecosystem. We use a range of minimum body sizes for the entry-size to the fishery, from $<$0.01g to 10g. These ranges are typical of industrial fisheries which are focused upon small zooplanktivorous species (Andersen and Pedersen, 2010), although previous studies have assumed fishing with a minimum entry-size to the fishery from 1g to 100g (Law et al., 2012) for a mackerel- or herring-like fish species, and 10g for an entire community of fish (Jacobsen et al., 2014). For each $(w_F, \tilde{\mu}_F)$-pairing, a no-fishing scenario is simulated for a year before being used as the initial condition for a ten year simulation, where either a size-at-entry or balanced harvesting strategy is practiced.

We measure the disturbance to the ecosystem in two ways:

1. The scaled time-averaged Euclidean distance between the phytoplankton populations when the fish community is harvested or not harvested
2. The period of the phytoplankton dynamics

5.3.1 Euclidean distance

Harvesting upon the fish community propagates through the marine ecosystem, and has a large impact upon the phytoplankton populations. Freund et al. (2006) utilised three distance measures in their study, to investigate the trajectories of phytoplankton and zooplankton concentrations under bloom and non-bloom modes. We use the same Euclidean distance measure here to see how close trajectories of the phytoplankton's population when the fish community is fished or not fished come to each other. d_P is defined as the time-averaged

Euclidean distance between the phytoplankton's density when the fish community is fished and not fished.

$$d_P = \left(\sum_{t}^{\tau} \sqrt{\left(P_F(t) - P_{NF}(t)\right)^2} \right) / \tau \tag{5.4}$$

where $P_F(t)$ is the phytoplankton density at time t when the fish community is harvested, $P_{NF}(t)$ is the phytoplankton density at time t when the fish community is not harvested and τ is the number of days which the distance measure is being averaged over. Similar distance measures were used for zooplankton, and for the entire ecosystem, but as the largest effects were seen in the phytoplankton population, we only present these results here.

When d_P is a small value, there is only a small qualitative change in the dynamics of the phytoplankton population (see Figure 5.2(a), where $d_P = 0.004$). A large qualitative change in behaviour is measured through a large distance value. Figure 5.2(b) shows $d_P = 0.104$, which is 2 magnitudes larger than before.

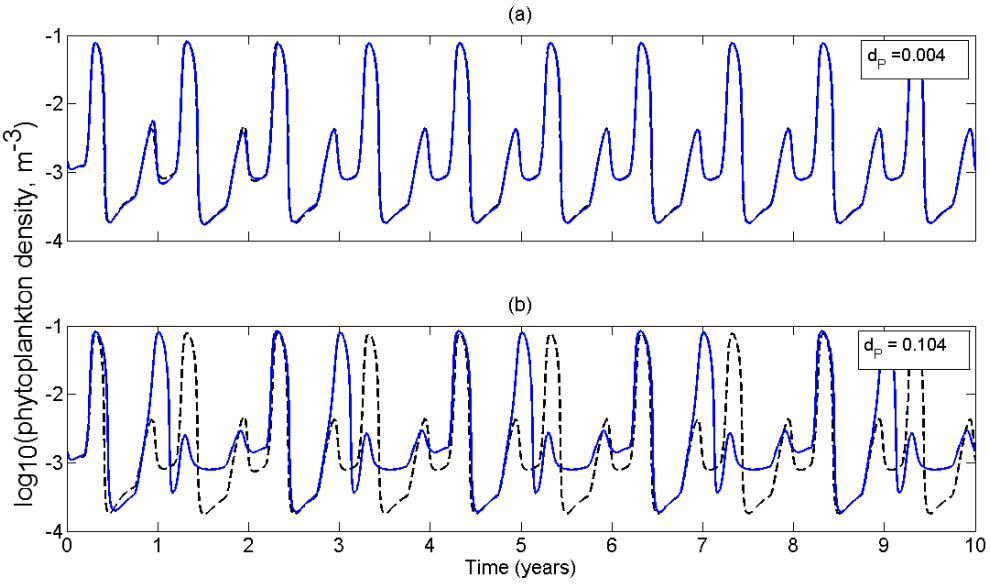

Figure 5.2: Two examples of the effect that harvesting upon the fish community has upon the phytoplankton density, where the phytoplankton density under a no-harvesting scenario for the fish community, $P_{NF}(t)$ (dashed black lines), is compared to the phytoplankton density when the fish community is harvested, $P_F(t)$ (solid blue lines). (a) A small change to the dynamics leads to a small value of $d_P = 0.004$ and (b) a large change to the dynamics leads to a larger value of $d_P = 0.104$.

Figure 5.3 shows the time-averaged Euclidean distance, and has been scaled to a value between 0 and 1 in order to allow for a comparison between the size-at-entry and balanced

(a)

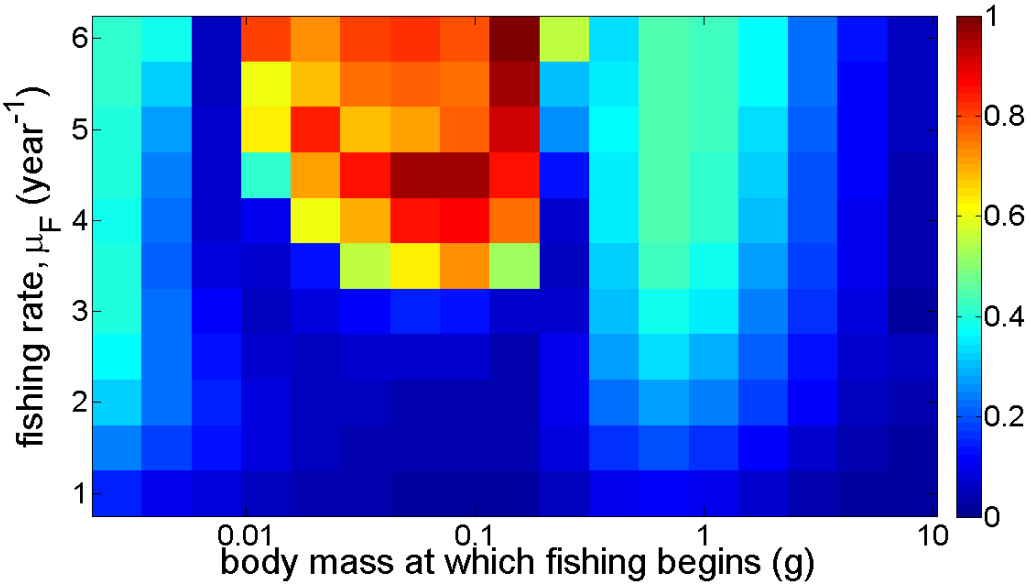

Figure 5.3: The time-averaged Euclidean distance between the phytoplankton populations when the fish community is harvested or not harvested for (a) the size-at-entry fishing strategy and (b) the balanced harvesting strategy.

harvesting strategies. The distance measure shows that the chosen minimum body-size at which fishing begins is the dominant factor in the disruption to the marine ecosystem. However, the distance measure for the balanced harvesting strategy (Figure 5.3b) shows minimal changes to the phytoplankton population when fishing begins at 1g, whereas the size-at-entry strategy shows a significant difference in this region between the phytoplankton populations when the fish community is harvested or not harvested. Overall, the balanced harvesting strategy can be applied over a much larger range of fishing $(w_F, \tilde{\mu}_F)$-scenarios than the size-at-entry strategy, whilst causing less disturbance to the phytoplankton populations.

When a minimum body-size of just under 0.01g is chosen for the fishery, then there is a notable change to the phytoplankton population. These are the size-classes of fish which are feeding predominantly on the zooplankton population. The higher mortality rate upon these fish leads to a release in the predation pressure upon zooplankton, thus the zooplankton population increases. This in turn leads to a decrease in the phytoplankton population as their predation pressures by the zooplankton increases. Hence this fishing strategy has a direct impact upon the marine ecosystem. Under a balanced harvesting strategy, these small-sized fish have a high productivity and are fished upon more intensely than under a size-at-entry strategy. This leads to a greater disruption to the phytoplankton population under lower fishing intensities when using a balanced harvesting approach.

The greatest impact to the phytoplankton population occurs when harvesting upon fish stocks begins with a chosen minimum body-size of about 0.1g. These are the size-classes of fish which are feeding predominantly on the planktivores. As before, there is a trophic cascade effect through the marine food web, due to the direct impact of fishing. It is a much more pronounced effect than the previously described case as there are more feedbacks occurring when fishing upon this trophic level. Fishing on individuals of body mass 0.1g leads to a decrease in the predation pressure upon the planktivores, whose population density then increases. This in turn decreases the zooplankton population and increases the phytoplankton population. However, by increasing the phytoplankton population, there is more food available for larval fish and planktivores, who uses the available food to grow quickly through the fish community. Thus the feedbacks that occur between the trophic levels can lead to the occurrence of complex dynamics.

There is a noticeable absence of a strong feedback to the dynamics of the phytoplankton when a minimum body-size of 1g or larger is chosen for the fishery. The trophic cascade that is initiated by fishing is damped as it travels further away from the perturbed trophic level (Andersen and Pedersen, 2010). Thus, when the cascade reaches the zooplanktivores (or other small fish that have a diet which includes zooplankton), the effect that it has upon them is minimal and does not trigger a strong reaction in the phytoplankton population.

5.3.2 Period of the phytoplankton dynamics

Section 5.3.1 shows that the choice of fishing strategies can lead to a large disruption of the marine ecosystem. One of the consequences to the marine ecosystem is the change in the periodic behaviour of the phytoplankton population. In general, phytoplankton undergoes a spring bloom due to increased temperature, nutrient availability and light intensity (McCauley and Murdoch, 1987; Moisan et al., 2002; Townsend et al., 1994). The phytoplankton then undergoes a smaller autumn bloom due to an increase in nutrients through mixing and diffusion into the upper mixed layer from the lower layer of the water column (Findlay, 2006). This behaviour occurs on an annual basis, in other words, with a period of 1 year^{-1}.

Figure 5.4 shows that the periodicity of the phytoplankton population changes under different fishing scenarios. The size-at-entry and balanced harvesting fishing strategies cause six different dynamic behaviours within the phytoplankton population, from aperiodic (henceforth labelled as period-0) to period-5 dynamics.

To determine the periodicity of the phytoplankton population, a fast Fourier transform was applied to the phytoplankton data. The fast Fourier transform converts time to frequency, and thus can indicate the strongest frequencies that occur in time-series data. The period is simply the inverse of the frequency: the peaks of the fast Fourier transform indicate the strongest periodic behaviour within the phytoplankton behaviour. The fast Fourier transform can be written as:

$$\hat{f}(\xi) = \sum_{j=1}^{N} P(j) \left(e^{(-2\pi i)/N} \right)^{(j-1)(\xi-1)} \tag{5.5}$$

where N is the number of points the transform is applied to and P is the phytoplankton density over ten years.

Figure 5.5 shows the results of a fast Fourier transform, and the resultant dominant period of the phytoplankton's dynamics when there is no harvesting upon the fish community. As can be seen in Figure 5.5a, there is a strong peak at period 1, indicating that the dominant period is the recognised annual large spring bloom/small autumn bloom case.

Figure 5.6 shows the different periodic behaviours that the phytoplankton population undergoes, depending on particular $(w_F, \tilde{\mu}_F)$-fishing scenarios. As can be seen, the majority of the fishing scenarios do not disrupt the phytoplankton population's seasonal dynamics, as the

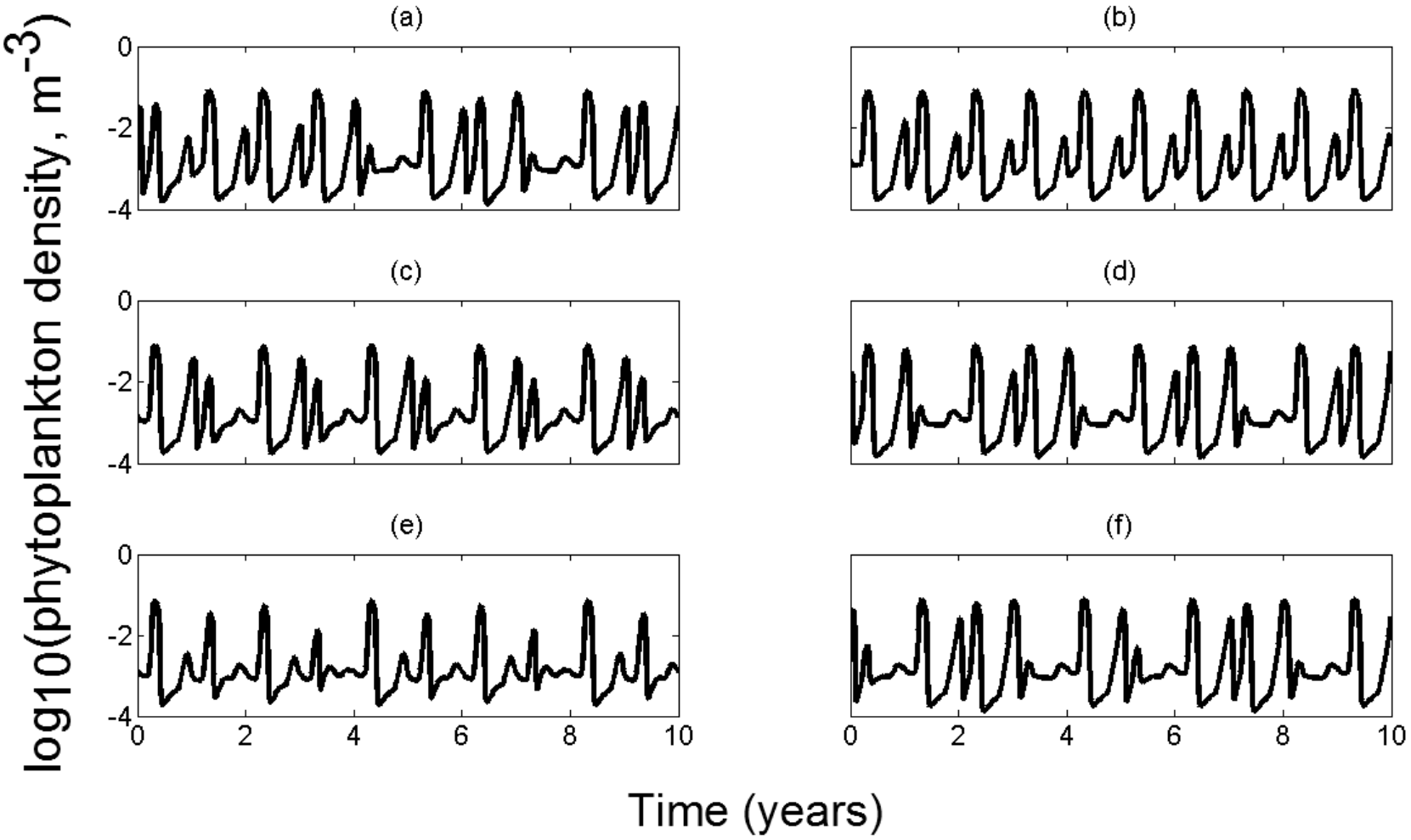

Figure 5.4: Different fishing scenarios lead to six types of dynamics occurring in the phytoplankton population. (a) Period-0 (or aperiodic) (b) period-1 (c) period-2 (d) period-3 (e) period-4 and (f) period-5 dynamics, shown over a ten year simulation. See later for Figure 5.6 for examples of fishing scenarios which lead to these different dynamical behaviours.

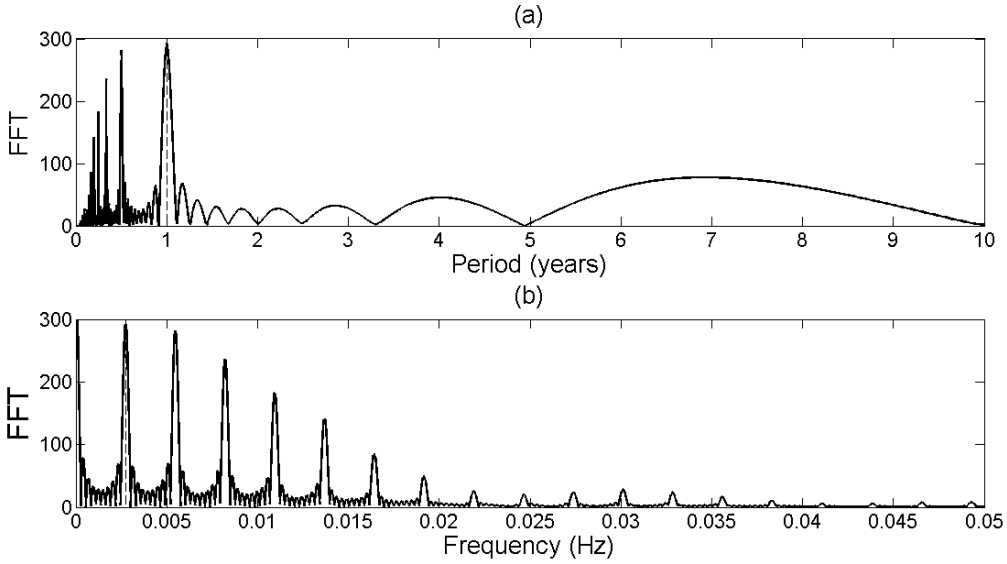

Figure 5.5: When there is no fishing on the marine ecosystem, the phytoplankton population exhibit period 1 dynamics. The fast Fourier transform (FFT) indicates the dominant (a) frequency and (b) period in the phytoplankton population.

period-1 behaviour is the most dominant.

The size-at-entry fishing strategy shows three clear regions of disturbance to the dynamics of the phytoplankton population, which refine those regions distinguished by the Euclidean distance measure (see Figure 5.3a). The regions centred at fishing with a minimum body mass $<$0.01g and 1g were the least affected by the fishing strategy, and can be seen in Figure 5.6a that the phytoplankton population has period-2 or period-4 dynamics within these regions. Thus, the phytoplankton population undergo a large spring bloom, followed by a smaller autumn bloom every two years (which is of the same magnitude as in the period-1 case), but then has a relatively small spring bloom and no significant autumn bloom in the second year (see Figure 5.4c). The region centred at fishing with a minimum body mass 0.1g shows the largest range of periodic dynamics within the phytoplankton population, with period-0, period-2 and period-3 dynamics occurring under these fishing scenarios.

The balanced harvesting strategy shows only two clear regions of dynamical change in the behaviour of the phytoplankton. As with the size-at-entry strategy, there is a region of disturbance centred around fishing scenarios which begin harvesting at body mass $<$0.01g, and this region again shows period-2 dynamics. The second region of disturbance, centred around fishing with a minimum body mass 0.1g, covers less potential $(w_F, \tilde{\mu}_F)$-scenarios than under the size-at-entry strategy. The region spans fishing scenarios where harvesting begins on fish of size 0.01g to about 0.15g, whereas the comparable region for the size-at-entry strategy spans a range of 0.01g to 0.25g. However, the balanced harvesting strategy also shows that significant changes to the phytoplankton population can occur under less in-

(a)

(b)

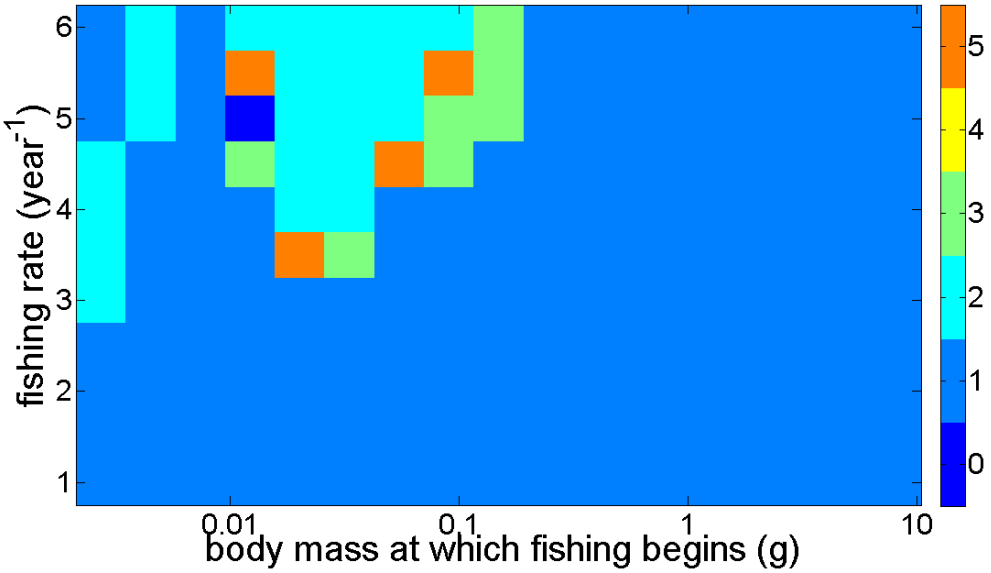

Figure 5.6: The periodicity of the phytoplankton's dynamics when the fish community is harvested using (a) the size-at-entry fishing strategy and (b) the balanced harvesting strategy. The choice of body mass at which fishing begins and the intensity of the fishing pressure leads to six different types of dynamical behaviours occurring in the phytoplankton population (from period 0 to period 5), as seen in Figure 5.4. In general, the fishing intensity has to be greater than 3 year^{-1} to impact the phytoplankton population.

tensive fishing pressures: within this region, a fishing pressure of 3.5 year^{-1} can drastically affect the periodic behaviour of the phytoplankton, whereas a fishing pressure of 4 year^{-1} is needed under the size-at-entry strategy to impact the phytoplankton's dynamics.

The changes in the periodic behaviour of the phytoplankton are caused by the changes in the fish community's dynamics when it is harvested upon, and in particular, the rate at which the fish graze upon the zooplankton population. Figure 5.7 shows the predation rate of fish upon zooplankton for three different fishing intensities. These scenarios were chosen as the phytoplankton's dynamics transition across three different periodic behaviours under these fishing intensities, under the balanced harvesting strategy. For the size-at-entry strategy, the phytoplankton has period-1 dynamics under each fishing intensity shown. Figure 5.7a shows that the exploitation of fish is minimal, and thus there is no significant difference change to the phytoplankton's dynamics.

When the fishing rate is increased from 3 year^{-1} to 3.5 year^{-1}, the phytoplankton's dynamics alter from period-1 to period-5 under a balanced harvesting strategy. As can be seen in Figure 5.7b, the peak in $A_Z(u)$ can occur earlier than at a lower fishing intensity. When this happens, there is a sudden drop in the zooplankton's abundance due to the increased pressure from predation, which releases the phytoplankton population and allows it to bloom to high abundances. A dynamical phase-plane analysis of the effect of increasing fishing intensities has upon the phytoplankton and zooplankton populations can be found online, where three movies of these described scenarios show the range of behaviours that can occur (please visit http://www.youtube.com/playlist?list=PLWBS2IgRW2JT7bx-7MPM6K2hwYLW4jios to view these movies).

The reaction of the phytoplankton population to different fishing scenarios could have a major impact upon sustainable fisheries management. If the seasonal behaviour of the phytoplankton varies yearly (or over multiple years), this could mean that the yield achieved by fisheries becomes much more variable. This would have economic and ecological consequences.

5.3.3 Yield

Yield is measured as the total biomass obtained through harvesting the fish community, and can be calculated as $Y = \int w_0 e^x \mu_F(x,t) u(x,t) dx$ (with units g day^{-1} m^{-3}).

Figure 5.8 shows that when the dynamics of the marine ecosystem are considerably affected by exploitation, this can have a significant impact upon the yield. Figure 5.8b and c show

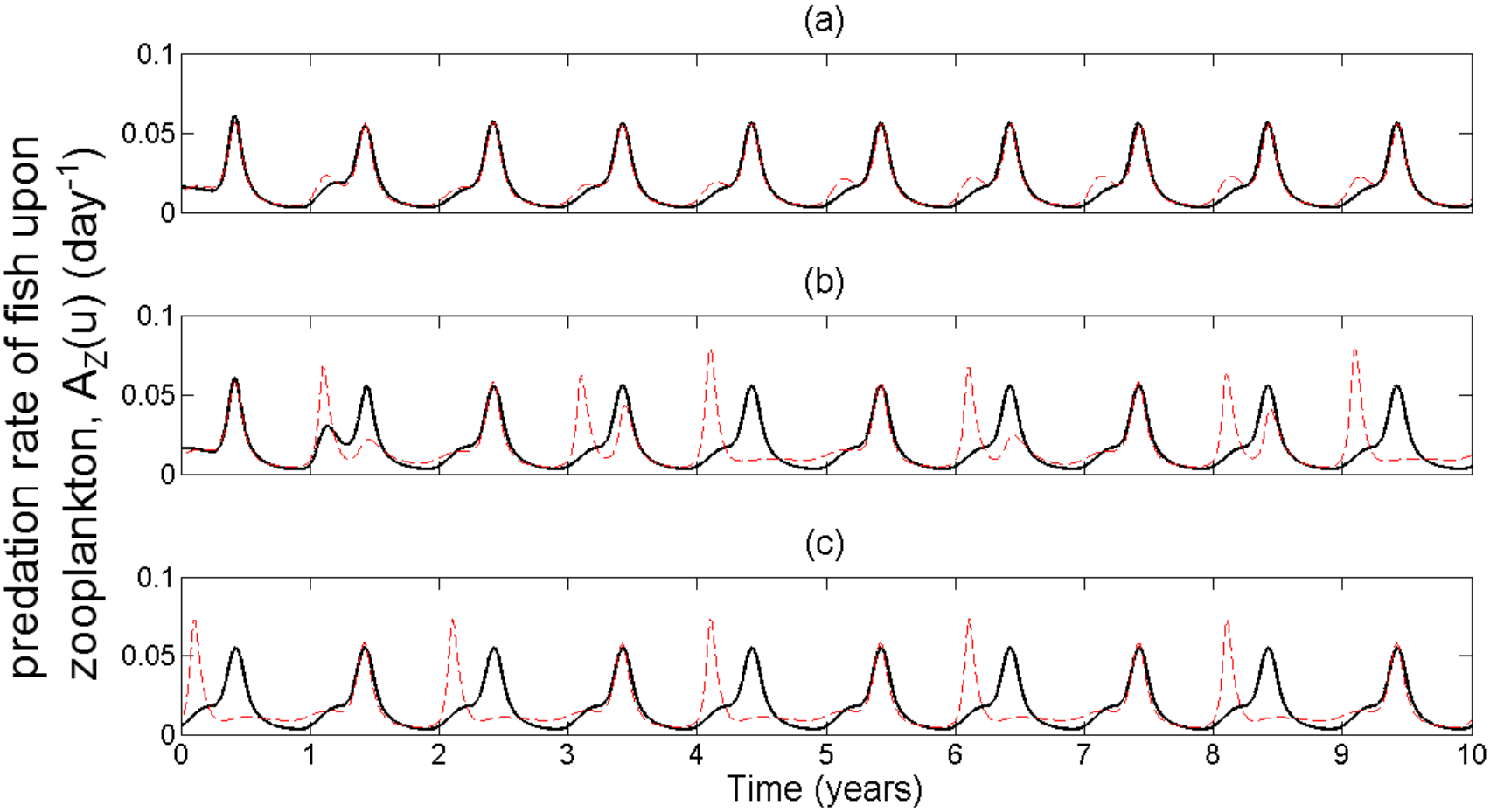

Figure 5.7: The dynamics of the fish community has a direct effect upon the zooplankton population, via their predation upon them. This impact upon the zooplankton population feeds back to the phytoplankton population, and has major consequences to their periodic dynamics. Three fishing intensities, where harvesting begins on individuals of body mass 0.02g, are shown and contrasted, with the size-at-entry strategy represented by the solid black lines and the balanced harvesting strategy represented by the dashed red lines. The periodic dynamics under the size-at-entry fishing strategy remains at period-1 for each fishing intensity, but varies for the balanced harvesting strategy. (a) $\tilde{\mu}_F = 3$ year^{-1} leads to period-1 dynamics, (b) $\tilde{\mu}_F = 3.5$ year^{-1} leads to period-5 dynamics and (c) $\tilde{\mu}_F = 4$ year^{-1} leads to period-2 dynamics

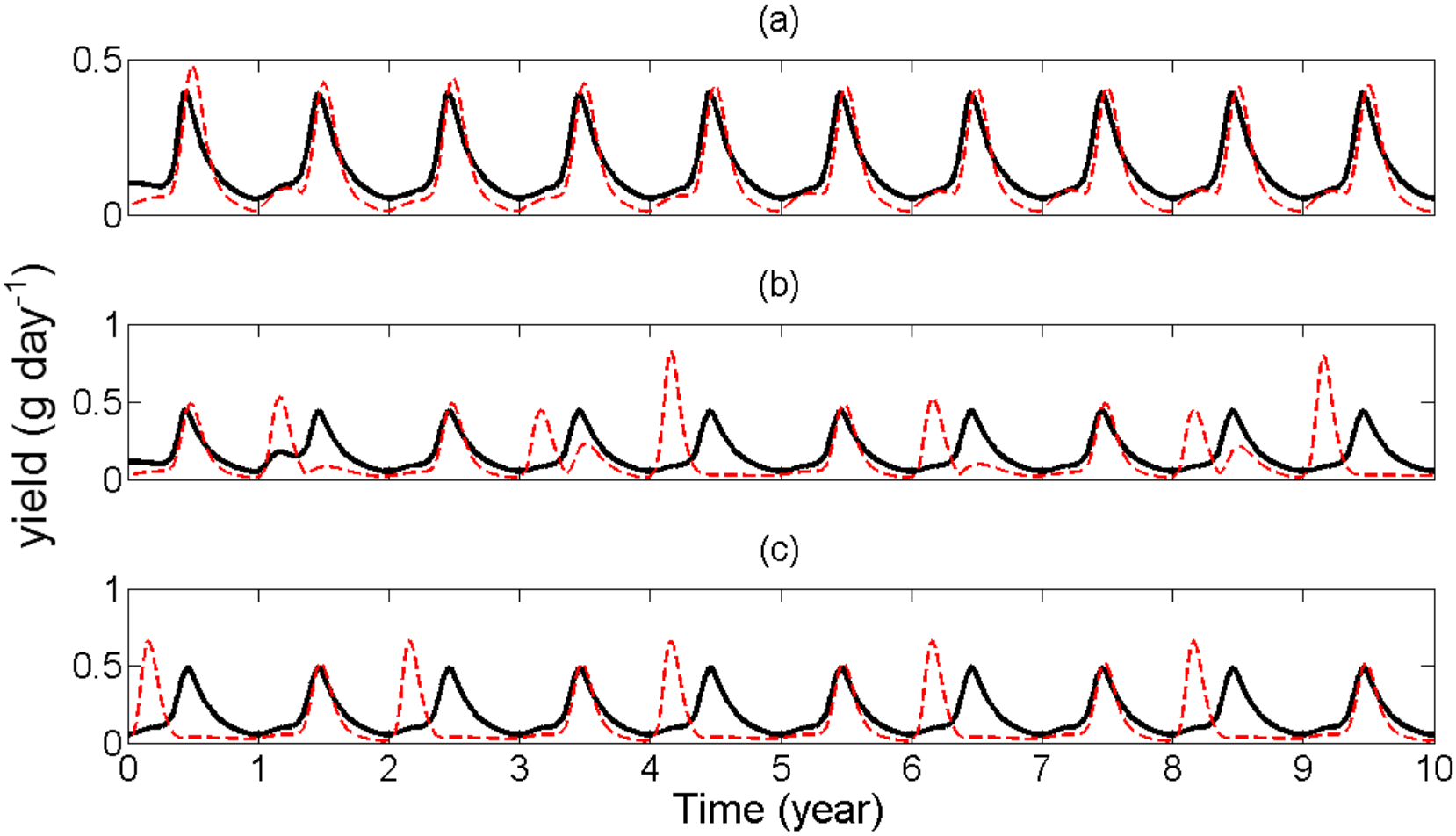

Figure 5.8: The yield obtained under the size-at-entry strategy (solid black line) and the balanced harvesting strategy (dashed red line), when fishing begins on individuals of body mass 0.02g for three different fishing intensities: (a) $\tilde{\mu}_F = 3$ year^{-1}, (b) $\tilde{\mu}_F = 3.5$ year^{-1} and (c) $\tilde{\mu}_F = 4$ year^{-1}

that when the natural period-1 dynamics of the phytoplankton are disrupted, the yield can appear more variable and unpredictable. Consider the period-2 dynamics case: when there is a year with a relatively small spring bloom, this impacts the zooplankton population which also has a relatively low density season. Thus, there is less food available for the planktivores in the fish community, and less biomass overall within the fish community. This leads to a relatively low-yield year.

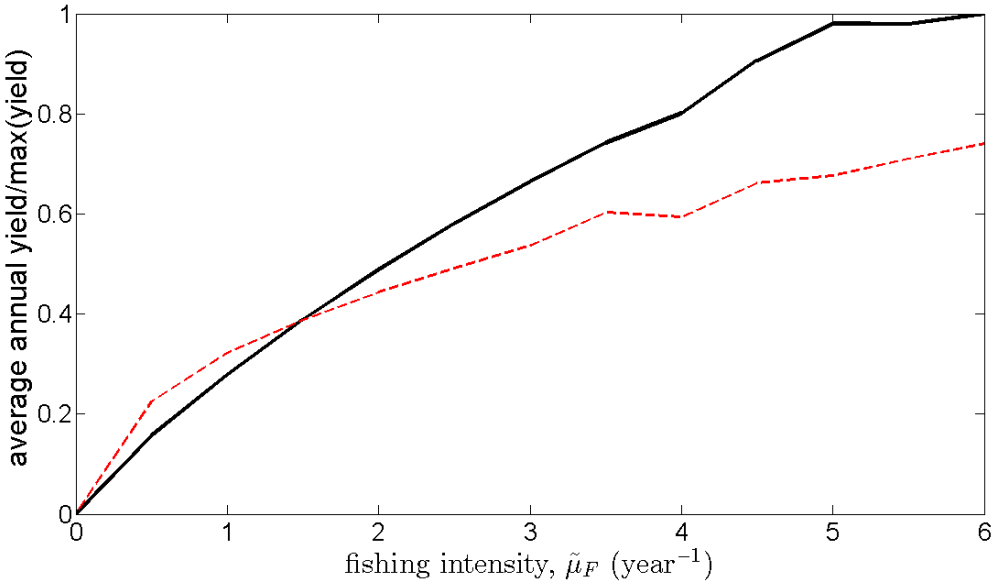

Figure 5.9: The averaged annual yield (normalised by dividing over the maximum obtained yield) for the size-at-entry strategy (solid black line) and the balanced harvesting strategy (dashed red line), when fishing begins on individuals of body mass 0.02g.

Figure 5.9 compares the averaged annual yields obtained under the size-at-entry and balanced harvesting strategies (where the yields were averaged over ten years), for the scenario where fishing begins upon individuals of body mass 0.02g. The results show that under low fishing intensities, the balanced harvesting strategy achieves a higher average annual yield than the size-at-entry strategy. However, once a fishing pressure of about 1.5 year^{-1} is exerted upon the ecosystem, the size-at-entry strategy achieves the higher average annual yield.

5.4 Discussion

The results of this study show that harvesting fish populations can have a significant impact upon the dynamics of phytoplankton. Whether a size-selective or balanced harvesting strategy is exerted upon a marine ecosystem, small changes in the fishing intensity can cause the phytoplankton dynamics to shift from a predictable annual pattern, to something much less

predictable where there are bloom and non-bloom years.

There have been several investigations into the potential trophic cascades that can occur in marine ecosystems due to over exploitation of top predators. Casini et al. (2008) showed that a reduction of cod in the Baltic Sea had direct effects upon its main prey, the zooplanktivorous sprat, but also indirect effects upon the zooplankton and phytoplankton populations. Thus, a top-down cascade could feedback all the way down to the level of the primary producers, highlighting the importance of an ecosystem-scale approach to sustainable fisheries management. Casini et al. (2008) also proposed that, while the intensity of the spring bloom is mainly affected by the previous winter's nutrient level, the summer (or early autumn) bloom is a top-down driven process caused by the interactions with the fish community. Our results indicate that the causes of the spring and autumn blooms are not easily separated into top-down and bottom-up (nutrient-driven) reasonings, but rather that the relationship between fish and the lower-trophic-level organisms leads to dynamical changes which occur over a long time-scale.

Figure 5.4 shows that the phytoplankton dynamics can shift from the typical period-1 dynamics observed in temperate marine ecosystems, to much more complex behaviours such as period-5 and period-0 dynamics. Zohary (2004) analysed the phytoplankton record from Lake Kinneret, the only freshwater lake in Israel, from 1969 to 2002. She shows that there exists two distinct periods within this record. Firstly, between 1969 and 1993, the phytoplankton dynamics exhibited distinctly stable periodic dynamics which occurred annually, centred on a spring bloom of dinoflagellate. However, the second period occurs between 1994 and 2002, where there is a loss of the previously predictable pattern: instead, there are bloom and non-bloom years which occur. There were two major perturbations which took place in Lake Kinneret between these periods: (i) the collapse of the fishery of Kinneret Bleak and (ii) the re-flooding of dried peat-soils in the lake's catchment. The collapse of the fishery led to a 'bleak dilution program', where sub-commercially sized fish were harvested annually, as well as the over-fishing of other commercial species. Although a cause-and-effect relationship between the bleak fishery and the major changes in the phytoplankton dynamics cannot be inferred, our results show that under intensive harvesting of fish stocks, the dynamics of the phytoplankton population can dramatically shift behaviours.

Figure 5.3 and Figure 5.6 both indicate that there are distinct regions within potential fishing scenarios which lead to a disturbance in phytoplankton dynamics. This is likely a model artefact, due to the aggregation of phytoplankton populations into one group, and similarly for zooplankton. Thus, the largest changes to the phytoplankton's dynamics occur when fishing pressure is exerted directly upon those fish species which have the strongest linkage to the phytoplankton and zooplankton populations. Although such noticeable trophic cascades can occur in marine ecosystems, such as the cod-induced cascade in the Baltic Sea (Casini et al.,

2008) or the fishing-induced cascade in the Black Sea (Daskalov et al., 2007), these circumstances are rare. Further work is needed to explore the consequences of the aggregation of the phytoplankton and zooplankton populations, as we would expect more 'diluted' regions of disturbances to occur when considering a less amalgamated approach.

Implications for fisheries management

Regardless of the strategy applied for harvesting fish populations, our results have shown the clear consequences that exploitation of top predators has upon primary producers. Figure 5.8 shows the clear link between primary production and fisheries yields, and highlights the importance of a holistic view towards fisheries management (Chassot et al., 2007; Travers et al., 2007). The results show an absence of a strong feedback to the dynamics of the phytoplankton population for fisheries with a size-at-entry of 1g and larger, and while North Sea fisheries operate with entry sizes of 100g to 1000g (Law et al., 2012; Jacobsen et al., 2014; Andersen and Pedersen, 2010), understanding the potential impact of fishing at lower limits for the size-at-entry is important for developing future strategies. For example, the balanced harvesting strategy would predominantly harvest fish of a very small size (likely with a body mass less than 1g), as these fish have the highest productivity in the marine ecosystem.

Size-selective fishing strategies can lead to major disturbances in the marine ecosystem (O'Brien et al., 2000; Hutchinson, 2008; Reznick and Ghalambor, 2005; Enberg et al., 2011), and these disturbances can potentially occur over a wider range of fishing scenarios than a balanced harvesting approach. A balanced harvesting strategy can still have the same significant impact upon the dynamics of the primary producers, but it can also reduce the disruption to the size distribution of the marine ecosystem (Law et al., 2012), thereby preserving the structure and biodiversity of the ecosystem. However, the major disadvantage to using a balanced harvesting strategy is the ability to parameterise it accordingly to the natural productivities of species (Jacobsen et al., 2014). Compromises could be made for practical implementation, whereby the natural productivity is measured per season of the year rather than per day.

Balanced harvesting is a promising management strategy which protects the size-structure of marine ecosystems whilst achieving higher fisheries yields than a size-at-entry strategy. Yet it can have the same disruptive influence upon the underlying phytoplankton's dynamics as size-selective fishing strategies, with the shifts in the phytoplankton's dynamics leading to more variable fisheries yields.

Acknowledgements

We thank Gustav Delius and Jamie Wood for their helpful insights. This research was supported by a joint studentship to CW from the Centre for Environmental Fisheries and Aquaculture Science UK and the University of York UK.

Chapter 6

General Discussion

6.1 Summary and Synthesis

Marine ecosystems are of huge importance to human society: as a source of food, for economic growth and for mitigating climate change (Vitousek et al., 1997; Botsford et al., 1997; Levin and Lubchenco, 2008; Boyd and Doney, 2002; Hoegh-Guldberg and Bruno, 2010; Jin et al., 2003). Human activities, such as the overexploitation of commercially important fish stocks (Worm et al., 2009), have led to large-scale changes in the fish communities. One such change has been in the size and species composition of the fish communities (Jennings et al., 2002). These changes have consequences in the yield obtained through fishing, where the catch is dominated by smaller-sized fish (Reznick and Ghalambor, 2005; Enberg et al., 2011), as well as the biodiversity within the marine ecosystems (Bianchi, 2000). Human activities have also had an indirect effect upon marine ecosystems through climate change (Hoegh-Guldberg and Bruno, 2010): the warming of the sea surface temperatures have affected biological processes (such as the growth rate of phytoplankton (Moisan et al., 2002)), as well as depleted oceanic oxygen leading to dead zones in the ocean (Diaz and Rosenberg, 2008). The potential role of the ocean in mitigating climate change by acting as a sink for atmospheric carbon dioxide (Siegenthaler and Sarmiento, 1993; Boyd and Doney, 2002; Yool et al., 2013) has also lead to humans having a direct influence upon marine ecosystems, through large-scale iron fertilisation experiments (Coale et al., 1996; Blain et al., 2007).

Marine ecosystems are complex systems, where lower-trophic-level organisms interact with higher-trophic-level organisms, and their dynamics are intricately affected by each other. Taking account of their interactions and their consequences for managing fisheries sustainability is the basis for an ecosystem-based approach to fisheries management (Rose et al., 2010; Fulton, 2010).

Over the last ten years, there has been a huge interest in 'end-to-end' (E2E) modelling, where hydrodynamic models (representing the environmental forcing of the ocean), biogeochemical models (representing the utilisation of nutrients by the lower-trophic-level (LTL) organisms) and fish production models (representing higher-trophic-level (HTL) organisms) are coupled together into one framework (Rose et al., 2010). The common approach for constructing E2E models has been to couple together existing submodels that represent the LTL and HTL organisms (Aydin et al., 2005; Libralato and Solidoro, 2009; Travers et al., 2009; Fennel, 2010; Kishi et al., 2011). Biogeochemical models of LTLs tend to represent the organisms through functional groups (Kishi et al., 2007; Travers et al., 2009), whereas fish production models are frequently species-centric. Thus, the "structure" of the coupled models are significantly different. There is also a vast difference in the "resolutions" used in the isolated submodels: LTL models divide the functional groups into 1-3 size-classes at most (such as small, large and carnivorous), whilst HTL models use a much finer resolution. Travers et al. (2009) used 11 size-structured fish populations within their E2E model, whilst Fennel (2010) used 7 size-classes to represent the life cycle of cod. Only by understanding the implication of coupling together models which differ at the component level can E2E models be used to predict ecosystem changes due to environmental stressors. This thesis provides a systematic investigation into the effects of coupling together models which differ in their "structure" and "resolution", to aid in the differentiation between ecosystem-scale effects and numerical artefacts due to these fundamental differences.

6.1.1 The discretisation of size-structured models

Size-structured models are commonly used in E2E models to represent the population dynamics of HTL organisms (Travers et al., 2009; Maury, 2010). There are many advantages to size-structured models, particularly for E2E modelling, as they promote model simplicity and tractability in complex frameworks, as well as providing useful indicators for measuring the status of an ecosystem (Pope et al., 2006). The McKendrick-von Foerster partial differential equation models an age-structured population (Kot, 2001), and a variant of this equation has been widely used to model size-structured populations (Benoît and Rochet, 2004; Andersen and Beyer, 2006; Law et al., 2009), where the abundance of the population is dependent on body size and time.

Partial differential equations (PDEs) are usually studied using numerical methods due to the challenges faced with formal mathematical analysis, although great strides have been taken in this direction by assuming scale invariance (Capitán, 2010; Datta et al., 2011). Numerical methods involve partitioning the domain space into a grid and approximating the PDE at these discrete points (Lax, 1965; Press et al., 2007). Numerical methods require care to

ensure that they are numerically stable and that the integrations converge to the numerical approximation (Lax, 1965); these factors are dependent on the choice of discretized step sizes. In **Chapter 2** of this thesis, I studied the effect that the choice of numerical resolution had upon the large-scale behaviour of a size-structured fish community. I derived a numerical stability condition which showed that size spectrum models could be numerically stable under coarse resolutions (i.e. a large step size for the size-classes is chosen). However, whilst the system may be numerically stable when coarsely resolved, the level of discretisation also affects the slope of the size spectrum, and its mathematical stability.

The changes in the large-scale behaviour of the fish community under different discretisations of the numerical scheme are primarily due to the implementation of the feeding kernel (Baird and Suthers, 2007). At coarse resolutions, the predator has a limited number of prey available to feed upon, which limits its somatic growth and thus impacts the final abundances and slope of the size spectrum. As the discretisation becomes finer, the number of prey available to the predator increases: continuing the discretisation allows the range of available prey to converge to the continuous limit. With a greater number of prey available for feeding upon, the predator is able to allocate more biomass to somatic growth, and thus there is a higher abundance of large fish species at finer resolutions. The effect that the choice of numerical resolution has upon model behaviour has been shown in mathematical modelling studies (Baird and Suthers, 2007; Picard et al., 2010), as well as in the construction of empirical size-spectra (Han, 1998; Kerr, 1974; Sheldon et al., 1977; Mancinelli et al., 2008). The results from **Chapter 2** shows the necessity of recognising the role that the choice of numerical method has upon biological interpretations, and that consideration of numerical resolution must be addressed in size-structured modelling.

6.1.2 Model architecture and understanding its impact upon the dynamics of end-to-end models

Understanding the effect that model architecture has upon the large-scale behaviour of a model is as important as understanding the effect that the choice of numerical method has upon it. Historically, models of LTL and HTL organisms have been developed from very different perspectives. Biogeochemical models have been most commonly used for modelling LTL populations: these models focus on the flux of a key nutrient (usually nitrogen) through the biological components of phytoplankton and zooplankton. These biogeochemical models are coupled to hydrodynamic models which capture the physical elements of the ocean (such as the wind speed and sea surface temperature) (Blackford, 2004), and attempt to realistically model the dynamics of primary production. The population dynamics of HTL organisms have been developed from the perspective of fisheries management (Travers et al.,

2009), with a focus of optimising yields of exploited fish stocks whilst maintaining a strong spawning-stock population (Lassen and Medley, 2001; Magnusson, 1995). The different focus that has led to the development of biogeochemical and food web/fish population models has meant that these models vary significantly with the scales used (both spatial and temporal (Carlotti and Poggiale, 2010)), the structure of the biological components (from functional groups for LTL organisms and fish species for HTL organisms) and the resolution of the biological components (from 1-3 zooplankton groups (Steele et al., 2007) to finely-resolved (for approximating continuous PDEs) size-structured models with 101 size-classes (Maury et al., 2007).

Developing a dynamic E2E ecosystem model is not a straightforward task, particularly when coupling together models which were created for different purposes. Not only are there practical considerations (functional groups which are defined in the LTL model may not be in the HTL model, thus requiring a 'library' to be created to enable the two submodels to communicate), but the fundamental differences of the frameworks for the submodels may have consequences upon the ecosystem-scale behaviours. In **Chapter 3**, I developed a dynamic E2E model using a minimal framework (henceforth known as the PZ-Fish model): I represented the LTL organisms with two box components for the phytoplankton and zooplankton, and used a size-structured fish community model to represent the HTL organisms. This minimal framework mimics those used in current E2E models (Travers et al., 2009; Fennel, 2010; Megrey et al., 2007). I compare these results to the previously defined HTL model - the size-structured fish community model where the LTL organisms are represented by a static resource spectrum.

With this minimal framework, I studied the steady-state solutions of the ecosystem model. The results show that if only measures of the steady-state solutions are studied (such as the abundances of the organisms within the ecosystem, the total biomass within the ecosystem or the slope of the size-spectra), then the E2E model yields results which appear plausible and comparable to empirical observations. It is only when studying the underlying life histories within the model that the effect of the choice of model architecture can be seen. The growth trajectory of an individual larval fish in the E2E model grows much slower, and to a smaller maximum size, than a larval fish in the HTL model. Both models lead to fish growing at a slower rate and to a smaller maximum size than seen in real data. Santos et al. (2002) measured a range of species of fish of the Algarve coast, with maximum body sizes ranging from 8g to over 1000g, whereas the average fish in the HTL model grows to a maximum size of about 5g and to only 0.1g in the E2E model. The difference in the growth trajectories is due to the representation of the LTL organisms - the E2E model assumes that the LTL organisms are two compartments of phytoplankton and zooplankton and thus the larval fish are limited by the supply of prey available to them.

DeYoung et al. (2004) proposed that a rhomboid strategy be used for modelling pelagic ecosystems, where the trophic level or population of interest is modelled at the highest resolution, and that the resolution decreases at higher or lower trophic levels. Speirs et al. (2010) use the rhomboid strategy to explicitly model the populations dynamics of cod and the nine North Sea species which potentially have the strongest interaction with cod. Using this approach, Speirs et al. (2010) showed that the population of herring has a strong impact upon the cod populations, and in particular, that the maximum sustainable yield of cod is strongly dependent on the abundance of the herring population.

The results from this chapter shows that modelling different trophic levels at different resolutions can impact the trophic level of interest, and that this strategy should be used with caution. These types of frameworks can be used to understand the effect that higher and lower trophic levels have upon each other, and the feedbacks and interactions between these trophic levels, but should not be used for predicting the impact on the underlying life histories.

6.1.3 The importance of the zooplankton dynamics

The zooplankton population has long been under-represented in marine ecosystem models: in LTL models, a 'closure' term is implemented in the zooplankton's dynamics to represent predation by the fish populations, whereas in HTL models, the zooplankton is not modelled explicitly but is portrayed through a 'carrying capacity' parameter, or through a fixed 'pool' of resources (Rose et al., 2010; Travers et al., 2007; Morozov et al., 2012). The representation of the zooplankton is of key importance in E2E models, as they are the link between the lower and higher trophic levels (Rose et al., 2010). The zooplankton population has been modelled in many different ways, from a single box component (Franks, 2002; Steele and Hendersen, 1981), to a coarsely size-structured representation of small and large (Travers et al., 2009), using a completely stage-structured representation (Fennel, 2001; Moll and Stegert, 2007; Stegert et al., 2007) to a continuously size-structured population model (Fuchs and Franks, 2010).

The underlying dynamics of the zooplankton population, such as the modelling of the grazing of herbivorous zooplankton upon the phytoplankton populations (Morozov et al., 2012; Gentleman and Neuheimer, 2008), must also be investigated. In planktonic models, the zooplankton's grazing dynamics are commonly described by a function which has a satiating response to increasing prey availability (Franks, 2002), usually through a Holling Type II functional response (Travers et al., 2009; Scheffer et al., 2000) or an Ivlev-type function (Fennel, 2010; Kishi et al., 2007). It has been observed, historically, that the use of a satiating

response leads to a destabilization of the ecosystem (Gentleman and Neuheimer, 2008).

In **Chapter 3**, three different functional responses for the grazing of zooplankton upon phytoplankton are studied: the Holling Type I, II and III functional responses. The mathematical stability of the isolated LTL submodel (where the predation upon the phytoplankton and zooplankton populations by the HTLs is assumed to be a constant rate) shows that the steady-state solutions are strongly dependent upon the assumed predation rate of the fish upon the zooplankton population, particularly when a satiating functional response is assumed in the zooplankton's grazing rate. The results show that when a Type II functional response is used, the LTL submodel (and thus the coupled E2E ecosystem model) is predominantly unstable under most predation pressures by the HTL organisms. The Type III response is predominantly stable under most predation pressures, but can be unstable under particular scenarios. A Type III response is underused in planktonic models, yet it has the same satiating characteristics as a Type II response, and the mathematical formulation allows for the occurrence of "excitable" phenomena such as seasonal spring phytoplankton blooms (where a rapid growth in the phytoplankton biomass is followed by an equally rapid decline) (Truscott and Brindley, 1994; Freund et al., 2006; Winder and Cloern, 2010).

6.1.4 Climate change and the consequences to marine ecosystems

In temperate oceans, phytoplankton undergoes an annual occurrence known as a seasonal bloom. This typically occurs in the spring months, with a smaller bloom often occurring in the autumn months (Truscott and Brindley, 1994; Winder and Cloern, 2010; Findlay, 2006). The spring bloom is caused by a number of environmental factors (increased nutrient availability, light intensity and temperature (McCauley and Murdoch, 1987; Moisan et al., 2002; Townsend et al., 1994)), whilst the autumn bloom is caused by destratification leading to an influx of fresh nutrients from the lower layers of the water column (Findlay, 2006).

Climate change is predicted to lead to an increase of 1.1°C to 6.4°C in sea surface temperature over the next 100 years (Huertas et al., 2011). In this thesis, I focus on the effect of sea surface temperature upon the seasonal phytoplankton blooms, and the impact upon the rest of the marine ecosystem. In particular, in **Chapter 4**, I investigate the effect of a future warming scenario across a marine ecosystem, where the mean sea surface temperature increases by 3°C over 100 years. The PZ-Fish model developed in **Chapter 3**, with a Holling Type III functional response assumed for the zooplankton's grazing function upon phytoplankton, was used to model the dynamics of the marine ecosystem. In this chapter, it is assumed that temperature has a direct influence upon the phytoplankton growth rate (an increase in temperature leads to an increase in the phytoplankton growth rate), and the results show that the

warming temperature leads to a shift to an earlier occurrence of the phytoplankton bloom. This is in agreement with several empirical studies investigating the timing of the spring blooms (Edwards et al., 2002; Wiltshire and Manly, 2004).

The warming of the sea surface temperatures also leads to an increase in the duration of the spring phytoplankton bloom, which has a direct impact upon the autumn blooms. Due to the extended duration of the spring bloom, there is not enough time for an autumn bloom to occur: thus under a warming climate, this thesis predicts a loss of the autumn bloom. These results have been found in a modelling study by Molen et al. (2012), as well as in empirical observations (Martinez et al., 2011).

This thesis shows the importance of ecosystem-scale models, and the need to include the interactions between LTL and HTL organisms in one framework. The extended duration of the spring phytoplankton bloom is due to the increased grazing pressures of the fish community upon the zooplankton community. The zooplankton population declines, which in turn decreases the grazing pressure of the zooplankton upon the phytoplankton population and leads to a longer phytoplankton bloom. If a 'closure' term were used, representing the predation of the fish community as a fixed mortality rate upon the phytoplankton and zooplankton dynamics, the full implication of a warming climate would not be realised. Whilst the occurrence of an earlier bloom would emerge (as this is a direct effect of a warming climate), the predicted loss of the autumn bloom would not as this is due to the complex interactions of the phytoplankton and zooplankton populations with the fish community.

6.1.5 The impact of fishing on marine ecosystems

Fishing upon marine ecosystems is a practice which has occurred over hundreds of years (Pauly et al., 2005), and the management of fisheries is an area which attempts to protect those resources whilst maximising the yield obtained (Botsford et al., 1997; Caddy and Cochrane, 2001). This has led to the development of quantitative stock assessment methods, such as the use of mathematical models of the population dynamics of fish (Schnute and Richards, 2001). These mathematical models focus on exploited fish species, either in a single-species (Lassen and Medley, 2001) or multi-species context (Magnusson, 1995). These models focus solely on the HTL organisms, and do not explicitly include the dynamics of the LTL organisms within their frameworks. Fisheries managers have begun adopting an ecosystem approach to their strategies, where the targeted fish stocks are not the only consideration in exploitation practices but also the LTL organisms such as phytoplankton and zooplankton, and the socioeconomic effects (Plagányi, 2007; Hall and Mainprize, 2004). This has been one of the driving factors in the development of E2E models.

In **Chapter 5**, I use the dynamic PZ-Fish model developed in **Chapter 3** and simulate two fishing strategies in order to understand the implications that exploitation of fish stocks has upon the phytoplankton population. A traditional size-at-entry strategy, where fish of a minimum body size enter the fishery before being harvested, and a recently developed balanced harvesting strategy, where fishing occurs on all size-classes of fish in the community but in proportion to their natural productivity (Law et al., 2012; Garcia et al., 2012; Zhou et al., 2010), were studied in this chapter. I explore the fishing scenarios that would be representative of an industrial fishery focussed upon small zooplanktivorous species. The results show that each of these fishing strategies can significantly affect the dynamics of the phytoplankton population, shifting the stable annual patterns to unpredictable periodic behaviours. This finding is supported by empirical results which show that the seasonal dynamics of phytoplankton are strongly affected by the fish community (Casini et al., 2008; Zohary, 2004). The balanced harvesting strategy also achieves a greater biomass yield under low intensity fishing scenarios than the size-at-entry strategy, but can also lead to a greater disturbance in the phytoplankton population. These results show the potential dangers of fishing down to body sizes so small that large feedbacks occur into the plankton. Thus, this thesis makes a useful contribution to the ongoing debate about top-down (changes due to the fish population) and bottom-up (changes due to the nutrients and plankton population) control in marine ecosystem dynamics.

These findings show that exploitation of the fish community can have a strong influence upon the dynamics of the phytoplankton, and supports the need for ecosystem-based fisheries management. However, the fishing scenarios used in this modelling study are only representative of fisheries which are focused upon small zooplanktivorous species. Fishing scenarios which assumed a size-at-entry strategy upon larger fish (for example, a minimum body size of 10g) did not show any significant changes upon the dynamics of the phytoplankton population. This is due to the size-structured fish community: when a size-spectrum model is perturbed (for example, through fishing), the trophic cascade is damped as it comes further away from the perturbed trophic level (Andersen and Pedersen, 2010). This effect is amplified in the size-structured fish community model due to the assumption of each size-class contributing to the reproductive rate of the community. Thus, when fishing occurs on larger fish, the trophic cascade is damped to such a degree that when it affects the zooplanktivores (and other small fish which have a strong feeding preference upon the phytoplankton and zooplankton), it does not have a significant effect upon the phytoplankton's dynamics.

6.2 Future perspectives and priorities

In this thesis, a systematic investigation into the effect of model architecture upon the large-scale behaviours of models of marine ecosystems has been conducted, and an understanding of the interactions and feedbacks between the higher and lower trophic level organisms has been achieved. A minimal framework was used to develop a dynamic E2E model which mimics those used in recent studies, which couples together a box-compartmental model of phytoplankton and zooplankton and a size-structured fish community. Using this framework, it has been possible to study the implications of coupling together two models which vary significantly in their structure and resolution, as well as highlighting the importance of E2E models for addressing ecosystem-scale questions, such as the impact of climate change and fishing. In doing so, ways to improve the model have become evident, as well as avenues for future work.

The aim of this thesis was to understand the consequences of coupling together models which differ significantly in their structure and resolution. In **Chapter 3**, a phytoplankton-zooplankton-fish model was developed as the basis of this investigation. The amalgamation of several plankton functional types into two compartments of phytoplankton and zooplankton has had a significant impact upon the individual life histories of larval fish. Results from **Chapter 3** has shown that having only two prey items to feed upon leads to a slower growth trajectory for larval fish as well as a smaller body mass after five years, when compared to an assumption of a fixed resource which is numerically resolved to the same degree as the fish community. This is partly due to the formulation of the feeding kernel (the preference that an individual fish has for feeding upon phytoplankton or zooplankton), and one route that could be explored is the extension of the feeding kernel to represent feeding on a range of size-classes of phytoplankton (or zooplankton). This would retain the minimal framework of the PZ-Fish model, which allows for tractability of the model when different forcing scenarios are explored, and allows the interactions between the trophic levels to be the focus of investigations.

However, to fully understand the effect of the aggregation of plankton functional types into a limited number of size-classes, this modelling framework should be extended. The zooplankton needs to be methodically resolved into a population which is consistent with the modelled fish community, by first dividing it into two size-classes (of large and small zooplankton) and eventually extending it to a fully size-structured population (Fuchs and Franks, 2010). A similar approach can then be undertaken for resolving the phytoplankton population. However, the dynamics of the phytoplankton population cannot be modelled using the McKendrick-von Foerster equation as phytoplankton does not grow through consumption of smaller phytoplankton. Fuchs and Franks (2010) model a continuous population of size-

structured phytoplankton by assuming that the maximum specific growth rate scales with body size. This approach could be adopted when developing a size-structured phytoplankton population.

The size-structured fish community model also has limitations: in reality, the ocean consists of hundreds of species of fish with individual life histories, and by modelling these species within one framework restricts the emergence of behaviours such as diet shifting (Claessen and Dieckmann, 2002) or regime shifts (Shannon et al., 2004; Andrades, 2012). A multi-species approach for the fish community could be used, for example, by determining species by their asymptotic size and thus using a trait- and size-based model (Andersen and Beyer, 2006; Hartvig et al., 2010). Whilst this proposal would lead to a more complex model for the fish community, it would also allow for more realistic scenarios to be explored such as size-at-entry fisheries with a minimum body size of 100g (Jacobsen et al., 2014).

Another limitation to the size-structured fish community model is the assumption of continuous reproduction, an assumption made in most size-structured models (Hartvig et al., 2010; de Roos et al., 2008; Law et al., 2012). In reality, most fish will spawn once a year and the timing of the spawning period can be vital for the survival of the larval fish (Cushing, 1975; Wright and Trippel, 2009). Thygesen et al. (2005) show that when reproduction occurs once a year in a size-structured mode, it affects the strategy of optimal allocation of energy between growth and reproduction. This is a feature which could have ecosystem-scale consequences. By modelling reproduction as a seasonal 'pulse', ideas such as the 'match-mismatch' hypothesis (the proposal that the timing of egg hatching and the timing of spring phytoplankton blooms must overlap for optimal growth of the larval fish (Cushing, 1975)) can be studied, and the interaction between the phytoplankton and the fish community is better represented.

In **Chapter 4**, the impact of a warming climate upon the seasonal dynamics of phytoplankton was studied, where the sea surface temperature directly affected the phytoplankton growth rate. However, temperature also affects other processes in biological organisms, such as metabolic rates (Richardson, 2008), optimal growth rates (Peck and Daewel, 2007) and egg-hatching times (Pepin et al., 1997). Temperature can also have an indirect effect upon physiological processes through changing the oxygen content of the ocean waters, which again impacts the somatic growth rates of fish (Cheung et al., 2012; Pörtner and Knust, 2007). Thus, climate change will not just affect the seasonal dynamics of the phytoplankton, but will also have a direct impact upon the survival rate of fish within the ecosystem. A warming climate may have a stronger influence upon the dynamics of marine ecosystems than the study in this thesis suggests, as the fish community is also directly affected by sea surface temperatures and creates additional feedbacks within the ecosystem that are not captured in the modelling study in **Chapter 4**.

Variability has not been fully implemented into this work, yet it plays an important role in marine ecosystems, either through environmental effects (O'Brien et al., 2000), the seasonal variation found in the timing of phytoplankton blooms (Gaedke, 1992; Townsend et al., 1994) or in fish recruitment (Kristiansen et al., 2011). An initial investigation into a variable warming climate was conducted, and showed that decreasing the variance of the temperature profile can also affect the seasonal dynamics of phytoplankton, leading to a small spring bloom and no autumn bloom. As variability is a key factor in the timing of phytoplankton blooms and fish recruitment (Burrow et al., 2011), it is an important avenue to explore in the context of E2E modelling.

To conclude, this thesis presents an initial investigation into the effect that coupling together models that differ significantly in their structure and resolution has upon large-scale behaviours of marine ecosystems. Whilst steady-state solutions of E2E models can yield results which superficially appear credible, by studying the underling life-histories of the fish community, discrepancies can be found. However, using a minimal modelling framework can still allow an understanding of the basic interactions and feedbacks that occur in an ecosystem-scaled system to be gained, and the work in this thesis highlights the importance of those interrelationships. This thesis is the necessary first step in the development of E2E models, and will aid research in the field of ecosystem based management. There are many avenues of possibilities for future work, starting with the extension of the zooplankton compartment into a fully size-structured, dynamic population. This will give a complete and thorough understanding of the effect that model architecture has upon E2E models that describe the dynamics of marine ecosystems.

"So long, and thanks for all the fish."
- Douglas Adams (1984)

Bibliography

(2012). World review of fisheries and aquaculture. Technical report.

Ackleh, A. S. and Ito, K. (1997). An implicit finite difference scheme for the nonlinear size-structured population model. *Numerical Functional Analysis and Optimization*, 18(9&10):865–884.

Andersen, K. and Beyer, J. (2006). Asymptotic size determines species abundance in the marine size spectrum. *The American Naturalist*, 168(1):54–61.

Andersen, K. H. and Pedersen, M. (2010). Damped trophic cascades driven by fishing in model marine ecosystems. *Proceedings of the Royal Society B*, 277:795–802.

Andersen, K. P. and Ursin, E. (1977). A multispecies extension to the Beverton and Holt theory of fishing, with accounts of phosphorus circulation and primary production. *Meddelelser fra Danmarks Fiskeri- og Havundersøgelser*, pages 319–435.

Anderson, T. R. (2005). Plankton functional type modelling: running before we can walk? *Journal of Plankton Research*, 27(3).

Andrades, T. M. C. (2012). *Size-based dynamics of the pelagic fish community off Northern Chile*. PhD thesis, York.

Arino, O., Shin, Y.-J., and Mullon, C. (2004). A mathematical derivation of size spectra in fish populations. *Comptes Rendus Biologies*, 327(3):245–254.

Armstrong, R. (1999). Stable model structures for representing biogeochemical diversity and size spectra in plankton communities. *Journal of Plankton Research*, 21(3):445–464.

Aydin, K., Mcfarlane, G., King, J., Megrey, B., and Myers, K. (2005). Linking oceanic food webs to coastal production and growth rates of Pacific salmon (Oncorhynchus spp.), using

models on three scales. *Deep Sea Research Part II: Topical Studies in Oceanography*, 52(5-6):757–780.

Baird, M. E. and Suthers, I. M. (2007). A size-resolved pelagic ecosystem model. *Ecological Modelling*, 203(3-4):185–203.

Baretta, J. (1995). The European regional seas ecosystem model, a complex marine ecosystem model. *Netherlands Journal of Sea Research*, 33(3-4):233–246.

Beaugrand, G. and Kirby, R. R. (2010). Climate, plankton and cod. *Global Change Biology*, 16(4):1268–1280.

Benoît, E. and Rochet, M.-J. (2004). A continuous model of biomass size spectra governed by predation and the effects of fishing on them. *Journal of Theoretical Biology*, 226(1):9–21.

Beverton, R. J. and Holt, S. J. (1993). *On the dynamics of exploited fish populations*. Springer.

Bianchi, G. (2000). Impact of fishing on size composition and diversity of demersal fish communities. *ICES Journal of Marine Science*, 57(3):558–571.

Blackford, J. (2004). Ecosystem dynamics at six contrasting sites: a generic modelling study. *Journal of Marine Systems*, 52(1-4):191–215.

Blain, S., Quéguiner, B., Armand, L., Belviso, S., Bombled, B., Bopp, L., Bowie, A., Brunet, C., Brussaard, C., Carlotti, F., Christaki, U., Corbière, A., Durand, I., Ebersbach, F., Fuda, J.-L., Garcia, N., Gerringa, L., Griffiths, B., Guigue, C., Guillerm, C., Jacquet, S., Jeandel, C., Laan, P., Lefèvre, D., Lo Monaco, C., Malits, A., Mosseri, J., Obernosterer, I., Park, Y.-H., Picheral, M., Pondaven, P., Remenyi, T., Sandroni, V., Sarthou, G., Savoye, N., Scouarnec, L., Souhaut, M., Thuiller, D., Timmermans, K., Trull, T., Uitz, J., van Beek, P., Veldhuis, M., Vincent, D., Viollier, E., Vong, L., and Wagener, T. (2007). Effect of natural iron fertilization on carbon sequestration in the Southern Ocean. *Nature*, 446(7139):1070–4.

Blanchard, J. L., Jennings, S., Law, R., Castle, M. D., McCloghrie, P., Rochet, M.-J., and Benoît, E. (2009). How does abundance scale with body size in coupled size-structured food webs? *The Journal of Animal Ecology*, 78(1):270–80.

Borrell, B. (2013). A big fight over little fish. *Nature*, 493:597–598.

Botsford, L. W., Castilla, J. C., and Peterson, C. H. (1997). The management of fisheries and marine ecosystems. *Science*, 277(5325):509–515.

Boyd, P. W. and Doney, S. C. (2002). Modelling regional responses by marine pelagic ecosystems to global climate change. *Geophysical Research Letters*, 29(16):53–1–53–4.

Brentnall, S. J., Richards, K. J., Brindley, J., and Murphy, E. (2003). Plankton patchiness and its effect on larger-scale productivity. *Journal of Plankton Research*, 25(2):121–140.

Burrow, J. F., Horwood, J. W., and Pitchford, J. W. (2011). The importance of variable timing and abundance of prey for fish larval recruitment. *Journal of Plankton Research*, 33(8):1153–1162.

Caddy, J. and Cochrane, K. (2001). A review of fisheries management past and present and some future perspectives for the third millennium. *Ocean & Coastal Management*, 44(9-10):653–682.

Calsina, A. and Saldafia, J. (1995). A model of physiologically structured population dynamics with a nonlinear individual growth rate. *Journal of Mathematical Biology*, 33:335–364.

Capitán, J. a. (2010). Scale-invariant model of marine population dynamics. *Physical Review E*, 81(6):061901.

Carlotti, F. and Poggiale, J. (2010). Towards methodological approaches to implement the zooplankton component in end to end food-web models. *Progress In Oceanography*, 84:20–38.

Casini, M., Lövgren, J., Hjelm, J., Cardinale, M., Molinero, J.-C., and Kornilovs, G. (2008). Multi-level trophic cascades in a heavily exploited open marine ecosystem. *Proceedings. Biological sciences / The Royal Society*, 275(1644):1793–801.

Caswell, H. and Neubert, M. G. (1998). Chaos and closure terms in plankton food chain models. *Journal of Plankton Research*, 20(9):1837–1845.

Chassot, E., Mélin, F., Le Pape, O., and Gascuel, D. (2007). Bottom-up control regulates fisheries production at the scale of eco-regions in European seas. *Marine Ecology Progress Series*, 343:45–55.

Cheung, W. W. L., Sarmiento, J. L., Dunne, J., Frölicher, T. L., Lam, V. W. Y., Deng Palomares, M. L., Watson, R., and Pauly, D. (2012). Shrinking of fishes exacerbates impacts of global ocean changes on marine ecosystems. *Nature Climate Change*, 3(3):254–258.

Christensen, V. and Pauly, D. (1992). ECOPATH II - a software for balancing steady-state ecosystem models and calculating network characteristics *. *Ecological Modelling*, 61(681):169–185.

Claessen, D. and Dieckmann, U. (2002). Ontogenetic niche shifts and evolutionary branching in size-structured populations. *Evolutionary Ecology Research*, 4:189–217.

Clark, R. A., Fox, C. J., Viner, D., and Livermore, M. (2003). North Sea cod and climate change modelling the effects of temperature on population dynamics. *Global Change Biology*, (9):1669–1680.

Coale, K. H., Johnson, K. S., Fitzwater, S. E., Gordon, R. M., Tanner, S., Chavez, F. P., Ferioli, L., Sakamoto, C., Rogers, P., Millero, F., Steinberg, P., Nightingale, P., Cooper, D., Cochlan, W. P., Landry, M. R., Constantinou, J., Rollwagen, G., Trasvina, A., and Kudela, R. (1996). A massive phytoplankton bloom induced by an ecosystem-scale iron fertilization experiment in the equatorial Pacific Ocean. *Nature*, 383:495–501.

Cohen, J. E., Pimm, S. L., Yodzis, P., and Saldana, J. (1993). Body sizes of animal predators and animal prey in food webs. *Journal of Animal Ecology*, 62(1):67.

Currie, W. J. S., Claereboudt, M. R., and Roff, J. C. (1998). Gaps and patches in the ocean : a one-dimensional analysis of planktonic distributions. *Marine Ecology Progress Series*, 171:15–21.

Cushing, D. (1975). *Marine Ecology and Fisheries*. Cambridge University Press.

Daewel, U., Peck, M. a., Schrum, C., and St John, M. a. (2007). How best to include the effects of climate-driven forcing on prey fields in larval fish individual-based models. *Journal of Plankton Research*, 30(1):1–5.

Daskalov, G. M., Grishin, A. N., Rodionov, S., and Mihneva, V. (2007). Trophic cascades triggered by overfishing reveal possible mechanisms of ecosystem regime shifts. *Proceedings of the National Academy of Sciences of the United States of America*, 104(25):10518–23.

Datta, S. (2011). *A mathematical analysis of marine size spectra*. PhD thesis.

Datta, S., Delius, G. W., and Law, R. (2010). A jump-growth model for predator-prey dynamics: derivation and application to marine ecosystems. *Bulletin of Mathematical Biology*.

Datta, S., Delius, G. W., Law, R., and Plank, M. J. (2011). A stability analysis of the power-law steady state of marine size spectra. *Journal of Mathematical Biology*, 63(4):779–99.

de Roos, A., Diekmann, O., and Metz, J. a. J. (1992). Studying the dynamics of structured population models: a versatile technique and its application to Daphnia. *The American Naturalist*, 139(1):123–147.

de Roos, A. M., Diekmann, O., Getto, P., and Kirkilionis, M. (2010). Numerical equilibrium analysis for structured consumer resource models. *Bulletin of Mathematical Biology*, 72(2):259–97.

de Roos, A. M. and Persson, L. (2002). Size-Dependent Life-History Traits Promote Catastrophic Collapses of Top Predators. *Proceedings of the National Academy of Sciences*, 99(20):12907–12912.

de Roos, A. M., Schellekens, T., Van Kooten, T., Van De Wolfshaar, K., Claessen, D., and Persson, L. (2008). Simplifying a physiologically structured population model to a stage-structured biomass model. *Theoretical Population Biology*, 73(1):47–62.

DeYoung, B., Heath, M., Werner, F., Chai, F., Megrey, B., and Monfray, P. (2004). Challenges of modeling ocean basin ecosystems. *Science (New York, N.Y.)*, 304(5676):1463–6.

Diaz, R. J. and Rosenberg, R. (2008). Spreading dead zones and consequences for marine ecosystems. *Science (New York, N.Y.)*, 321(5891):926–9.

Dickie, L., Kerr, S., and Boudreau, P. (1987). Size-dependent processes underlying regularities in ecosystem structure. *Ecological Monographs*, 57(3):233–250.

Edwards, A. and Brindley, J. (1999). Zooplankton mortality and the dynamical behaviour of plankton population models. *Bulletin of Mathematical Biology*, 61(2):303–39.

Edwards, A. M. and Yool, A. (2000). The role of higher predation in plankton population models. *Journal of Plankton Research*, 22(6):1085–1112.

Edwards, M., Beaugrand, G., Reid, P. C., Rowden, A. A., and Jones, M. B. (2002). Ocean climate anomalies and the ecology of the North Sea. *Marine Ecology Progress Series*, 239:1–10.

Elliott, J. A., Jones, I. D., and Thackeray, S. J. (2006). Testing the sensitivity of phytoplankton communities to changes in water temperature and nutrient load, in a temperate lake. *Hydrobiologia*, 559(1):401–411.

Enberg, K., Jø rgensen, C., Dunlop, E. S., Varpe, O. y., Boukal, D. S., Baulier, L., Eliassen, S., and Heino, M. (2011). Fishing-induced evolution of growth: concepts, mechanisms and the empirical evidence. *Marine Ecology*, pages 1–25.

Farkas, J. and Hagen, T. (2007). Stability and regularity results for a size-structured population model. *Journal of Mathematical Analysis and Applications*, 328(1):119–136.

Fasham, M. J. R. (1993). Modelling the marine biota. In *The Global Carbon Cycle*, pages 457–504. Springer-Verlag, New York.

Fasham, M. J. R., Ducklow, H. W., and McKelvie, S. M. (1990). A nitrogen-based model of plankton dynamics in the oceanic mixed layer. *Journal of Marine Research*, 48(3):591–639.

Fennel, W. (2001). Modeling of copepods with links to circulation models. *Journal of Plankton Research*, 23(11):1217–1232.

Fennel, W. (2009). Parameterizations of truncated food web models from the perspective of an end-to-end model approach. *Journal of Marine Systems*, 76(1-2):171–185.

Fennel, W. (2010). A nutrient to fish model for the example of the Baltic Sea. *Journal of Marine Systems*, 81(1-2):184–195.

Field, J., Francis, R., and Aydin, K. (2006). Top-down modeling and bottom-up dynamics: Linking a fisheries-based ecosystem model with climate hypotheses in the Northern California Current. *Progress In Oceanography*, 68:238–270.

Findlay, H. S. (2006). Modelling of autumn plankton bloom dynamics. *Journal of Plankton Research*, 28(2):209–220.

Franks, P. J. (2002). NPZ Models of Plankton Dynamics: Their Construction, Coupling to Physics, and Application. *Journal of Oceanography*, 58:379–387.

Franks, P. J. S., Wroblewski, J. S., and Flierl, G. R. (1986). Behavior of a simple plankton model with food-level acclimation by herbivores. *Marine Biology*, 91(1):121–129.

Freund, J. A., Mieruch, S., Scholze, B., Wiltshire, K., and Feudel, U. (2006). Bloom dynamics in a seasonally forced phytoplankton zooplankton model: trigger mechanisms and timing effects. *Ecological Complexity*, 3(2):129–139.

Fuchs, H. and Franks, P. (2010). Plankton community properties determined by nutrients and size-selective feeding. *Marine Ecology Progress Series*, 413:1–15.

Fulton, E. A. (2010). Approaches to end-to-end ecosystem models. *Journal of Marine Systems*, 81(1-2):171–183.

Fulton, E. A., Link, J. S., Kaplan, I. C., Savina-Rolland, M., Johnson, P., Ainsworth, C., Horne, P., Gorton, R., Gamble, R. J., Smith, A. D. M., and Smith, D. C. (2011). Lessons in modelling and management of marine ecosystems: the Atlantis experience. *Fish and Fisheries*, 12(2):171–188.

Fulton, E. A., Smith, A. D., and Johnson, C. R. (2003a). Mortality and predation in ecosystem models: is it important how these are expressed? *Ecological Modelling*, 169(1):157–178.

Fulton, E. A., Smith, A. D., and Johnson, C. R. (2004). Effects of spatial resolution on the performance and interpretation of marine ecosystem models. *Ecological Modelling*, 176(1-2):27–42.

Fulton, E. A., Smith, A. D. M., and Johnson, C. R. (2003b). Effect of complexity on marine ecosystem models. *Marine Ecology Progress Series*, 253:1–16.

Gaedke, U. (1992). The size distribution of plankton biomass in a large lake and its seasonal variability. *Limnology and Oceanography*, 37(6):1202–1220.

Gaedke, U. (1995). A comparison of whole-community and ecosystem approaches (biomass size distributions , food web analysis , network analysis , simulation models) to study the structure , function and regulation of pelagic food webs. *Journal of Plankton Research*, 17(6):1273–1305.

Garcia, S. M., Kolding, J., Rice, J., Rochet, M., Zhou, S., Arimoto, T., Beyer, J. E., Borges, L., Bundy, A., Dunn, D., Fulton, E. A., Hall, M., Heino, M., Law, R., and Makino, M. (2012). Reconsidering the Consequences of Selective Fisheries. *Science*, 335:1045–1047.

Gentleman, W. C. and Neuheimer, a. B. (2008). Functional responses and ecosystem dynamics: how clearance rates explain the influence of satiation, food-limitation and acclimation. *Journal of Plankton Research*, 30(11):1215–1231.

Gislason, H., Daan, N., Rice, J. C., and Pope, J. G. (2010). Size, growth, temperature and the natural mortality of marine fish. *Fish and Fisheries*, 11(2):149–158.

Hall, S. J. and Mainprize, B. (2004). Towards ecosystem-based fisheries management. *Fish and Fisheries*, 5:1–20.

Han, B. (1998). Size dependence of biomass spectra and population density I. The effects of size scales and size intervals. *Journal of Theoretical Biology*, 191(3):259–265.

Hartvig, M., Andersen, K. H., and Beyer, J. E. (2010). Food web framework for size-structured populations. *Journal of Theoretical Biology*, 272(1):113–122.

Heath, M. R. (2012). Ecosystem limits to food web fluxes and fisheries yields in the North Sea simulated with an end-to-end food web model. *Progress in Oceanography*, 102:42–66.

Heath, M. R., Speirs, D. C., and Steele, J. H. (2014). Understanding patterns and processes in models of trophic cascades. *Ecology letters*, 17(1):101–14.

Hoegh-Guldberg, O. and Bruno, J. F. (2010). The impact of climate change on the world's marine ecosystems. *Science (New York, N.Y.)*, 328(5985):1523–8.

Holling, C. (1959). The components of predation as revealed by a study of small-mammal predation of the European pine sawfly. *The Canadian Entomologist*, 91(5):293–320.

Huertas, I. E., Rouco, M., López-Rodas, V., and Costas, E. (2011). Warming will affect phytoplankton differently: evidence through a mechanistic approach. *Proceedings of the Royal Society B*, 278(1724):3534–43.

Hughes, T. P. (1984). Population dynamics based on individual size rather than age: a general model with a reef coral example. *The American Naturalist*, 123(6):778–795.

Hutchinson, W. F. (2008). The dangers of ignoring stock complexity in fishery management: the case of the North Sea cod. *Biology letters*, 4(6):693–5.

Jacobsen, N. S., Gislason, H., Andersen, K. H., and B, P. R. S. (2014). The consequences of balanced harvesting of fish communities. *Proceedings of the Royal Society B*, 281.

James, A., Pitchford, J. W., and Brindley, J. (2003). The relationship between plankton blooms, the hatching of fish larvae, and recruitment. *Ecological Modelling*, 160(1-2):77–90.

Jennings, S. and Dulvy, N. (2005). Reference points and reference directions for size-based indicators of community structure. *ICES Journal of Marine Science*, 62(3):397–404.

Jennings, S., Greenstreet, S., Hill, L., Piet, G., Pinnegar, J., and Warr, K. (2002). Long-term trends in the trophic structure of the North Sea fish community: evidence from stable-isotope analysis, size-spectra and community metrics. *Marine Biology*, 141(6):1085–1097.

Jin, D., Hoagland, P., and Morin Dalton, T. (2003). Linking economic and ecological models for a marine ecosystem. *Ecological Economics*, 46(3):367–385.

Kamioka, K. (2005). Mathematical analysis of an age-structured population model with space-limited recruitment. *Mathematical Biosciences*, 198(1):27–56.

Kelley, C. (1995). *Iterative methods for linear and nonlinear equations*. Society for Industrial and Applied Mathematics.

Kerr, S. (1974). Theory of size distribution in ecological communities. *Journal of the Fisheries Research Board of Canada*, 31(12):1859–1862.

Kishi, M., Kashiwai, M., Ware, D., Megrey, B., Eslinger, D., Werner, F., Noguchiaita, M., Azumaya, T., Fujii, M., and Hashimoto, S. (2007). NEMUROa lower trophic level model for the North Pacific marine ecosystem. *Ecological Modelling*, 202(1-2):12–25.

Kishi, M. J., Ito, S.-i., Megrey, B. a., Rose, K. a., and Werner, F. E. (2011). A review of the NEMURO and NEMURO.FISH models and their application to marine ecosystem investigations. *Journal of Oceanography*, 67(1):3–16.

Kot, M. (2001). *Elements of mathematical ecology*. Cambridge University Press.

Kristiansen, T., Drinkwater, K. F., Lough, R. G., and Sundby, S. (2011). Recruitment variability in North Atlantic cod and match-mismatch dynamics. *PloS ONE*, 6(3):e17456.

Lassen, H. and Medley, P. (2001). *Virtual Population Analysis: A Practical Manual for Stock Assessment*. Food and Agriculture Organization of the United Nations.

Law, R. (2000). Fishing, selection, and phenotypic evolution. *ICES Journal of Marine Science*, 57(3):659–668.

Law, R., Kolding, J., and Plank, M. J. (2013). Squaring the circle: reconciling fishing and conservation of aquatic ecosystems. *Fish and Fisheries*, pages n/a–n/a.

Law, R., Plank, M. J., James, A., and Blanchard, J. L. (2009). Size-spectra dynamics from stochastic predation and growth of individuals. *Ecology*, 90(3):802–11.

Law, R., Plank, M. J., and Kolding, J. (2012). On balanced exploitation of marine ecosystems: results from dynamic size spectra. *ICES Journal of Marine Science*, 69:602–614.

Lax, P. (1965). Numerical solution of partial differential equations. *The American Mathematical Monthly*, 72(2):74–84.

Le Quéré, C., Harrison, S. P., Prentice, C., Buitenhuis, E. T., Aumont, O., Bopp, L., Claustre, H., Cotrim da Cunha, K., Kohfeld, K. E., Legendre, L., Manizza, M., Platt, T., Rivkin, R. B., Sathyendranath, S., Uitz, J., Watson, A. J., and Wolf-Gladrow, D. (2005). Ecosystem dynamics based on plankton functional types for global ocean biogeochemistry models. *Global*, 11:2016–2040.

Levin, S. a. and Lubchenco, J. (2008). Resilience, robustness, and marine ecosystem-based management. *BioScience*, 58(1):27.

Lewis, K. and Allen, J. (2009). Validation of a hydrodynamic-ecosystem model simulation with time-series data collected in the western English Channel. *Journal of Marine Systems*, 77(3):296–311.

Libralato, S. and Solidoro, C. (2009). Bridging biogeochemical and food web models for an end-to-end representation of marine ecosystem dynamics: The Venice lagoon case study. *Ecological Modelling*, 220(21):2960–2971.

Link, J. S., Fulton, E. a., and Gamble, R. J. (2010). The northeast US application of ATLANTIS: A full system model exploring marine ecosystem dynamics in a living marine resource management context. *Progress in Oceanography*, 87(1-4):214–234.

Magnusson, K. (1995). An overview of the multispecies VPA ? theory and applications. *Reviews in Fish Biology and Fisheries*, 5(2):195–212.

Mancinelli, G., Pinna, M., and Basset, A. (2008). Spatio-temporal variability of macrozoobenthos size structure of a coastal lagoon : the influence of spectrum resolution. *Transitional Waters Bulletin*, 2:81–92.

Martens, P. and Beusekom, J. E. E. (2008). Zooplankton response to a warmer northern Wadden Sea. *Helgoland Marine Research*, 62(1):67–75.

Martin, A. P., Richards, K. J., Bracco, A., and Provenzale, A. (2002). Patchy productivity in the open ocean. *Global Biogeochemical Cycles*, 16(2):9–1–9–9.

Martinez, E., Antoine, D., D'Ortenzio, F., and de Boyer Montégut, C. (2011). Phytoplankton spring and fall blooms in the North Atlantic in the 1980s and 2000s. *Journal of Geophysical Research*, 116(C11):C11029.

Maury, O. (2010). An overview of APECOSM, a spatialized mass balanced Apex Predators ECOSystem Model to study physiologically structured tuna population dynamics in their ecosystem. *Progress in Oceanography*, 84(1-2):113–117.

Maury, O., Shin, Y., Faugeras, B., Benari, T., and Marsac, F. (2007). Modeling environmental effects on the size-structured energy flow through marine ecosystems. Part 2: Simulations. *Progress In Oceanography*, 74(4):500–514.

Maxwell, S. M., Hazen, E. L., Morgan, L. E., Bailey, H., and Lewison, R. (2012). Finding balance in fisheries management. *Science*, 336(336):413.

McCauley, E. and Murdoch, W. W. (1987). Cyclic and stable populations : plankton as paradigm. *The American Naturalist*, 129(1):97–121.

Megrey, B. a., Rose, K. a., Klumb, R. a., Hay, D. E., Werner, F. E., Eslinger, D. L., and Smith, S. L. (2007). A bioenergetics-based population dynamics model of Pacific herring (Clupea harengus pallasi) coupled to a lower trophic level nutrientphytoplanktonzooplankton model: Description, calibration, and sensitivity analysis. *Ecological Modelling*, 202(1-2):144–164.

Mellin, C., Galzin, R., Ponton, D., and Vigliola, L. (2009). Detecting age-structured effects in growth performance of coral reef fish juveniles. *Aquatic Biology*, 6(August):31–39.

Moisan, J. R., Moisan, T. A., and Abbott, M. R. (2002). Modelling the effect of temperature on the maximum growth rates of phytoplankton populations. *Ecological Modelling*, 153(3):197–215.

Molen, J., Aldridge, J. N., Coughlan, C., Parker, E. R., Stephens, D., and Ruardij, P. (2012). Modelling marine ecosystem response to climate change and trawling in the North Sea. *Biogeochemistry*, 113(1-3):213–236.

Moll, A. and Stegert, C. (2007). Modelling Pseudocalanus elongatus stage-structured population dynamics embedded in a water column ecosystem model for the northern North Sea. *Journal of Marine Systems*, 64(1-4):35–46.

Mooij, W., De Senerpont Domis, L., and Hülsmann, S. (2008). The impact of climate warming on water temperature, timing of hatching and young-of-the-year growth of fish in shallow lakes in the Netherlands. *Journal of Sea Research*, 60(1-2):32–43.

Morozov, A., Poggiale, J.-C., and Cordoleani, F. (2012). Implementation of the zooplankton functional response in plankton models: State of the art, recent challenges and future directions. *Progress in Oceanography*, 103:80–91.

Murray, A. (2001). The use of simple models in the design and calibration of a dynamic 2D model of a semi-enclosed Australian bay. *Ecological Modelling*, 136(1):15–30.

Nisbet, R., McCauley, E., and Johnson, L. (2010). Dynamic energy budget theory and population ecology: lessons from Daphnia.

O'Brien, C. M., Fox, C. J., Planque, B., and Casey, J. (2000). Climate variability and North Sea cod. *Nature*, 404:142.

Pahl-wostl, C. (1997). Dynamic structure of a food web model : comparison with a food chain model. *Ecological Modelling*, 100:103–123.

Pauly, D. (2000). Ecopath, Ecosim, and Ecospace as tools for evaluating ecosystem impact of fisheries. *ICES Journal of Marine Science*, 57(3):697–706.

Pauly, D., Watson, R., and Alder, J. (2005). Global trends in world fisheries: impacts on marine ecosystems and food security. *Philosophical transactions of the Royal Society of London. Series B, Biological sciences*, 360(1453):5–12.

Peck, M. and Daewel, U. (2007). Physiologically based limits to food consumption, and individual-based modeling of foraging and growth of larval fishes. *Marine Ecology Progress Series*, 347:171–183.

Peeters, F., Straile, D., Lorke, A., and Livingstone, D. M. (2007). Earlier onset of the spring phytoplankton bloom in lakes of the temperate zone in a warmer climate. *Global Change Biology*, 13(9):1898–1909.

Pepin, P., Orr, D. C., and Anderson, J. T. (1997). Time to hatch and larval size in relation to temperature and egg size in Atlantic cod (Gadus morhua). *Canadian Journal of Fisheries and Aquatic Sciences*, 54(S1):2–10.

Perrin, N. and Sibly, R. M. (1993). Dynamic models of energy allocation and investment. *Annual Review of Ecology and Systematics*, 24(1993):379–410.

Picard, N., Ouédraogo, D., and Bar-hen, A. (2010). Choosing classes for size projection matrix models. *Ecological Modelling*, 221(19):2270–2279.

Pitchford, J. W. and Brindley, J. (2001). Prey patchiness, predator survival and fish recruitment. *Bulletin of mathematical biology*, 63(3):527–46.

Plagányi, E. E. (2007). Models for an ecosystem approach to fisheries.

Plank, M. J. and Law, R. (2011). Ecological drivers of stability and instability in marine ecosystems. *Theoretical Ecology*.

Platt, T. and Denman, K. (1977). Organisation in the pelagic ecosystem. *Helgoländer wissenschaftliche Meeresuntersuchungen*, 30:575–581.

Pope, J. G., Rice, J. C., Daan, N., Jennings, S., and Gislason, H. (2006). Modelling an exploited marine fish community with 15 parameters e results from a simple size-based model. *ICES Journal of Marine Science*, 63:1029–1044.

Pörtner, H. O. and Knust, R. (2007). Climate change affects marine fishes through the oxygen limitation of thermal tolerance. *Science*, 315:95–97.

Press, W. H., Teukolsky, S. A., Vetterling, W. T., and Flannery, B. P. (2007). *Numerical recipes: the art of scientific computing*. Cambridge University Press.

Quinones, R. (2003). Patterns of biomass-size spectra from oligotrophic waters of the Northwest Atlantic. *Progress In Oceanography*, 57(3-4):405–427.

Reid, P. C., Planque, B., and Edwards, M. (1998). Is observed variability in the long-term results of the Continuous Plankton Recorder survey a response to climate change? *Fisheries Oceanography*, 7(3-4):282–288.

Reznick, D. N. and Ghalambor, C. K. (2005). Can commercial fishing cause evolution ? Answers from guppies (Poecilia reticulata). *Canadian Journal of Fisheries and Aquatic Sciences*, 62:791–801.

Rice, J. (1996). Patterns of change in the size spectra of numbers and diversity of the North Sea fish assemblage, as reflected in surveys and models. *ICES Journal of Marine Science*, 53(6):1214–1225.

Richardson, A. J. (2008). In hot water : zooplankton and climate change. pages 279–295.

Rose, K. a. (2012). End-to-end models for marine ecosystems: Are we on the precipice of a significant advance or just putting lipstick on a pig? *Scientia Marina*, 76(1):195–201.

Rose, K. A., Allen, J. I., Artioli, Y., Barange, M., Blackford, J., Carlotti, F., Cropp, R., Daewel, U., Edwards, K., Flynn, K., Hill, S. L., Hille, R., Lambers, R., Huse, G., Mackinson, S., Megrey, B., Moll, A., Rivkin, R., Salihoglu, B., Schrum, C., Shannon, L., Shin, Y.-J., Smith, S. L., Smith, C., Solidoro, C., St. John, M., and Zhou, M. (2010). End-to-end models for the analysis of marine ecosystems: challenges, issues, and next steps. *Marine and Coastal Fisheries: Dynamics, Management, and Ecosystem Science*, 2:115–130.

Rossberg, A. G. (2012). A complete analytic theory for structure and dynamics of populations and communities spanning wide ranges in body size. In *Global Change in Multispecies Systems*, volume 46, pages 427–521. Elsevier Ltd., 1 edition.

Rudolf, V. H. W. (2007). Consequences of stage-structured predators: cannibalism, behavioral effects, and trophic cascades. *Ecology*, 88(12):2991–3003.

Santos, M. N., Gaspar, M. B., Vasconcelos, P., and Monteiro, C. C. (2002). Weight-length relationships for 50 selected fish species of the Algarve coast (southern Portugal). *Fisheries Research*, 59.

Scheffer, M. and Rinaldi, S. (2000). Minimal models of top-down control of phytoplankton. pages 265–283.

Scheffer, M., Rinaldi, S., and Kuznetsov, Y. A. (2000). Effects of fish on plankton dynamics : a theoretical analysis. *Canadian Journal of Fisheries and Aquatic Sciences*, 1219:1208–1219.

Schnute, J. T. and Richards, L. J. (2001). Use and abuse of fishery models. *Canadian Journal of Fisheries and Aquatic Sciences*, 58(1):10–17.

Shannon, L. J., Field, J. G., and Moloney, C. L. (2004). Simulating anchovysardine regime shifts in the southern Benguela ecosystem. *Ecological Modelling*, 172(2-4):269–281.

Shchepetkin, A. F. and McWilliams, J. C. (2005). The regional oceanic modeling system (ROMS): a split-explicit, free-surface, topography-following-coordinate oceanic model. *Ocean Modelling*, 9(4):347–404.

Sheldon, R., Prakash, A., and Sutcliffe Jr., W. (1972). The size distribution of particles in the ocean. *Limnology and Oceanography*, 17(3):327–340.

Sheldon, R., Sutcliffe Jr., W., and Paranjape, M. (1977). Structure of pelagic food chain and relationship between plankton and fish production. *Journal of the Fisheries Research Board of Canada*, 34(12):2344–2353.

Shin, Y.-j. and Cury, P. (2001). Exploring fish community dynamics through size-dependent trophic interactions using a spatialized individual-based model. *Aquatic Living Resources*, 14:65–80.

Shin, Y.-j., Travers, M., and Maury, O. (2010). Coupling low and high trophic level models: Towards a pathways oriented approach for end-to-end models. *Progress In Oceanography*, 84(1-2):105–112.

Shiomoto, A., Tadokoro, K., Nagasawa, K., and Ishida, Y. (1997). Trophic relations in the subarctic North Pacific ecosystem:possible feeding effect from pink salmon. *Marine Ecology Progress Series*, 150(1992):75–85.

Siegenthaler, U. and Sarmiento, J. (1993). Atmospheric carbon dioxide and the ocean. *Nature*, 365:119–125.

Silvert, W. and Platt, T. (1978). Energy flux in the pelagic ecosystem: A time-dependent equation. *Limnology and Oceanography*, 23(4):816–821.

Smith, A. D. M., Fulton, E. J., Hobday, A. J., Smith, D. C., Shoulder, P., and Scientific, P. (2007). Scientific tools to support the practical implementation of ecosystem-based fisheries management. *ICES Journal of Marine Science*, 64:633–639.

Song, H., Ji, R., Stock, C., and Wang, Z. (2010). Phenology of phytoplankton blooms in the Nova Scotian Shelf-Gulf of Maine region: remote sensing and modeling analysis. *Journal of Plankton Research*, 32(11):1485–1499.

Speirs, D., Guirey, E., Gurney, W., and Heath, M. (2010). A length-structured partial ecosystem model for cod in the North Sea. *Fisheries Research*, 106(3):474–494.

Steele, J., Collie, J., Bisagni, J., Gifford, D., Fogarty, M., Link, J., Sullivan, B., Sieracki, M., Beet, a., and Mountain, D. (2007). Balancing end-to-end budgets of the Georges Bank ecosystem. *Progress In Oceanography*, 74(4):423–448.

Steele, J. H. (2012). Prediction, scenarios and insight: The uses of an end-to-end model. *Progress in Oceanography*, 102:67–73.

Steele, J. H. and Hendersen, E. (1981). A Simple Plankton Model. *The American Naturalist*, 117(5):676–691.

Steele, J. H. and Henderson, E. W. (1992). The role of predation in plankton models. *Journal of Plankton Research*, 14(1):157–172.

Stegert, C., Kreus, M., Carlotti, F., and Moll, A. (2007). Parameterisation of a zooplankton population model for Pseudocalanus elongatus using stage durations from laboratory experiments. *Ecological Modelling*, 206(3-4):213–230.

Stock, C., Powell, T., and Levin, S. (2008). Bottomup and topdown forcing in a simple size-structured plankton dynamics model. *Journal of Marine Systems*, 74(1-2):134–152.

Thomas, A. C., Townsend, D. W., and Weatherbee, R. (2003). Satellite-measured phytoplankton variability in the Gulf of Maine. *Continental Shelf Research*, 23(10):971–989.

Thygesen, U. H. g., Farnsworth, K. D., Andersen, K. H., and Beyer, J. E. (2005). How optimal life history changes with the community size-spectrum. *Proceedings of the Royal Society B*, 272(1570):1323–31.

Townsend, D. W., Cammen, L. M., Holligan, P. M., Campbell, D. E., and Pettigrew, N. R. (1994). Causes and consequences of variability in the timing of spring phytoplankton blooms. *Deep Sea Research Part I: Oceanographic Research Papers*, 41(5):747–765.

Travers, M., Shin, Y., Jennings, S., and Cury, P. (2007). Towards end-to-end models for investigating the effects of climate and fishing in marine ecosystems. *Progress In Oceanography*, 75(4):751–770.

Travers, M., Shin, Y.-J., Jennings, S., Machu, E., Huggett, J., Field, J., and Cury, P. (2009). Two-way coupling versus one-way forcing of plankton and fish models to predict ecosystem changes in the Benguela. *Ecological Modelling*, 220(21):3089–3099.

Truscott, J. E. and Brindley, J. (1994). Ocean plankton populations as excitable media. *Bulletin of Mathematical Biology*, 56(5):981–998.

Vitousek, P. M., Mooney, H. A., Lubchenco, J., and Melillo, J. M. (1997). Human domination of Earth's ecosystems. *Science*, 277(5325):494–499.

Wiltshire, K. H., Malzahn, A. M., Wirtz, K., Greve, W., Janisch, S., Mangelsdorf, P., Manly, B. F. J., and Boersma, M. (2008). Resilience of North Sea phytoplankton spring bloom dynamics: An analysis of long-term data at Helgoland Roads. *Limnology and Oceanography*, 53(4):1294–1302.

Wiltshire, K. H. and Manly, B. F. J. (2004). The warming trend at Helgoland Roads, North Sea: phytoplankton response. *Helgoland Marine Research*, 58(4):269–273.

Winder, M. and Cloern, J. E. (2010). The annual cycles of phytoplankton biomass. *Philosophical transactions of the Royal Society of London. Series B, Biological sciences*, 365(1555):3215–26.

Worm, B., Hilborn, R., Baum, J. K., Branch, T. a., Collie, J. S., Costello, C., Fogarty, M. J., Fulton, E. a., Hutchings, J. a., Jennings, S., Jensen, O. P., Lotze, H. K., Mace, P. M., McClanahan, T. R., Minto, C., Palumbi, S. R., Parma, A. M., Ricard, D., Rosenberg, A. a., Watson, R., and Zeller, D. (2009). Rebuilding global fisheries. *Science*, 325(5940):578–85.

Wright, P. J. and Trippel, E. A. (2009). Fishery-induced demographic changes in the timing of spawning: consequences for reproductive success. *Fish and Fisheries*, 10(3):283–304.

Yool, a., Popova, E. E., Coward, a. C., Bernie, D., and Anderson, T. R. (2013). Climate change and ocean acidification impacts on lower trophic levels and the export of organic carbon to the deep ocean. *Biogeosciences*, 10(9):5831–5854.

Zhou, M. and Huntley, M. (1997). Population dynamics theory of plankton based on biomass spectra. *Marine Ecology Progress Series*, 159:61–73.

Zhou, S., Smith, A. D. M., Punt, A. E., Richardson, A. J., Gibbs, M., Fulton, E. a., Pascoe, S., Bulman, C., Bayliss, P., and Sainsbury, K. (2010). Ecosystem-based fisheries management requires a change to the selective fishing philosophy. *Proceedings of the National Academy of Sciences*, 107(21):9485–9.

Zohary, T. (2004). Changes to the phytoplankton assemblage of Lake Kinneret after decades of a predictable, repetitive pattern. *Freshwater Biology*, 49(10):1355–1371.